#3c
Revised

Appendix D: Species Distribution Model Outputs

Essential Fish Habitat Framework

Atlantic Sea Scallop Fishery Management Plan

Framework Adjustment 41

Northeast Multispecies Fishery Management Plan

Framework Adjustment 73

Draft

September 10, 2026

Prepared by the
New England Fishery Management Council
In consultation with the
National Marine Fisheries Service

1.0 TABLE OF CONTENTS

1.1 Tables

1.2 Figures

1.3 Acronyms

CFR	Code of Federal Regulations
EcoMon	Ecosystem Monitoring
EEZ	Exclusive Economic Zone
EFH	Essential Fish Habitat
FMP	Fishery management plan
FW	Framework
GARFO	Greater Atlantic Regional Fisheries Office
GB	Georges Bank
GLOBEC	Global Ocean Ecosystem Dynamics
GOM	Gulf of Maine
HAPC	Habitat Area of Particular Concern
HMA	Habitat Management Area
MADMF	Massachusetts Division of Marine Fisheries
MARMAP	Marine Resources Monitoring and Assessment and Prediction
MSA	Magnuson-Stevens Act; Magnuson-Stevens Fishery Conservation and Management Act
NEFMC	New England Fishery Management Council
NEFSC	Northeast Fisheries Science Center
NEPA	National Environmental Policy Act
NMFS	National Marine Fisheries Service
NOAA	National Oceanic and Atmospheric Administration
SNE	Southern New England
USC	United States Code
WOTUS	Waters of the United States

2.0 INTRODUCTION

The species distribution models (SDMs) that support essential fish habitat (EFH) designation are joint models for all species in this action except Atlantic halibut, Atlantic sea scallops, Atlantic wolffish, and offshore hake. The EFH designation updates for the latter four species are each supported by species-specific SDMs due to unique data needs and/or limitations. Some of the information provided in this document combines results across multiple species and life history stages, and other sections are presented by species. Generally, this information can be used to support EFH consultations as well as other management applications requiring an understanding of species distributions and the environmental drivers of those distributions. Additional model performance metrics are available upon request.

Note that the model uses a 'hurdle' approach. This means that the model is broken into a presence-absence component and a count component. The presence-absence component uses all observations of survey catch, coding anything greater than zero as present, and zero catches as absent. The count portion of the model uses just the positive catches, retaining the number of fish captured. In Section 4.0: Relationships with Environmental Variables, the results pertaining to these components are presented separately, as they provide slightly different information.

3.0 MODEL PERFORMANCE

Performance metrics were evaluated for the joint hurdle and species-specific SDMs using 5-fold cross-validation approach to assess the models' ability to generalize beyond the data used to train them. Table 1 documents the species- and life stage-specific performance using the following metrics: *Spearman's R* measures the rank correlation of model predictions to observations. *Root Mean Squared Log Error (RMSLE)* provides a measurement of error that is log-scaled to account for large differences in magnitude of species counts. *Mean Absolute Error* similarly measures error but uses the same units as the input data (species counts). *Area Under the Curve (AUC)* measures classification accuracy, primarily for the presence-absence component of the joint hurdle model; for species-specific, counts-based models, *AUC* was calculated by setting an arbitrary threshold, where ≥ 0.5 individuals per cell is considered a "presence".

Table 1. Model performance metrics for species distribution models (SDMs) supporting updated Essential Fish Habitat map designations in the 2025 EFH Framework and 2026 EFH Framework. Out-of-sample performance was measured on 5-fold cross-validation runs using the following metrics: *Spearman's R, Root Mean Squared Log Error (RMSLE), Mean Absolute Error*, and *Area Under the Curve (AUC)*. *AUC* is primarily for the presence-absence component of the joint hurdle model; for species-specific, counts-based models, *AUC* was calculated by setting an arbitrary threshold, where ≥ 0.5 individuals per cell is considered a "presence". "Pooled" refers to models that combine juvenile and adult data.

FMP	Species	Model Type	Life stage	*Spearman's R*	*RMSLE*	*MAE*	*AUC*
2025 Essential Fish Habitat Framework							
Northeast multispecies	Atlantic cod	Joint hurdle	Juvenile	0.524	0.844	11.086	0.935
			Adult	0.491	0.541	1.485	0.938
Atlantic herring	Atlantic herring	Joint hurdle	Juvenile	0.622	2.126	145.399	0.906
			Adult	0.532	1.238	12.189	0.919
Monkfish	Monkfish	Joint hurdle	Juvenile	0.595	0.476	0.846	0.919
			Adult	0.568	0.401	0.592	0.921
Skate complex	Barndoor skate	Joint hurdle	Pooled	0.491	0.401	0.615	0.955
Skate complex	Clearnose skate	Joint hurdle	Juvenile	0.579	0.46	1.007	0.979
			Adult	0.591	0.443	0.876	0.973
	Little skate	Joint hurdle	Juvenile	0.769	1.127	15.948	0.932

FMP	Species	Model Type	Life stage	*Spearman's R*	*RMSLE*	*MAE*	*AUC*
Skate complex			Adult	0.729	1.089	8.89	0.915
Skate complex	Rosette skate	Joint hurdle	Pooled	0.34	0.269	0.317	0.988
Skate complex	Smooth skate	Joint hurdle	Pooled	0.469	0.352	0.568	0.976
Skate complex	Thorny skate	Joint hurdle	Pooled	0.408	0.308	0.297	0.944
Skate complex	Winter skate	Joint hurdle	Juvenile	0.673	0.973	6.021	0.917
			Adult	0.497	0.488	0.923	0.913
2026 Essential Fish Habitat Framework							
Northeast multispecies	Acadian redfish	Joint hurdle	Juvenile	0.598	0.895	9.363	0.969
			Adult	0.493	0.862	15.234	0.984
Northeast multispecies	American plaice	Joint hurdle	Juvenile	0.668	0.557	4.26	0.98
			Adult	0.69	0.538	2.933	0.982
Northeast multispecies	Atlantic halibut	Trawl-only counts	Juvenile	0.225	0.137	0.0573	0.952
		Longline-trawl integrated counts	Adult	0.171	0.0882	0.0285	0.928
Atlantic sea scallop	Atlantic sea scallop	Dredge-trawl integrated counts	Adult[1]	*PENDING*			
				PENDING			
Northeast multispecies	Atlantic wolffish	Trawl-only counts	Juvenile	0.136	0.0977	0.0257	0.962
		Longline-trawl integrated counts	Adult	0.179	0.129	0.0450	0.948
Northeast multispecies	Haddock	Joint hurdle	Juvenile	0.555	1.353	43.464	0.928
			Adult	0.568	0.969	14.517	0.969
Northeast multispecies	Ocean pout	Joint hurdle	Juvenile	0.389	0.399	0.611	0.912
			Adult	0.512	0.547	1.272	0.922
Northeast multispecies	Offshore hake	Trawl-only counts	Juvenile	0.293	0.338	0.591	0.99
			Adult	0.336	0.238	0.254	0.989
Northeast multispecies	Pollock	Joint hurdle	Juvenile	0.293	0.511	1.57	0.885
			Adult	0.286	0.335	0.44	0.965
Northeast multispecies	Red hake	Joint hurdle	Juvenile	0.565	1.188	6.347	0.859
			Adult	0.755	1.101	15.682	0.947
Northeast multispecies	Silver hake	Joint hurdle	Juvenile	0.75	1.886	133.29	0.896
			Adult	0.818	1.384	66.103	0.956
Northeast multispecies	White hake	Joint hurdle	Juvenile	0.593	0.556	2.065	0.958
			Adult	0.588	0.415	0.962	0.974
Northeast multispecies	Windowpane flounder	Joint hurdle	Juvenile	0.502	0.722	1.952	0.848
			Adult	0.589	0.788	2.297	0.866
Northeast multispecies	Winter flounder	Joint hurdle	Juvenile	0.775	0.809	8.656	0.964
			Adult	0.721	0.786	3.972	0.938
Northeast multispecies	Witch flounder	Joint hurdle	Juvenile	0.551	0.471	1.224	0.974
			Adult	0.556	0.524	1.223	0.96
Northeast multispecies	Yellowtail flounder	Joint hurdle	Juvenile	0.415	0.446	0.901	0.934
			Adult	0.607	0.753	5.483	0.949

Notes:
[1] Atlantic sea scallops uses a single model to represent all life stages, but this model uses data from individuals with shell height > 75 mm. While juveniles actively swim to avoid predators up to ~80 mm shell height, these movements are generally at fine scales, and habitat preferences for settled juveniles and adults are expected to be the same.

4.0 RELATIONSHIPS WITH ENVIRONMENTAL VARIABLES

The importance of environmental covariates to model predictions was evaluated in two ways, predictor significance (demersal, Figure 1; pelagic, Figure 2) and variance partitioning (demersal, Figure 3; pelagic, Figure 4). The predictor significance plots depict whether covariates are statistically significant at the $p < 0.05$ level using analysis of variance (ANOVA) tests. The variance partitioning plots show how much variance in the response variable (presence/absence or abundance [counts]) is explained by including a given predictor in the model. Each figure has two panels; one illustrates the presence/absence component of the model, and the other illustrates the count component. Taken together, these figures illustrate which environmental covariates are generally important for predicting managed species' habitat.

Then, for each species and life stage, we include smooth-terms figures (Figures 5-20), which illustrate specific relationships between species' presence-absence or density (counts) and individual environmental covariates. Two plots are provided for each species and life stage combination modeled; the first is for the presence/absence component of the model, and the second is for the count component.

Table 2. Environmental covariates used in joint species distribution models (SDMs). Dynamic variables generally use monthly composites.

Model	Variable name	Covariate, data type	Source and link
Pelagic	SURFTEMP_DOPGLO_monthly_mean	Surface temperature; dynamic	2000-2006: Global Ocean Physics Reanalysis, available via the Copernicus Marine Environmental Monitoring Service (https://doi.org/10.48670/moi-00021) 2007-2019: "DoppioV3R3" ROMs-based (Regional Ocean Modeling System) assimilative reanalysis (Wilkin et al. 2022; https://doi.org/10.1016/j.pocean.2022.102919)
Demersal	BOTTEMP_DOPGLO_monthly_mean	Bottom temperature and salinity; dynamic	
Pelagic	SURFSALIN_DOPGLO_monthly_mean	Surface salinity; dynamic	
Demersal	BOTSALIN_DOPGLO_monthly_mean	Bottom salinity; dynamic	
Demersal	logGRAIN_km	Log sediment grain size; static	USGS sediment texture & USSEABED databases. https://woodshole.er.usgs.gov/project-pages/sediment/ and https://www.usgs.gov/programs/cmhrp/science/usseabed
Demersal	logDEPTH_km	Log depth; static	NCEI 1-arcsecond Coastal Relief Model. Source: National Centers for Environmental Information https://www.ncei.noaa.gov/products/coastal-relief-model
Demersal	logCOMPLEX_km	Log complexity; static	
Demersal	logBPI_km	Log bathymetric position index; static	
Pelagic	logSURFVELcm_DOP_month_clim_MAG_MEAN	Log surface current velocity; dynamic	2007-2019: "DoppioV3R3" ROMs-based (Regional Ocean Modeling System) assimilative reanalysis (Wilkin et al. 2022; https://doi.org/10.1016/j.pocean.2022.102919)

Model	Variable name	Covariate, data type	Source and link
Demersal	logBOTVELcm_DOP_month_clim_MAG_MEAN	Log wave bottom orbital velocity; dynamic	NREL WPTO wave hindcast, National Renewable Energy Laboratory Water Power Technologies Office https://www.nrel.gov/water/wave-hindcast-dataset
Pelagic, demersal	logTideVel_mean	Log tidal current velocity; dynamic	ADCIRC EC2015 Tidal Database. Includes the M2, S2, N2, K2, O1, K1, Q1, M4, M6 and STEADY tidal constituents. https://adcirc.org/
Pelagic	logMLD_DOPGLO_monthly_MEAN	Log mixed layer depth; dynamic	2000-2006: Global Ocean Physics Reanalysis, available via the Copernicus Marine Environmental Monitoring Service (https://doi.org/10.48670/moi-00021) 2007-2019: “DoppioV3R3” ROMs-based (Regional Ocean Modeling System) assimilative reanalysis (Wilkin et al. 2022; https://doi.org/10.1016/j.pocean.2022.102919)

4.1 PREDICTOR SIGNIFICANCE AND VARIANCE PARTITIONING

Figure 1. Predictor significance for demersal species. Statistical significance was evaluated at the p < 0.05 level using analysis of variance (ANOVA) tests for (A) the presence-absence component and (B) the zero-truncated negative binomial component of the joint hurdle species distribution model.

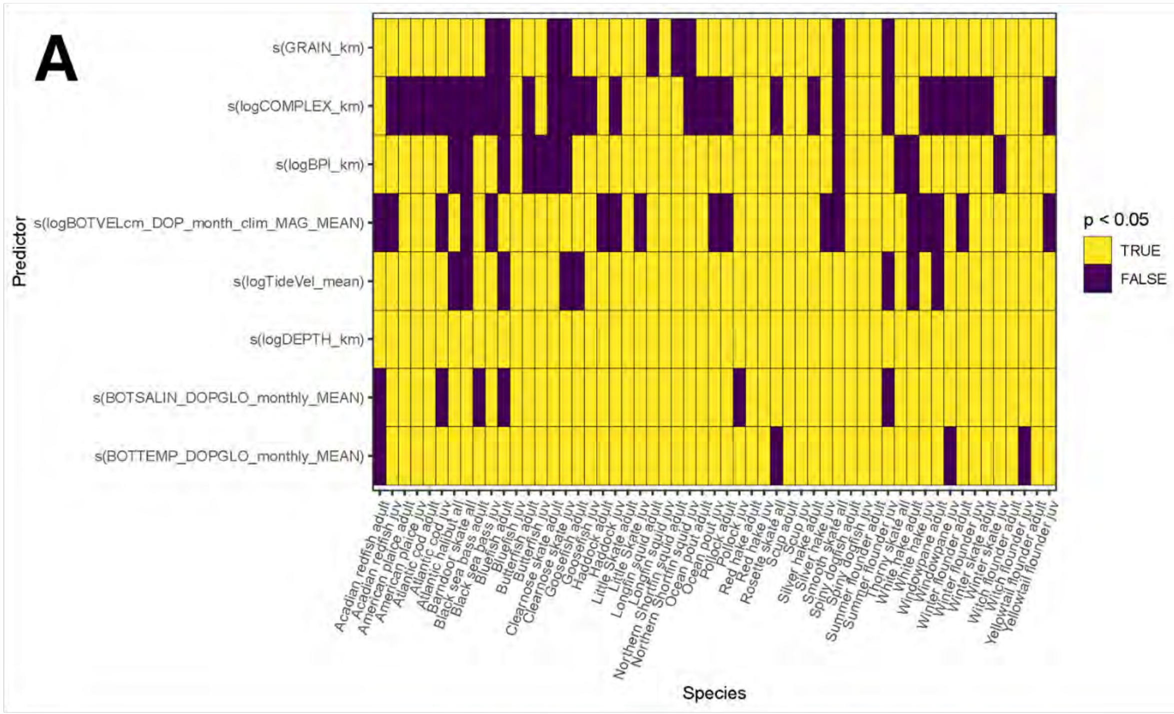

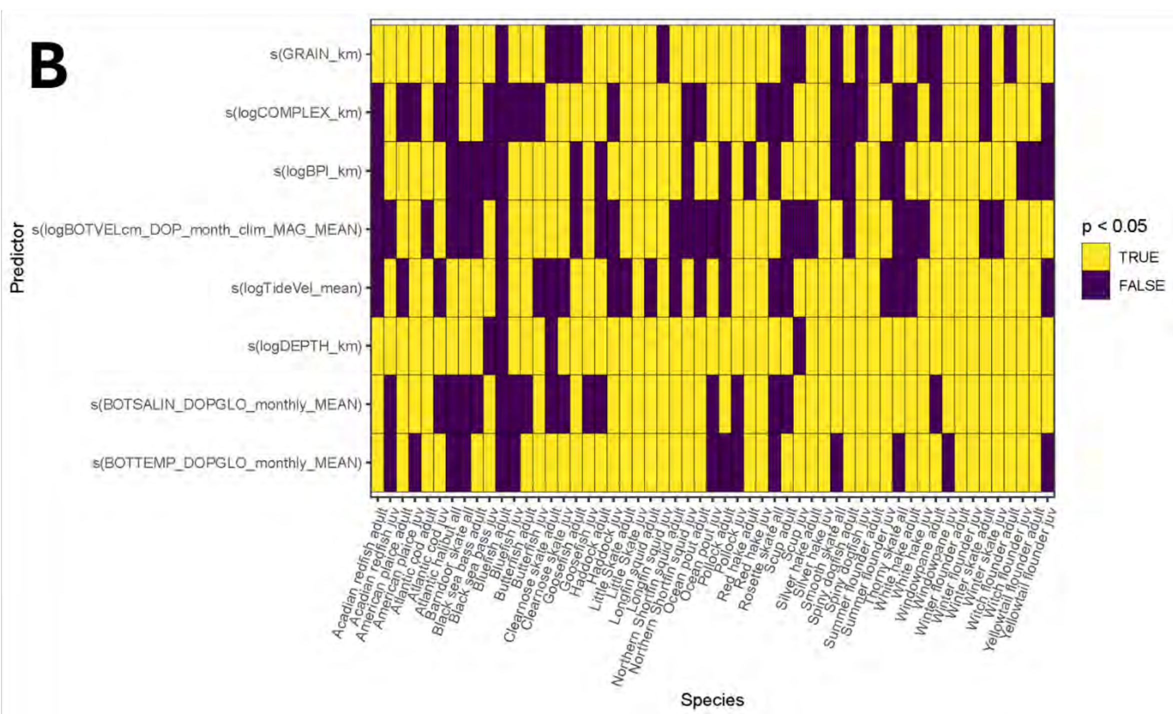

Figure 2. Predictor significance for pelagic species. Statistical significance was evaluated at the p < 0.05 level using analysis of variance (ANOVA) tests for (A) the presence-absence component and (B) the zero-truncated negative binomial component of the joint hurdle species distribution model.

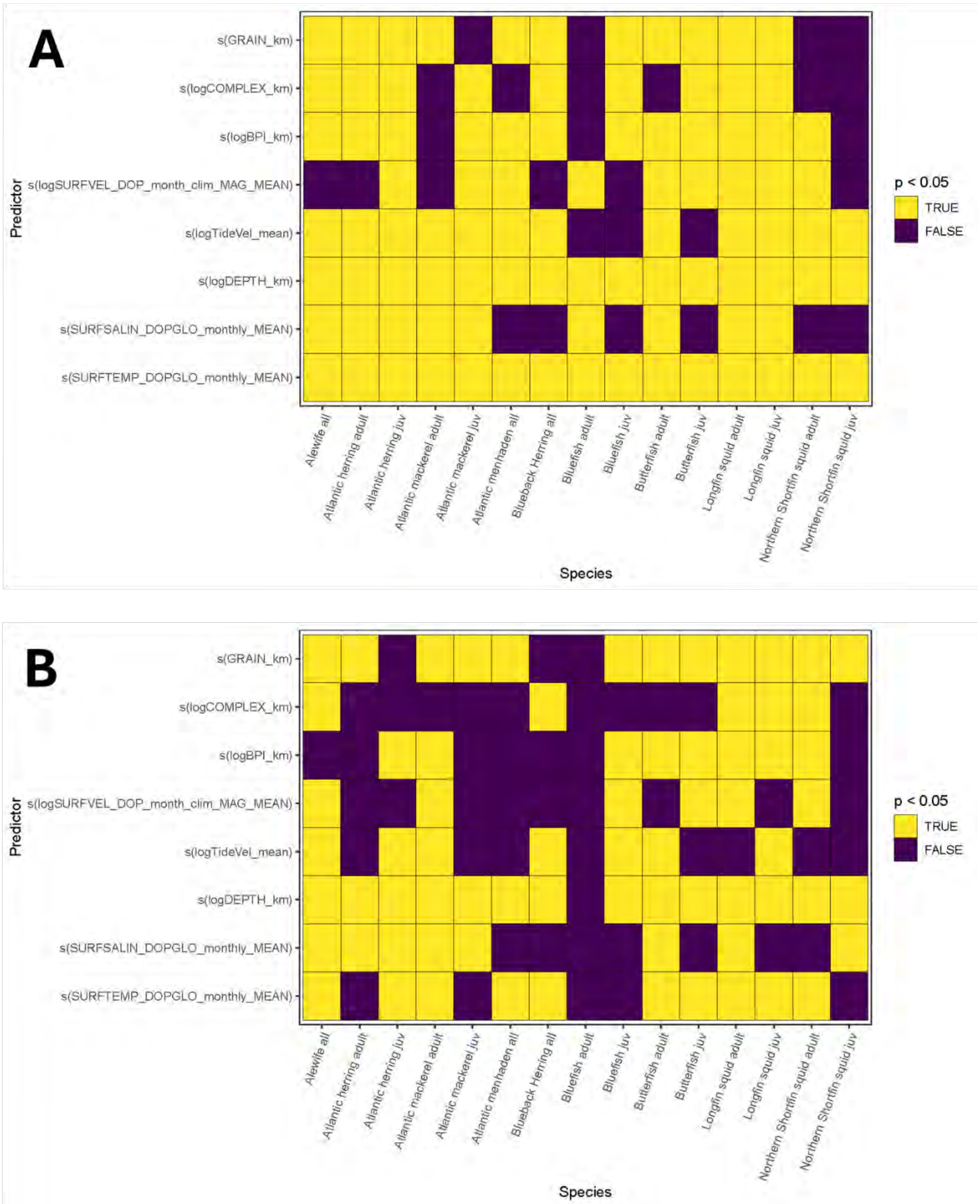

Figure 3. Variance partitioning for demersal species distribution models using a joint hurdle approach. (A) Presence-absence component of the hurdle model. (B) Count (zero-truncated negative binomial component) of the hurdle model.

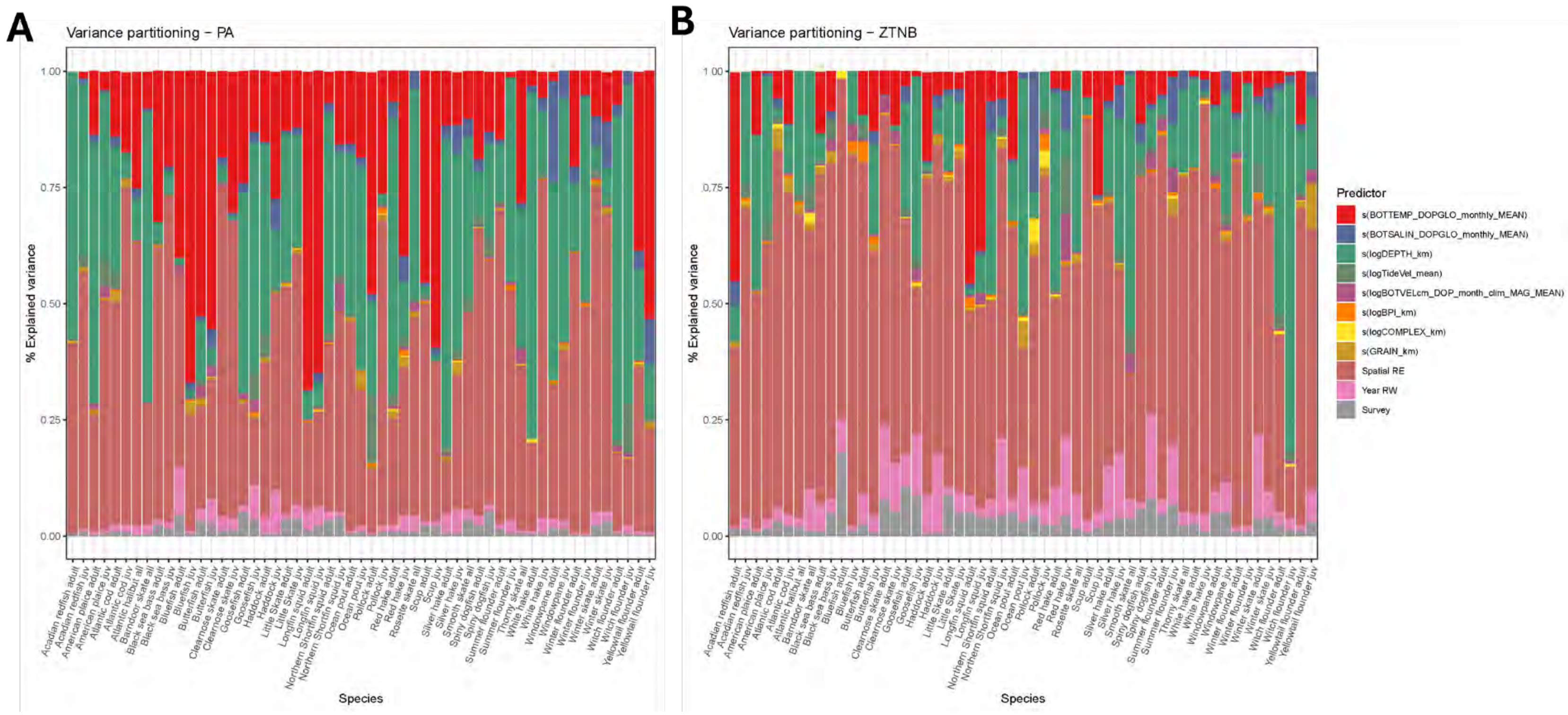

Figure 4. Variance partitioning for pelagic species distribution models using a joint hurdle approach. (A) Presence-absence component of the hurdle model. (B) Zero-truncated negative binomial component of the hurdle model.

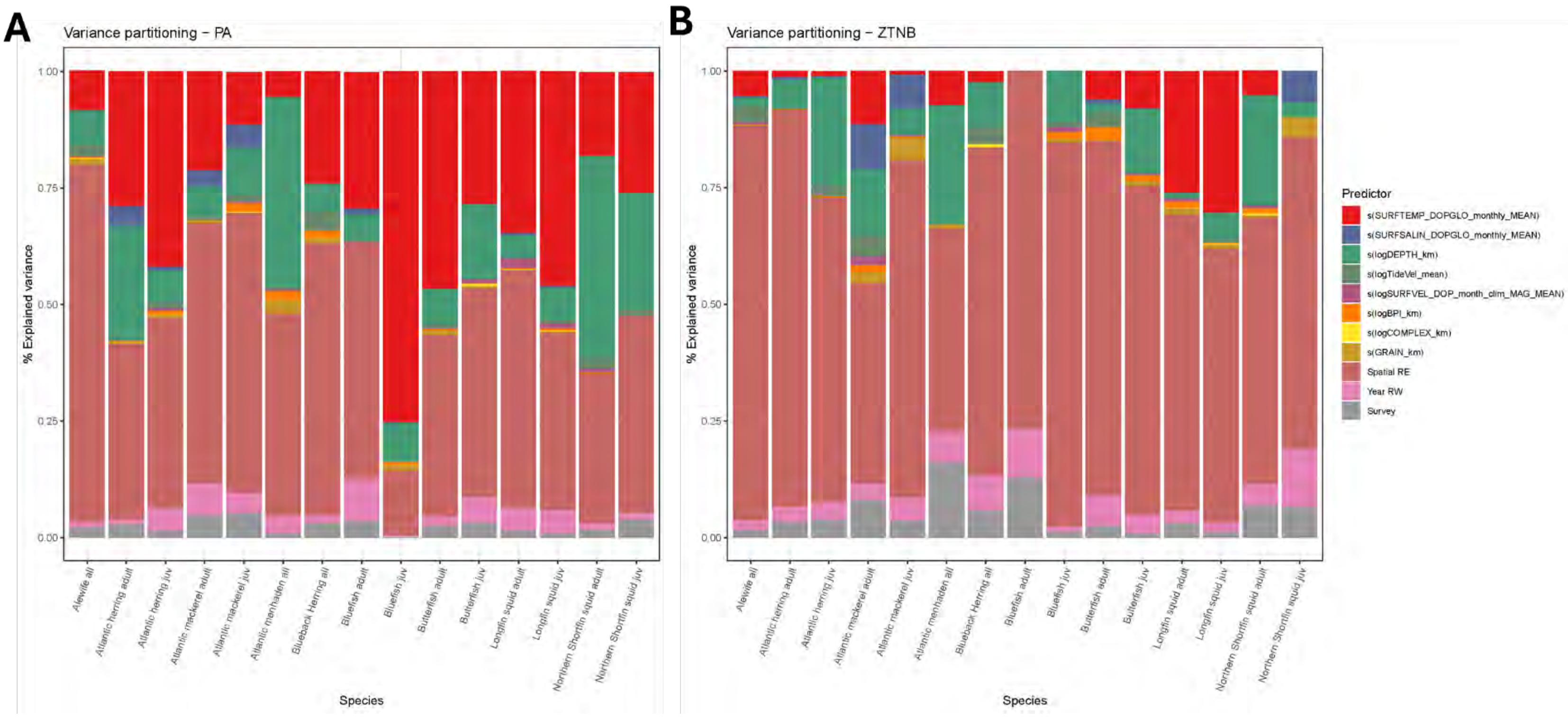

4.2 SMOOTH TERMS: SPECIES-SPECIFIC RELATIONSHIPS

4.2.1 Acadian redfish

Figure 5. Smooth terms graphs depicting relationships between species counts and individual environmental covariates for juvenile Acadian redfish (*Sebastes fasciatus*). (A) Presence-absence component. (B) Zero-truncated negative binomial (count) component of the joint hurdle species distribution model.

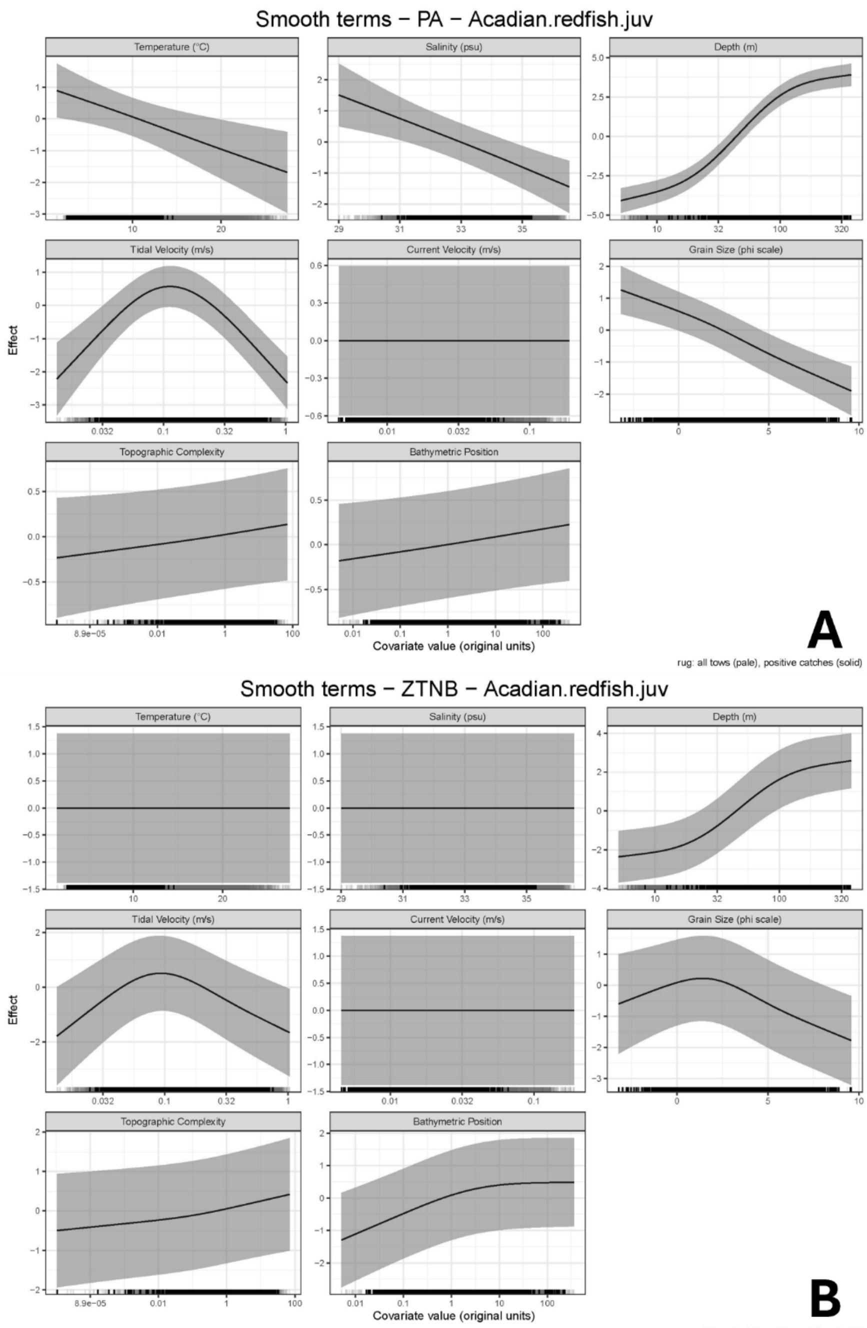

Figure 6. Smooth terms graphs depicting relationships between species counts and individual environmental covariates for adult Acadian redfish (*Sebastes fasciatus*). (A) Presence-absence component. (B) Zero-truncated negative binomial component of the joint hurdle species distribution model.

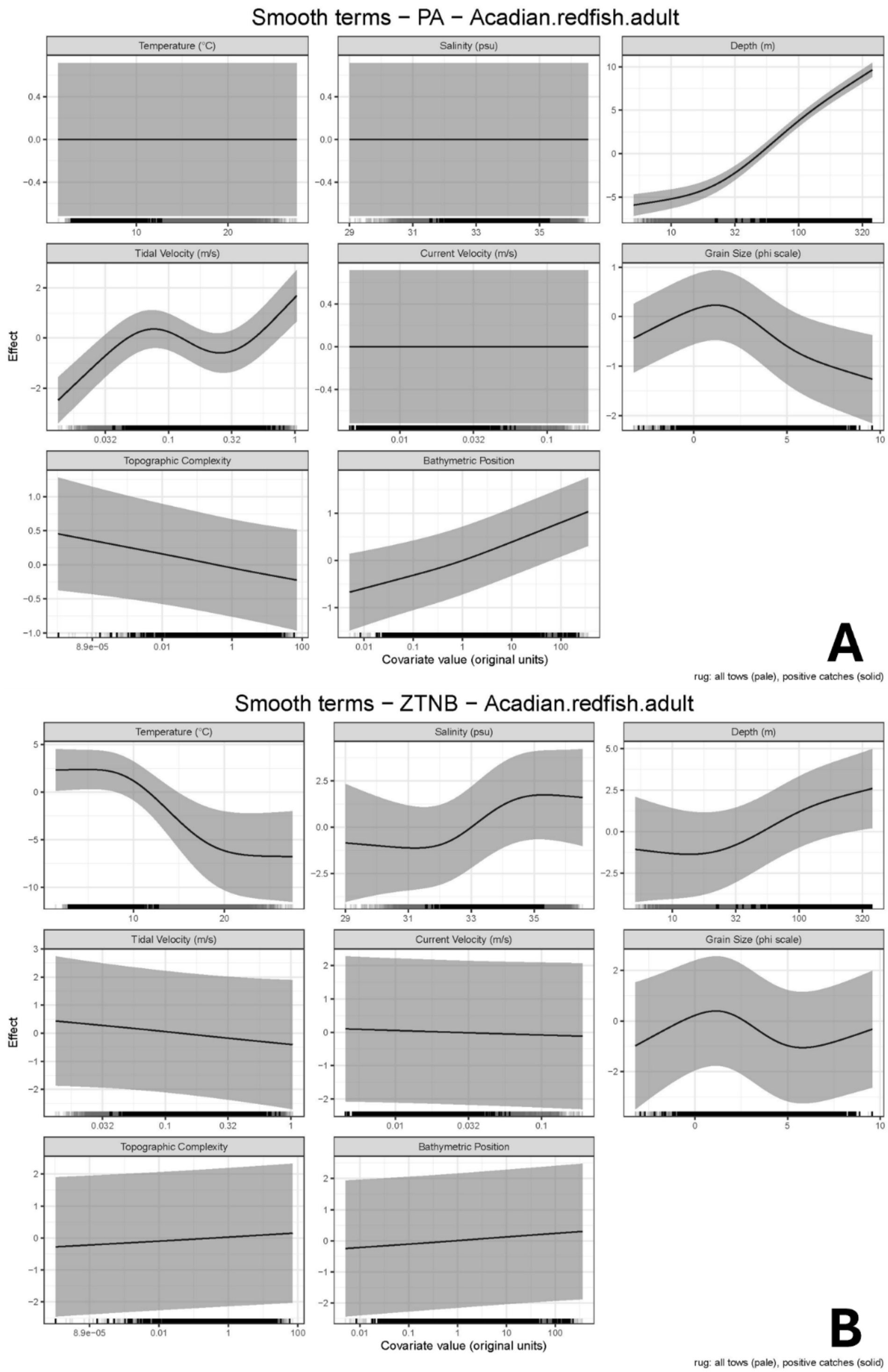

4.2.2 American plaice

Figure 7. Smooth terms graphs depicting relationships between species counts and individual environmental covariates for juvenile American plaice (*Hippoglossoides platessoides*). (A) Presence-absence component. (B) Zero-truncated negative binomial component of the joint hurdle species distribution model.

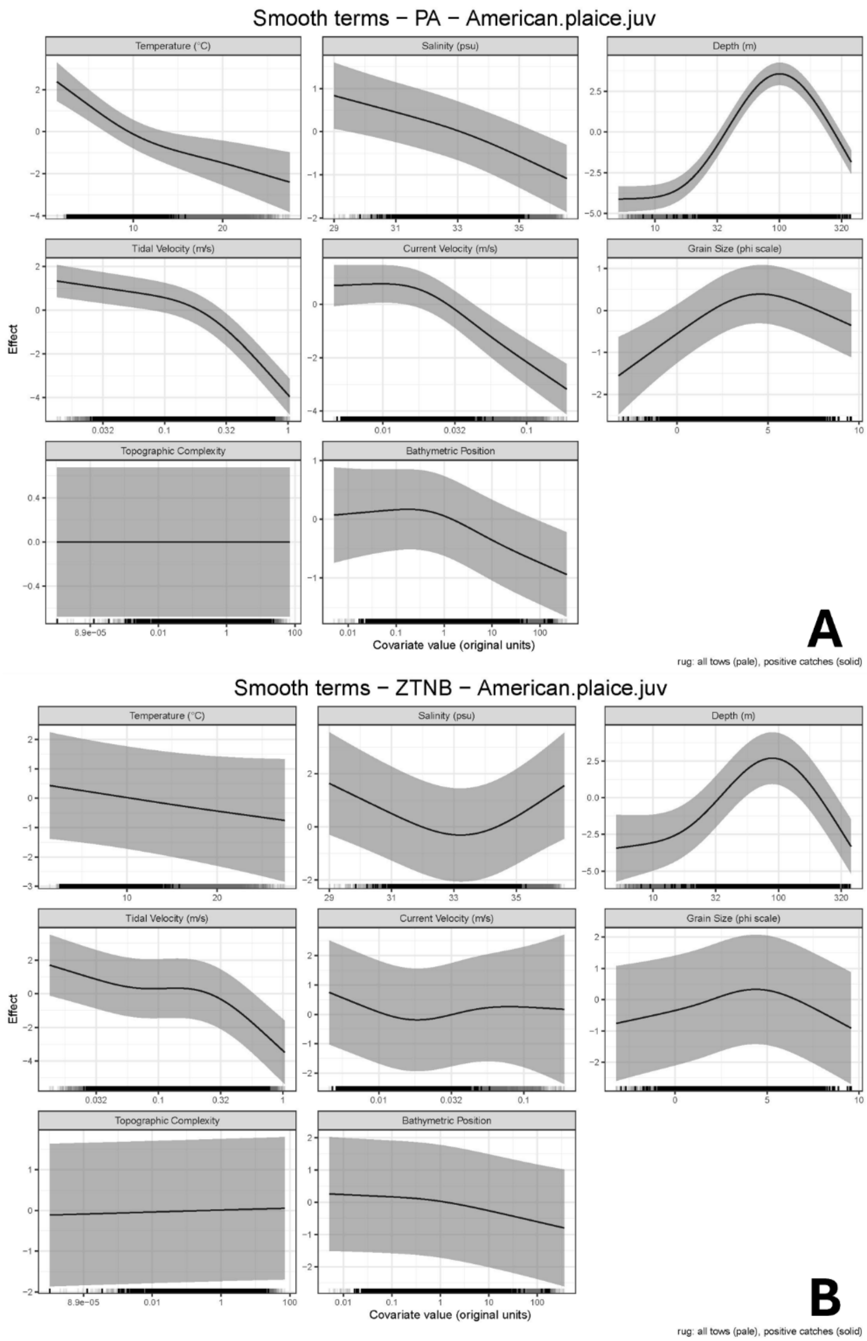

Figure 8. Smooth terms graphs depicting relationships between species counts and individual environmental covariates for adult American plaice (*Hippoglossoides platessoides*). (A) Presence-absence component. (B) Zero-truncated negative binomial component of the joint hurdle species distribution model.

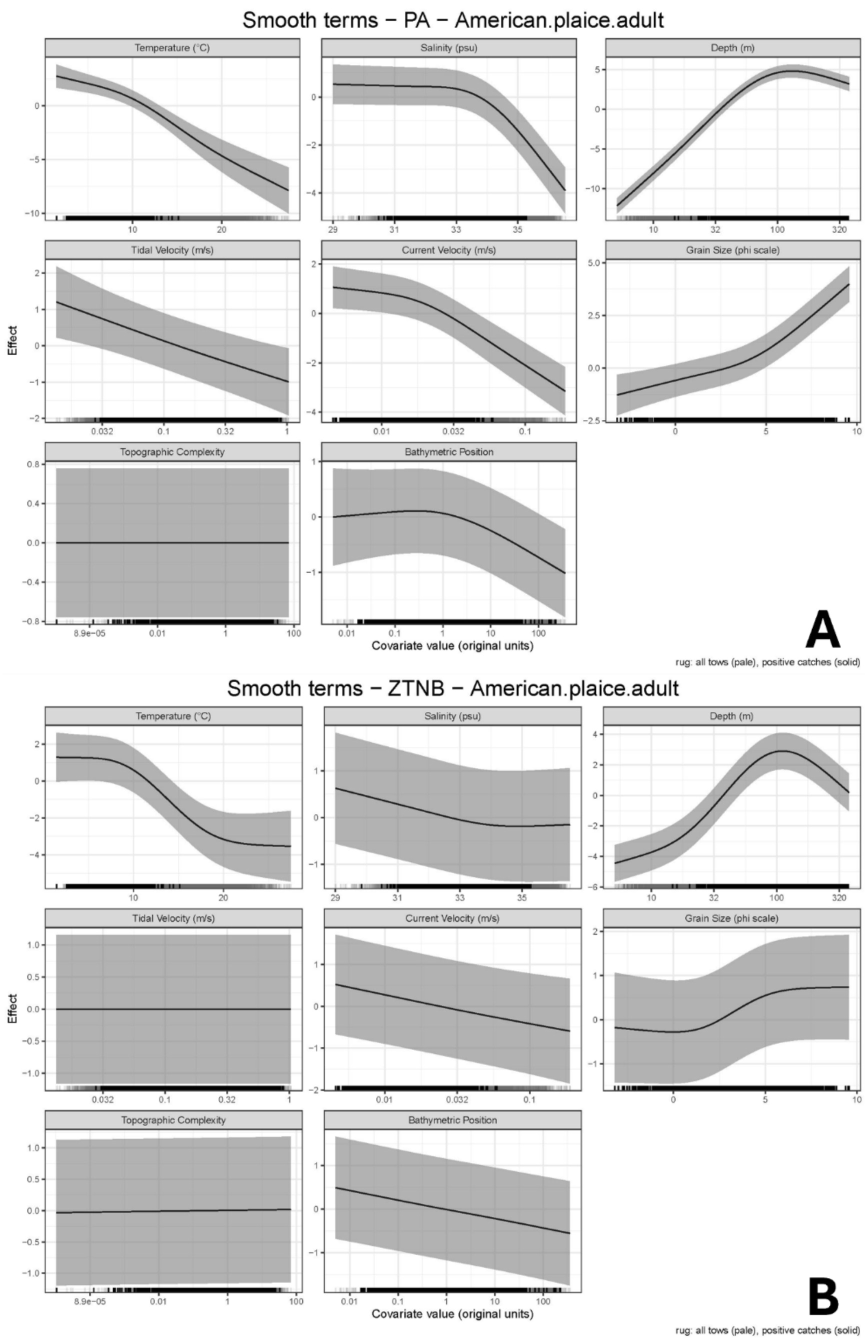

4.2.3 Atlantic halibut

Figure 9. Smooth terms graphs depicting relationships between species counts and individual environmental covariates for juvenile Atlantic halibut (*Hippoglossus hippoglossus*).

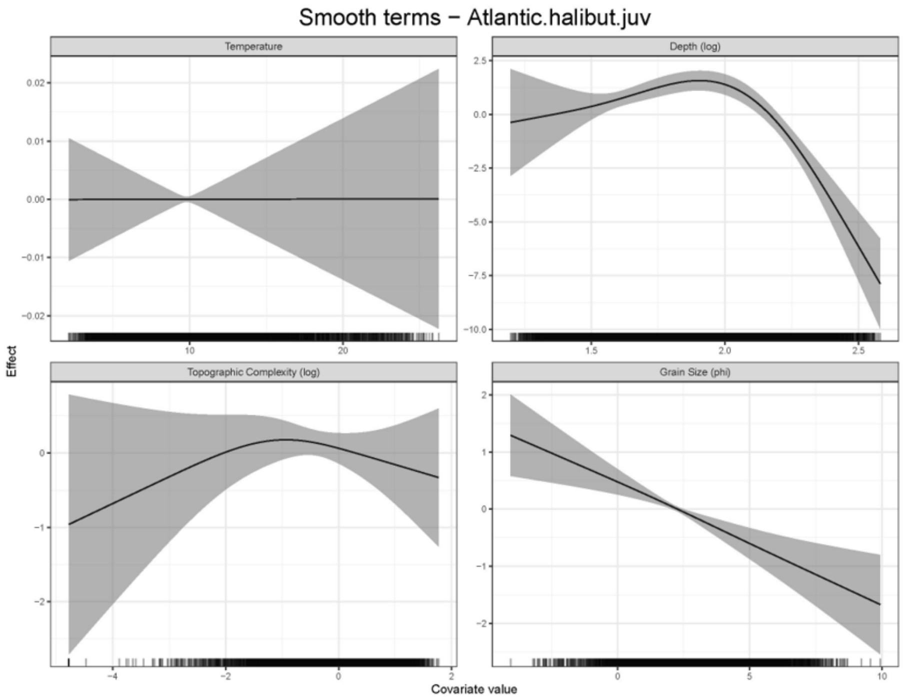

Figure 10. Smooth terms graphs depicting relationships between species counts and individual environmental covariates for adult Atlantic halibut (*Hippoglossus hippoglossus*).

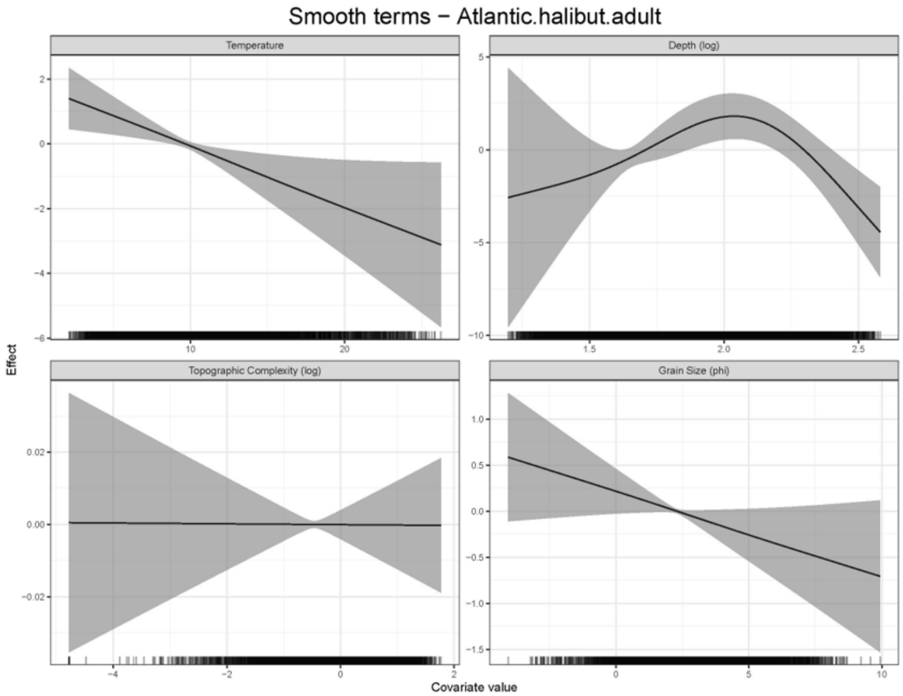

4.2.4 Atlantic sea scallop

Figure 11. Quadratic terms graphs depicting relationships between species counts and individual environmental covariates for adult Atlantic sea scallop (*Placopecten magellanicus*).

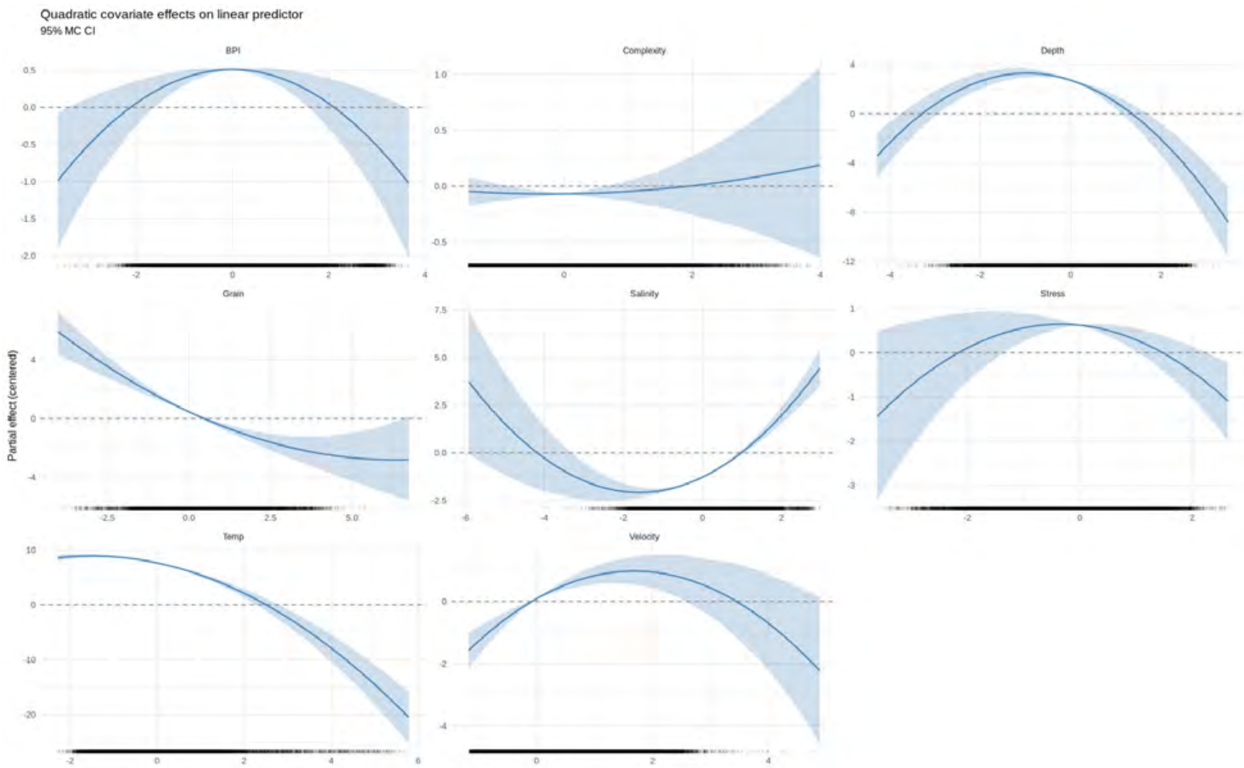

4.2.5 Atlantic wolffish

Figure 12. Smooth terms graphs depicting relationships between species counts and individual environmental covariates for juvenile Atlantic wolffish (*Anarhichas lupus*).

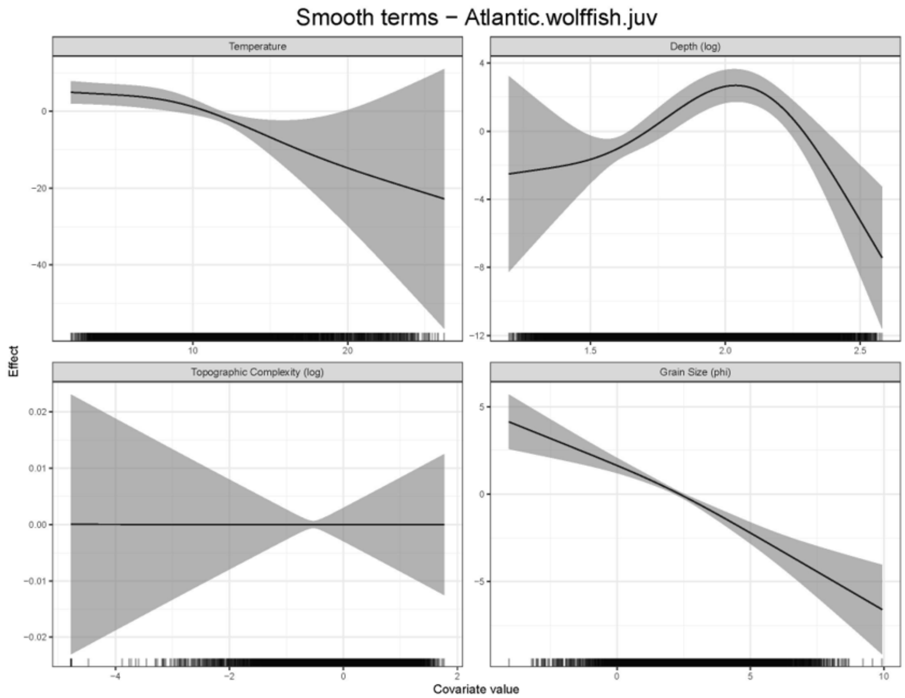

Figure 13. Smooth terms graphs depicting relationships between species counts and individual environmental covariates for adult Atlantic wolffish (*Anarhichas lupus*). (A) Presence-absence component. (B) Zero-truncated negative binomial component of the joint hurdle species distribution model.

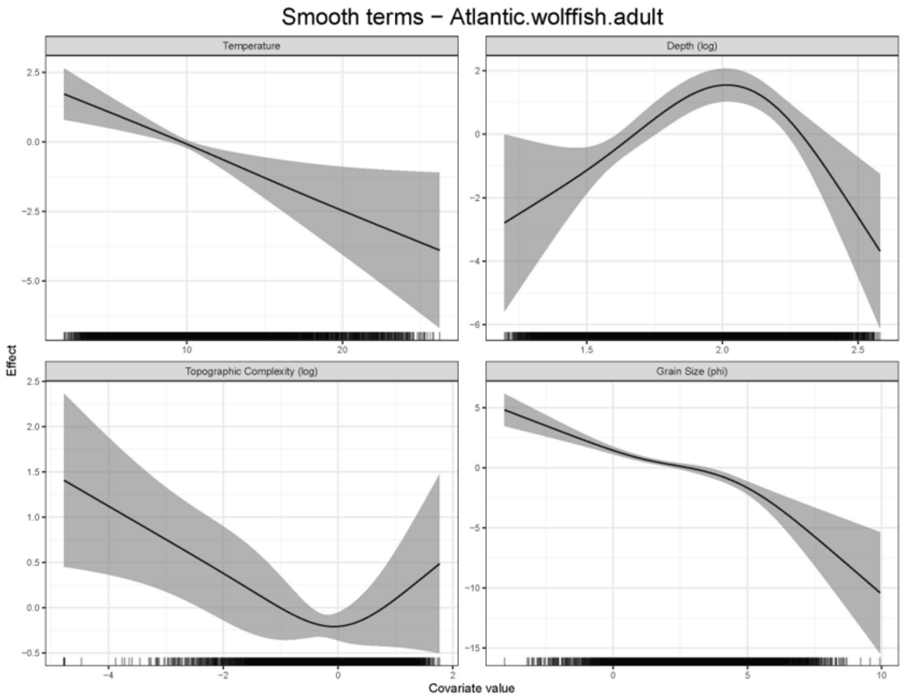

4.2.6 Haddock

Figure 14. Smooth terms graphs depicting relationships between species counts and individual environmental covariates for juvenile haddock (*Melanogrammus aeglefinus*). (A) Presence-absence component. (B) Zero-truncated negative binomial component of the joint hurdle species distribution model.

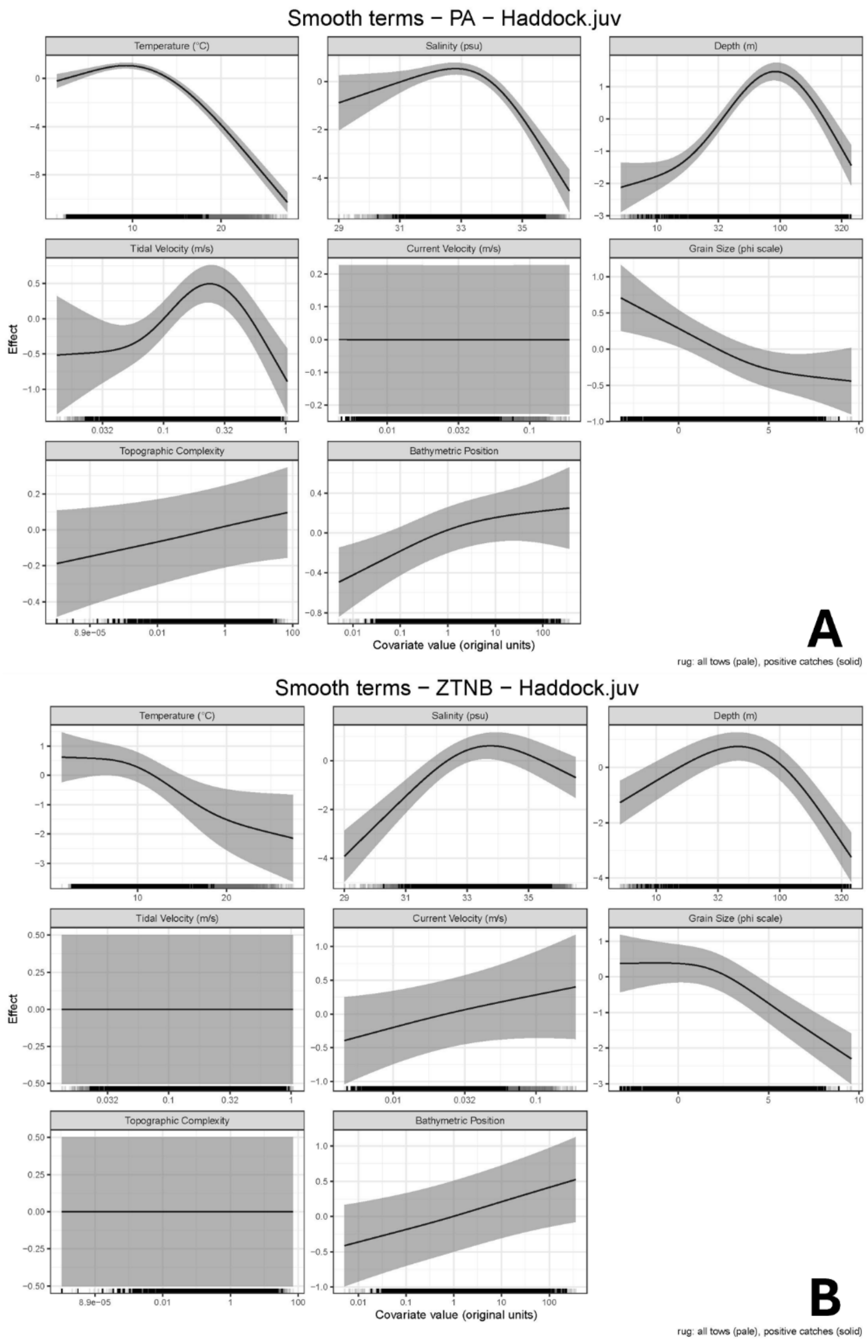

Figure 15. Smooth terms graphs depicting relationships between species counts and individual environmental covariates for adult haddock (*Melanogrammus aeglefinus*). (A) Presence-absence component. (B) Zero-truncated negative binomial component of the joint hurdle species distribution model.

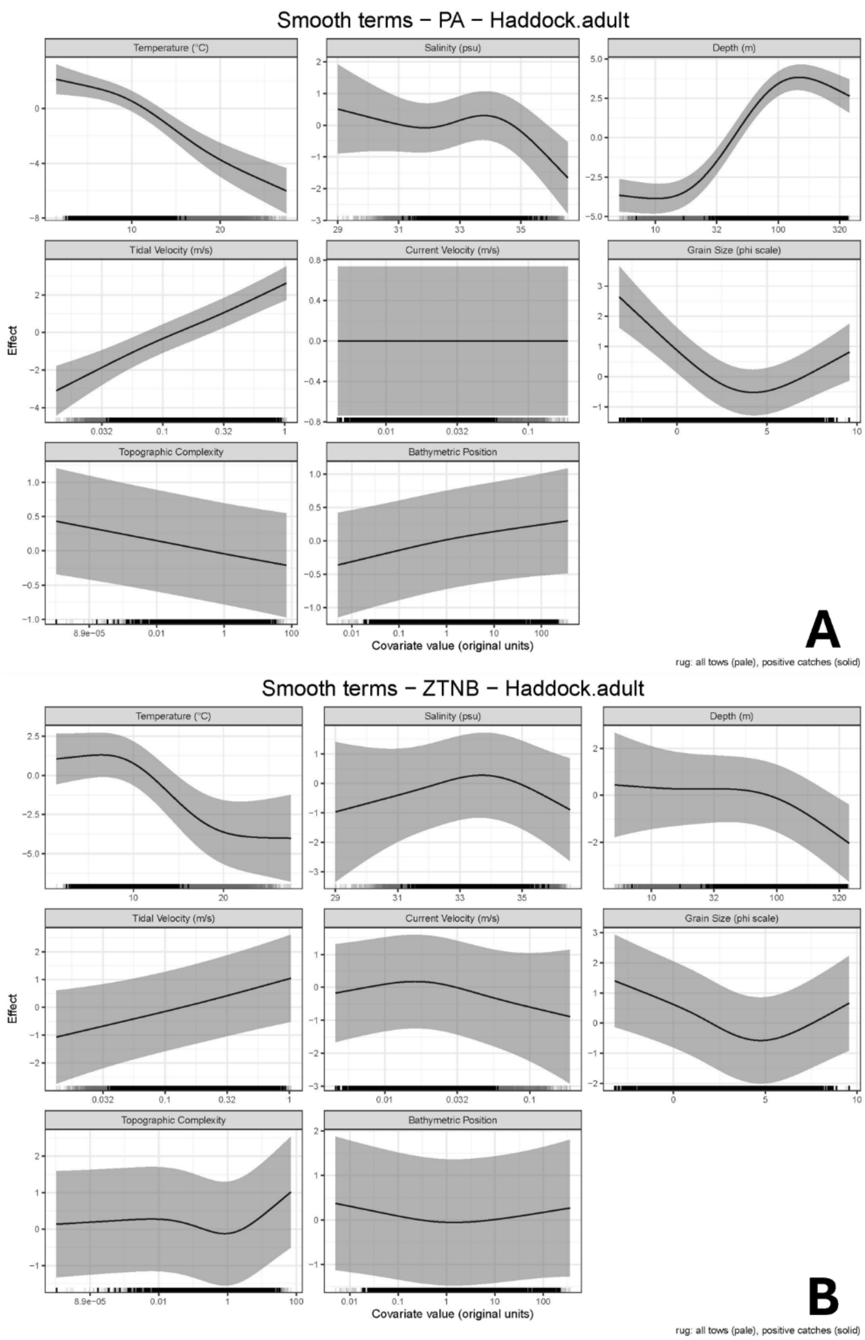

4.2.7 Ocean pout

Figure 16. Smooth terms graphs depicting relationships between species counts and individual environmental covariates for pooled juvenile ocean pout (*Macrozoarces americanus*). (A) Presence-absence component. (B) Zero-truncated negative binomial component of the joint hurdle species distribution model.

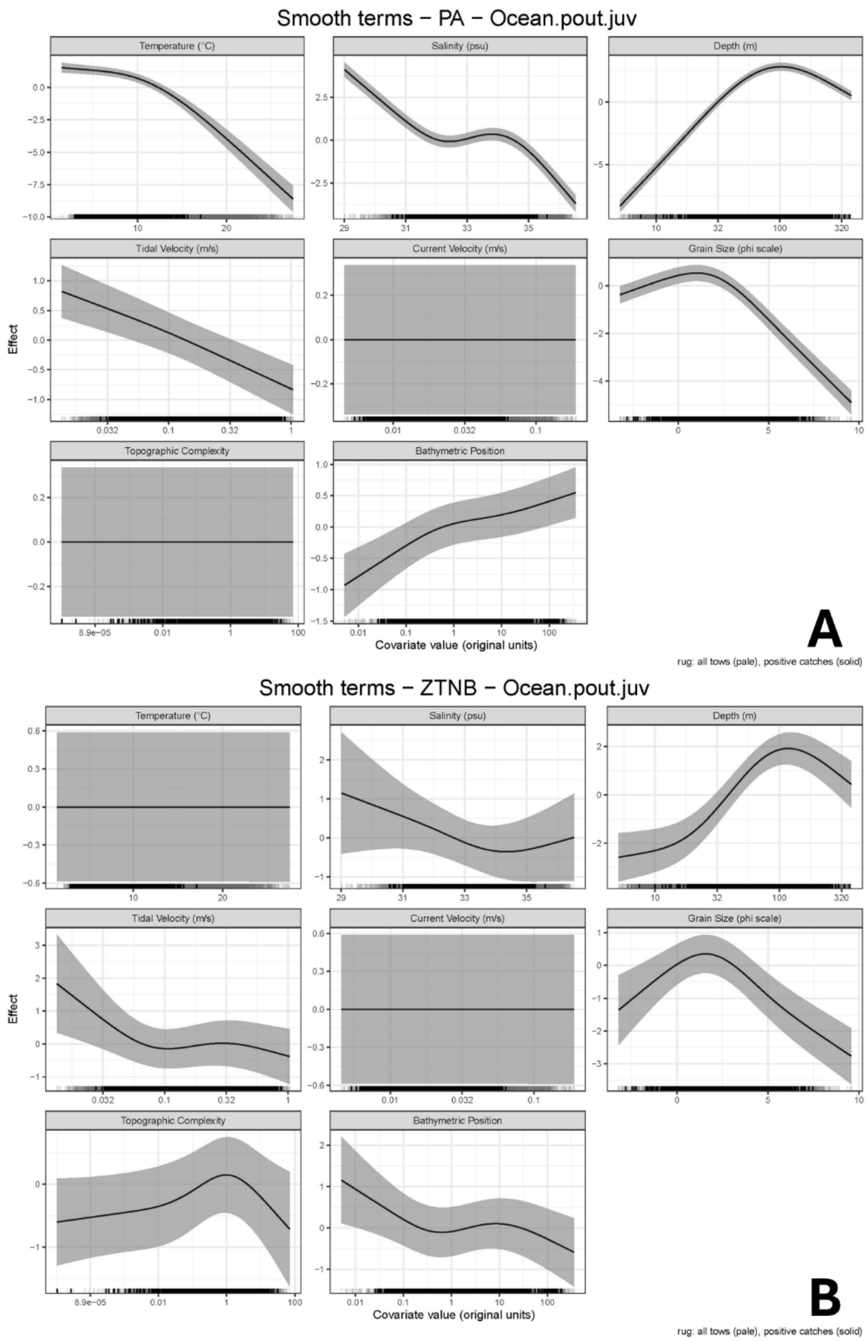

Figure 17. Smooth terms graphs depicting relationships between species counts and individual environmental covariates for adult ocean pout (*Macrozoarces americanus*). (A) Presence-absence component. (B) Zero-truncated negative binomial (count) component of the joint hurdle species distribution model.

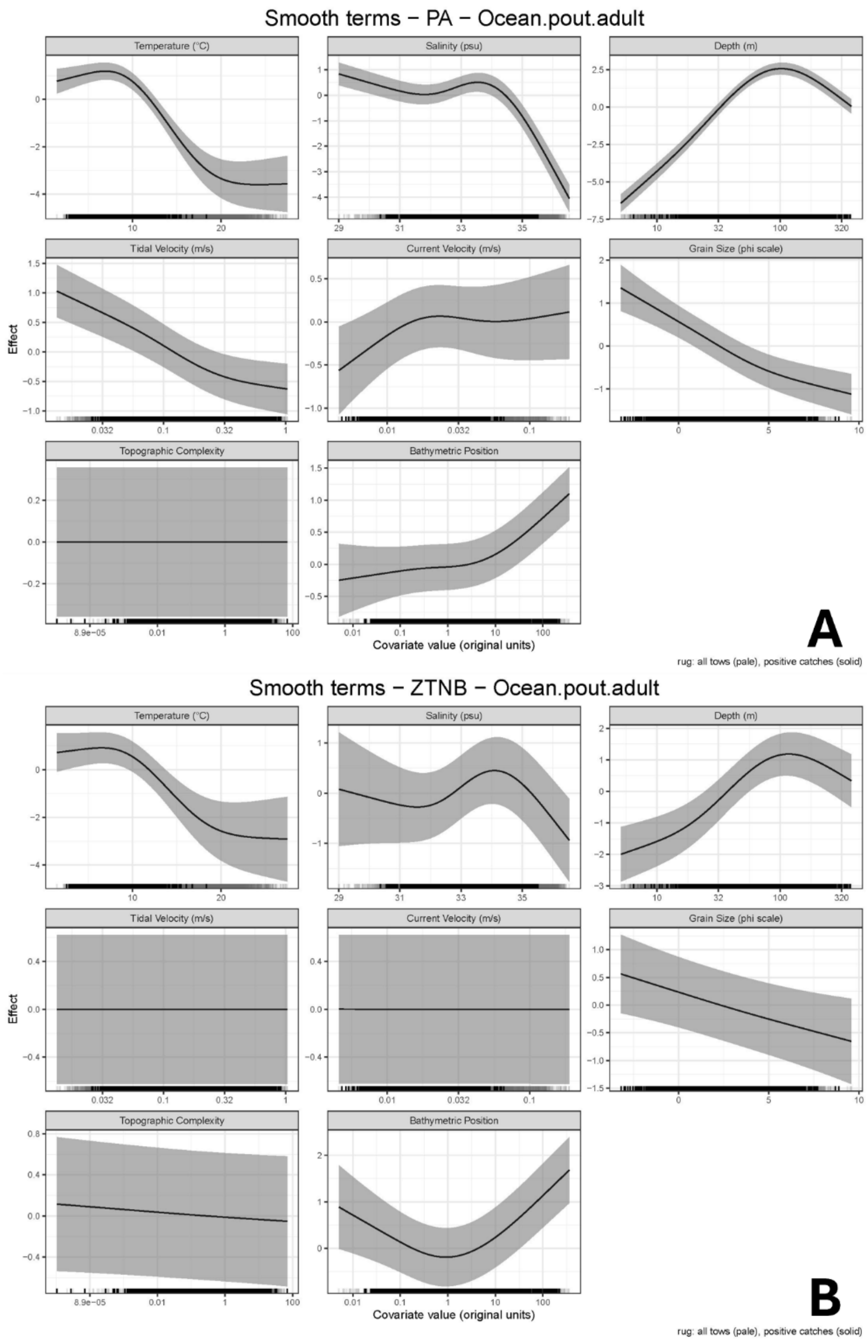

4.2.8 Offshore hake

Figure 18. Smooth terms graphs depicting relationships between species counts and individual environmental covariates for pooled juvenile offshore hake (*Merluccius albidus*).

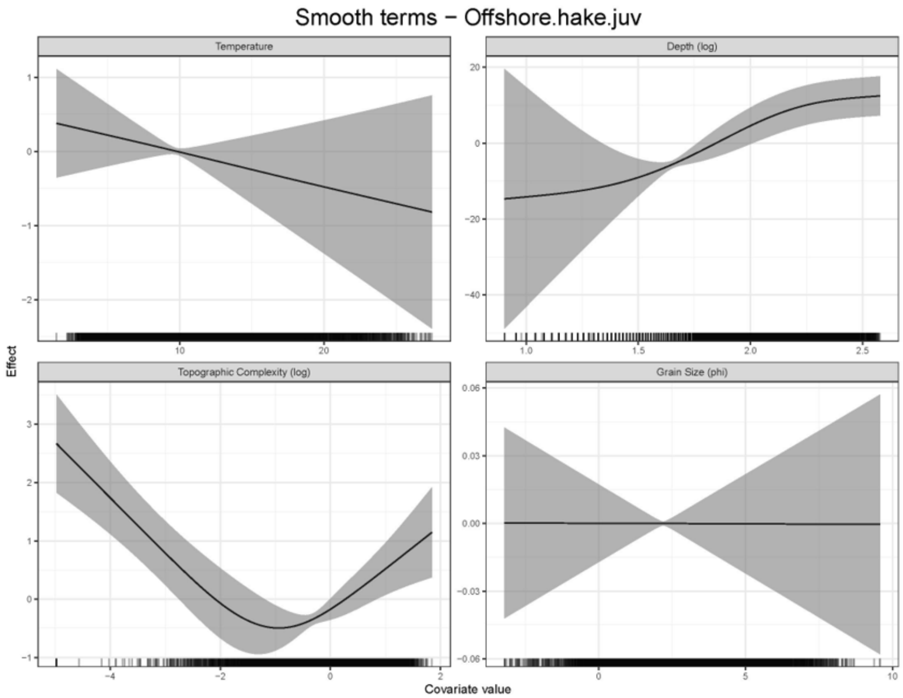

Figure 19. Smooth terms graphs depicting relationships between species counts and individual environmental covariates for adult offshore hake (*Merluccius albidus*).

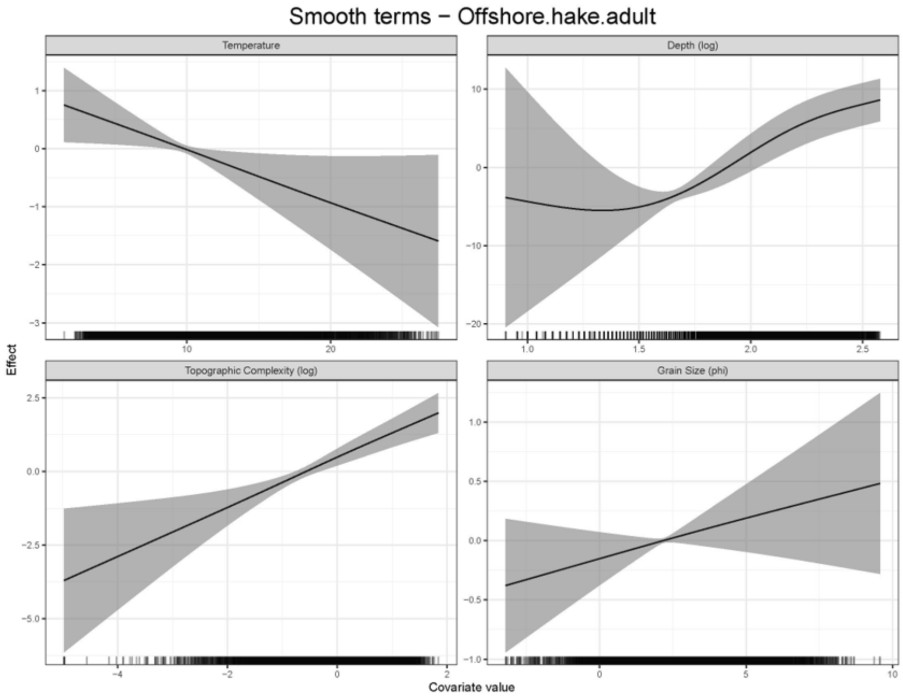

4.2.9 Pollock

Figure 20. Smooth terms graphs depicting relationships between species counts and individual environmental covariates for pooled juvenile pollock (*Pollachius virens*). (A) Presence-absence component. (B) Zero-truncated negative binomial component of the joint hurdle species distribution model.

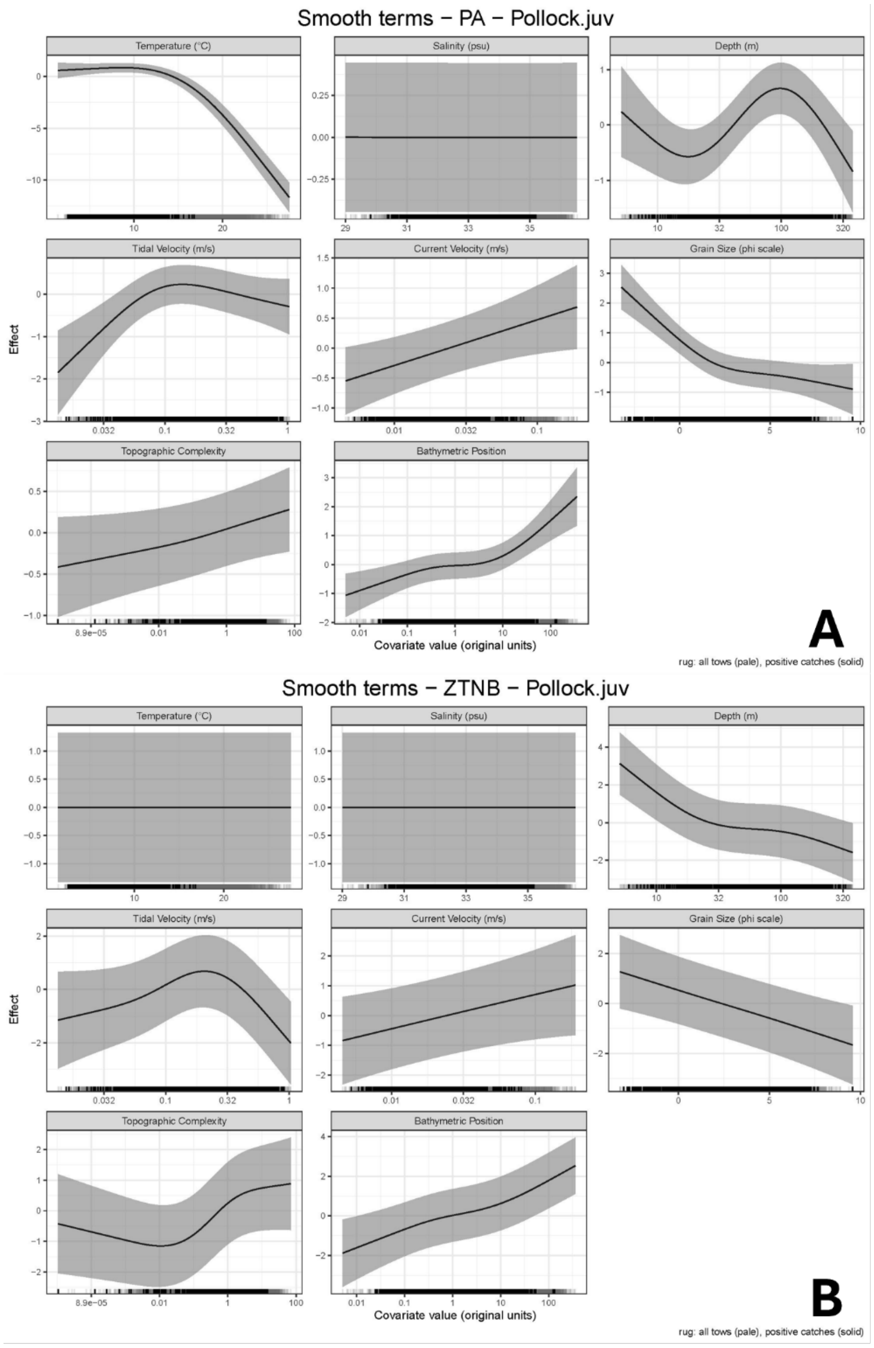

Figure 21. Smooth terms graphs depicting relationships between species counts and individual environmental covariates for adult pollock (*Pollachius virens*). (A) Presence-absence component. (B) Zero-truncated negative binomial (count) component of the joint hurdle species distribution model.

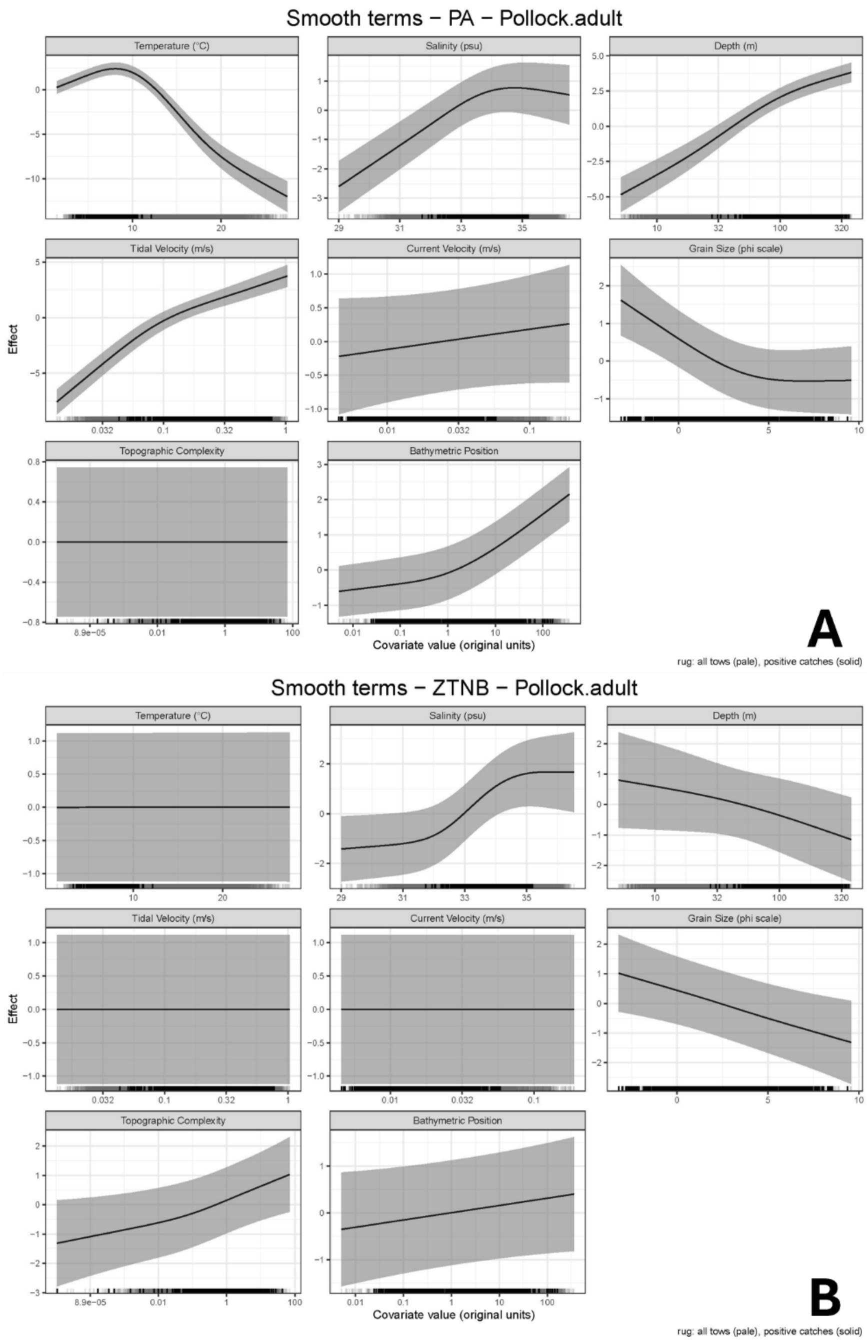

4.2.10 Red hake

Figure 22. Smooth terms graphs depicting relationships between species counts and individual environmental covariates for juvenile red hake (*Urophycis chuss*). (A) Presence-absence component. (B) Zero-truncated negative binomial component of the joint hurdle species distribution model.

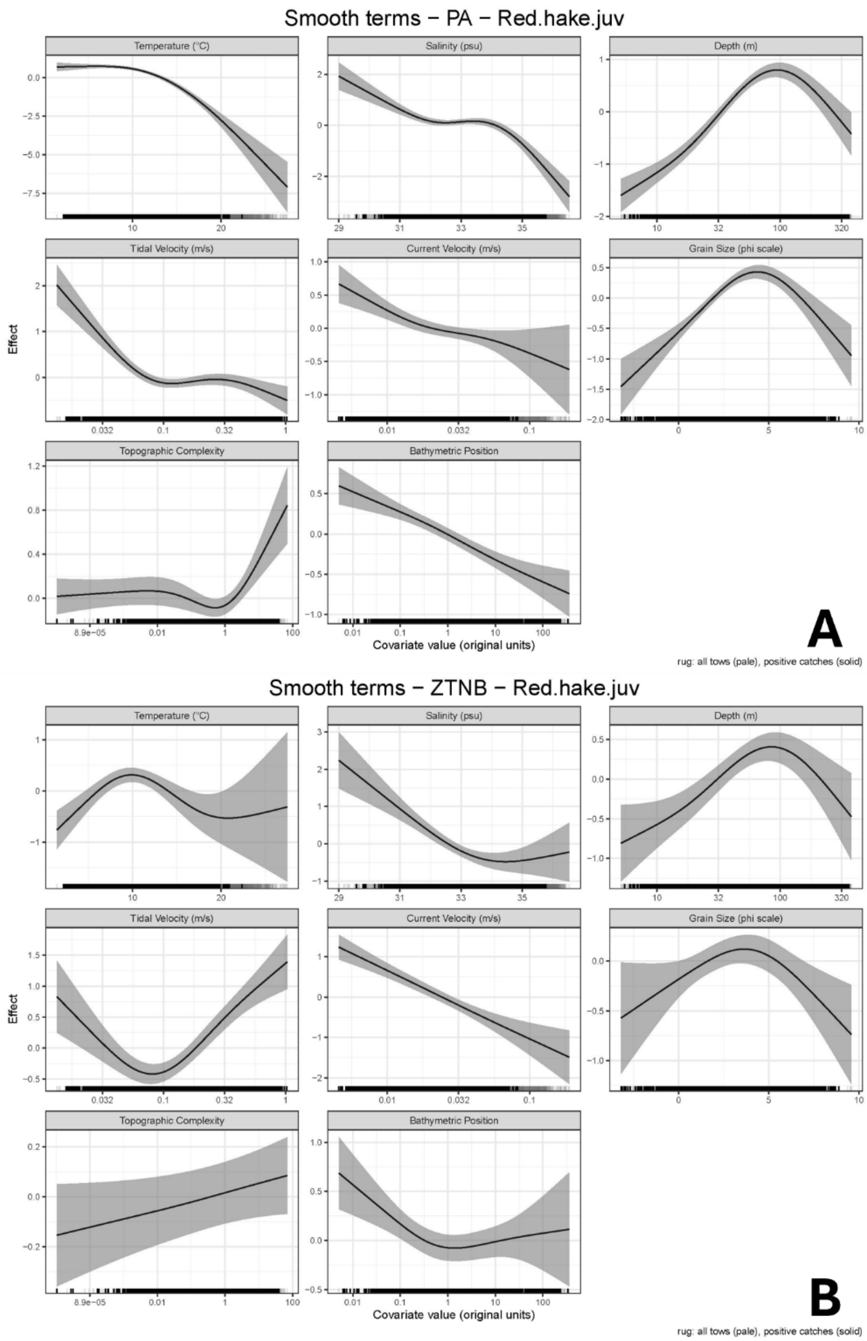

Figure 23. Smooth terms graphs depicting relationships between species counts and individual environmental covariates for adult red hake (*Urophycis chuss*). (A) Presence-absence component. (B) Zero-truncated negative binomial component of the joint hurdle species distribution model.

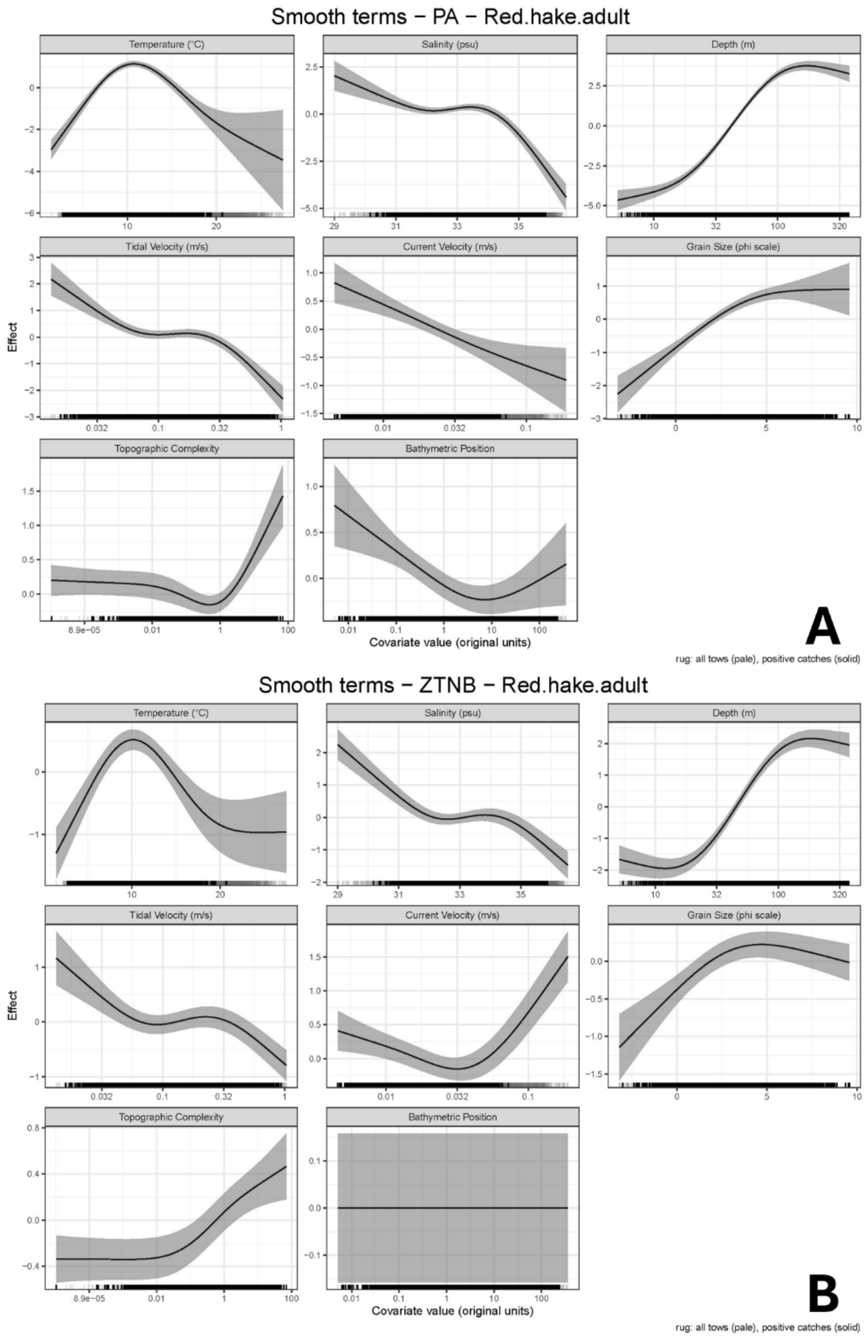

4.2.11 Silver hake

Figure 24. Smooth terms graphs depicting relationships between species counts and individual environmental covariates for juvenile silver hake (*Merluccius bilinearis*). (A) Presence-absence component. (B) Zero-truncated negative binomial (count) component of the joint hurdle species distribution model.

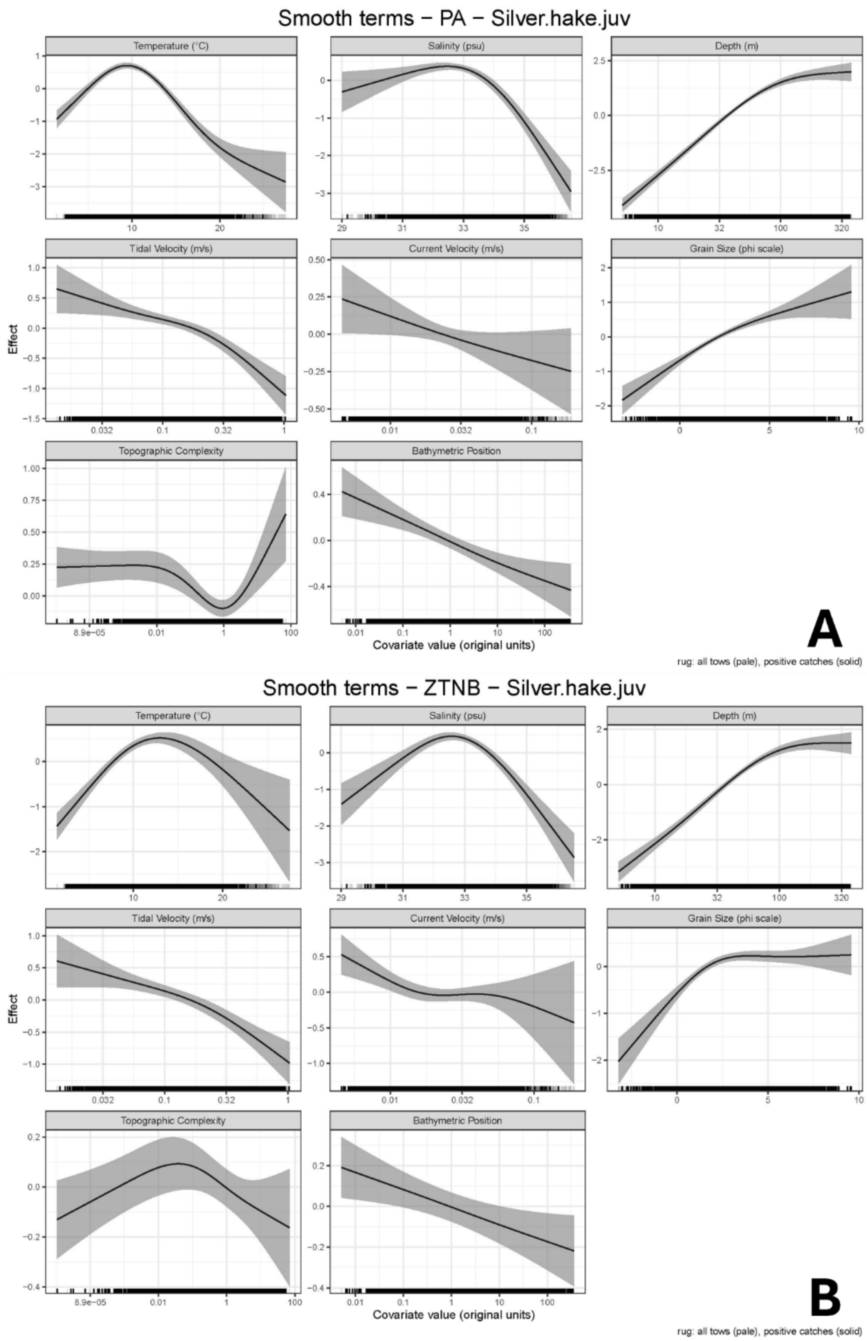

Figure 25. Smooth terms graphs depicting relationships between species counts and individual environmental covariates for adult silver hake (*Merluccius bilinearis*). (A) Presence-absence component. (B) Zero-truncated negative binomial (count) component of the joint hurdle species distribution model.

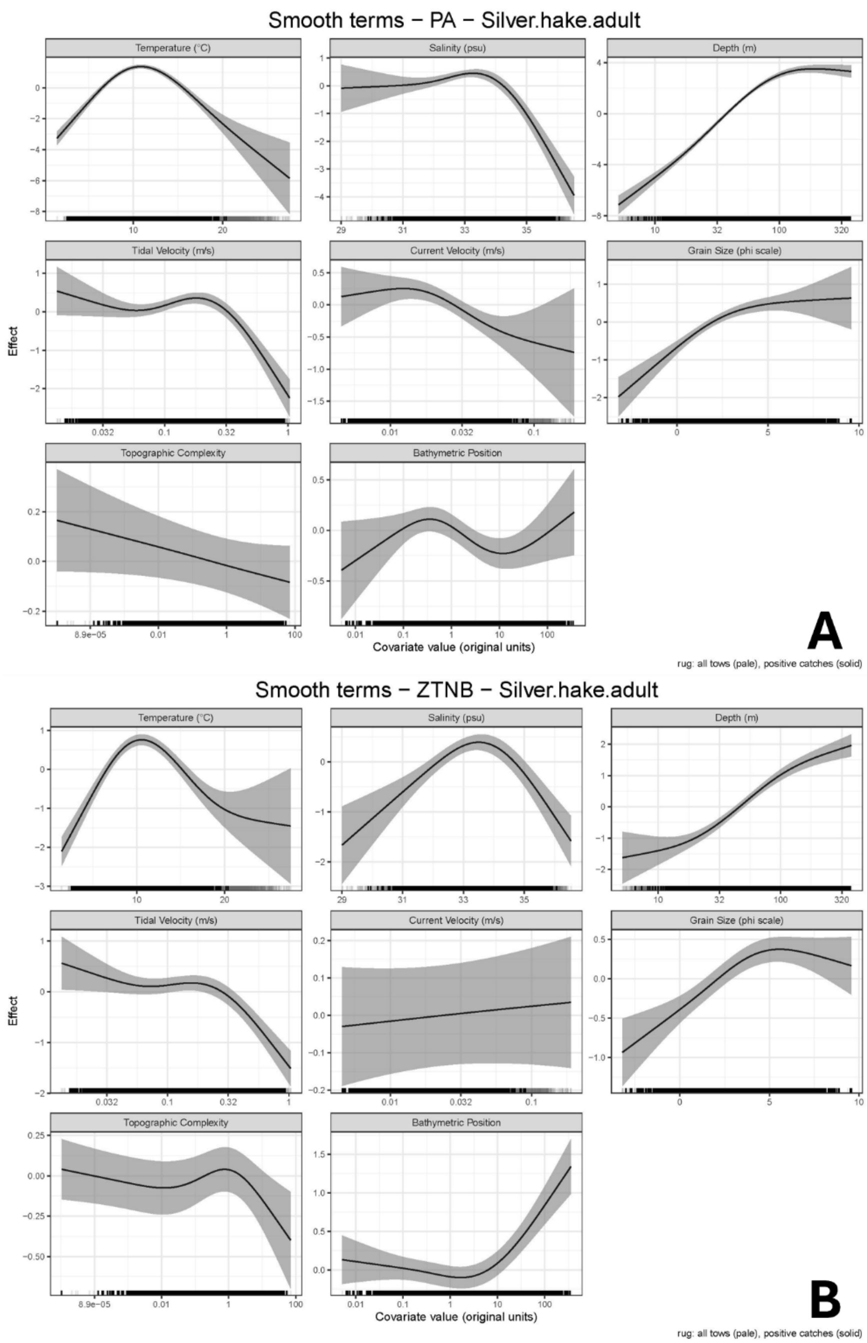

4.2.12 White hake

Figure 26. Smooth terms graphs depicting relationships between species counts and individual environmental covariates for juvenile white hake (*Urophycis tenuis*). (A) Presence-absence component. (B) Zero-truncated negative binomial (count) component of the joint hurdle species distribution model.

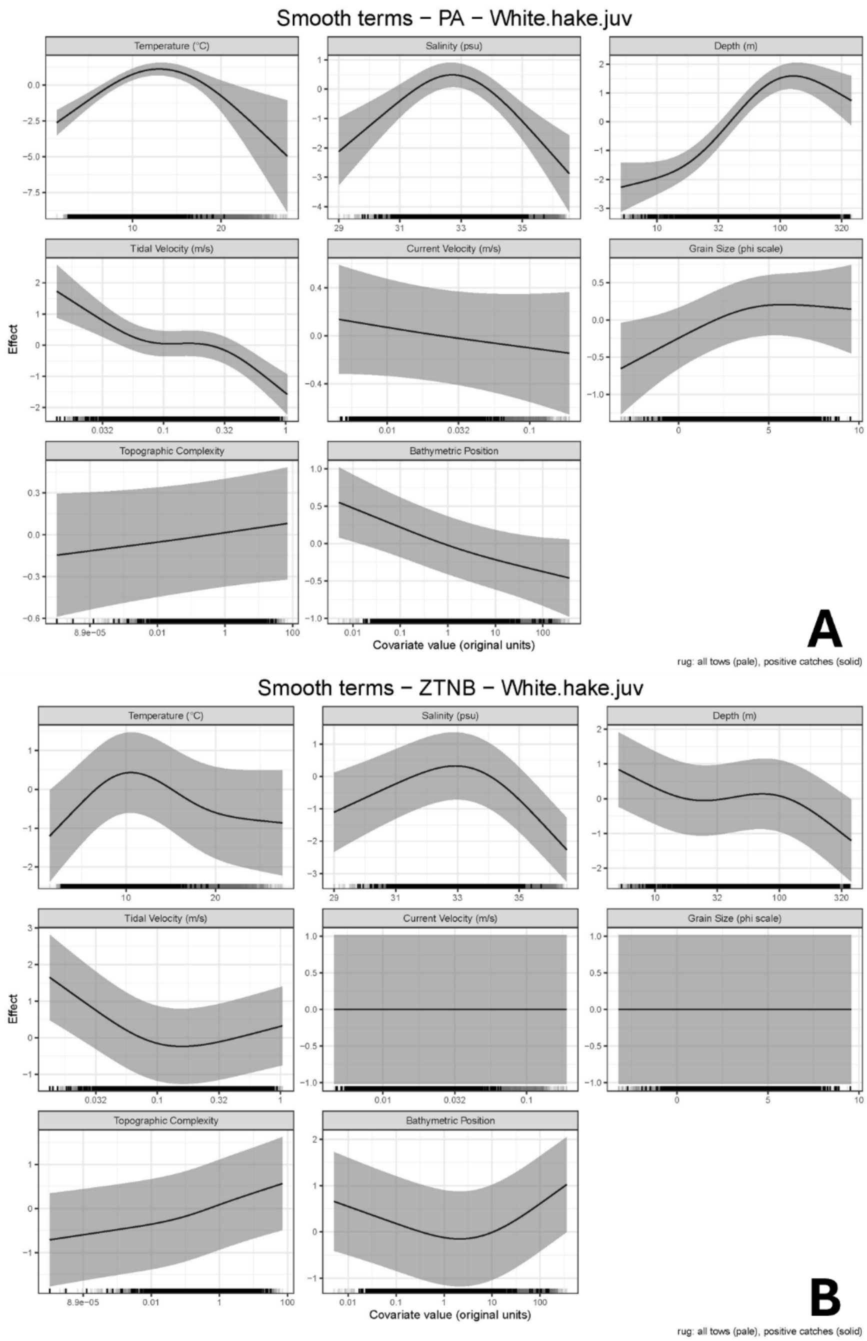

Figure 27. Smooth terms graphs depicting relationships between species counts and individual environmental covariates for adult white hake (*Urophycis tenuis*). (A) Presence-absence component. (B) Zero-truncated negative binomial (count) component of the joint hurdle species distribution model.

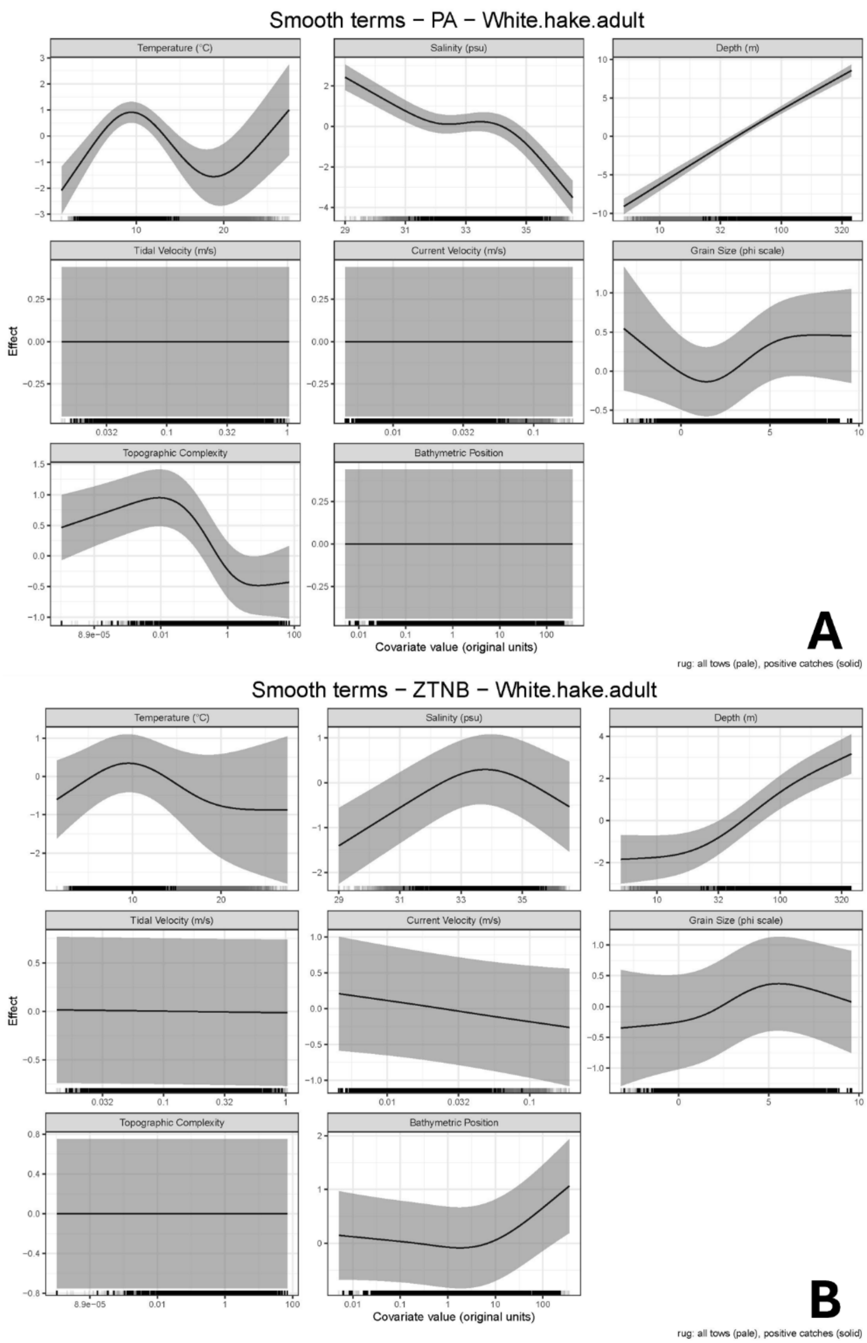

4.2.13 Windowpane flounder

Figure 28. Smooth terms graphs depicting relationships between species counts and individual environmental covariates for juvenile windowpane flounder (*Scophthalmus aquosus*). (A) Presence-absence component. (B) Zero-truncated negative binomial (count) component of the joint hurdle species distribution model.

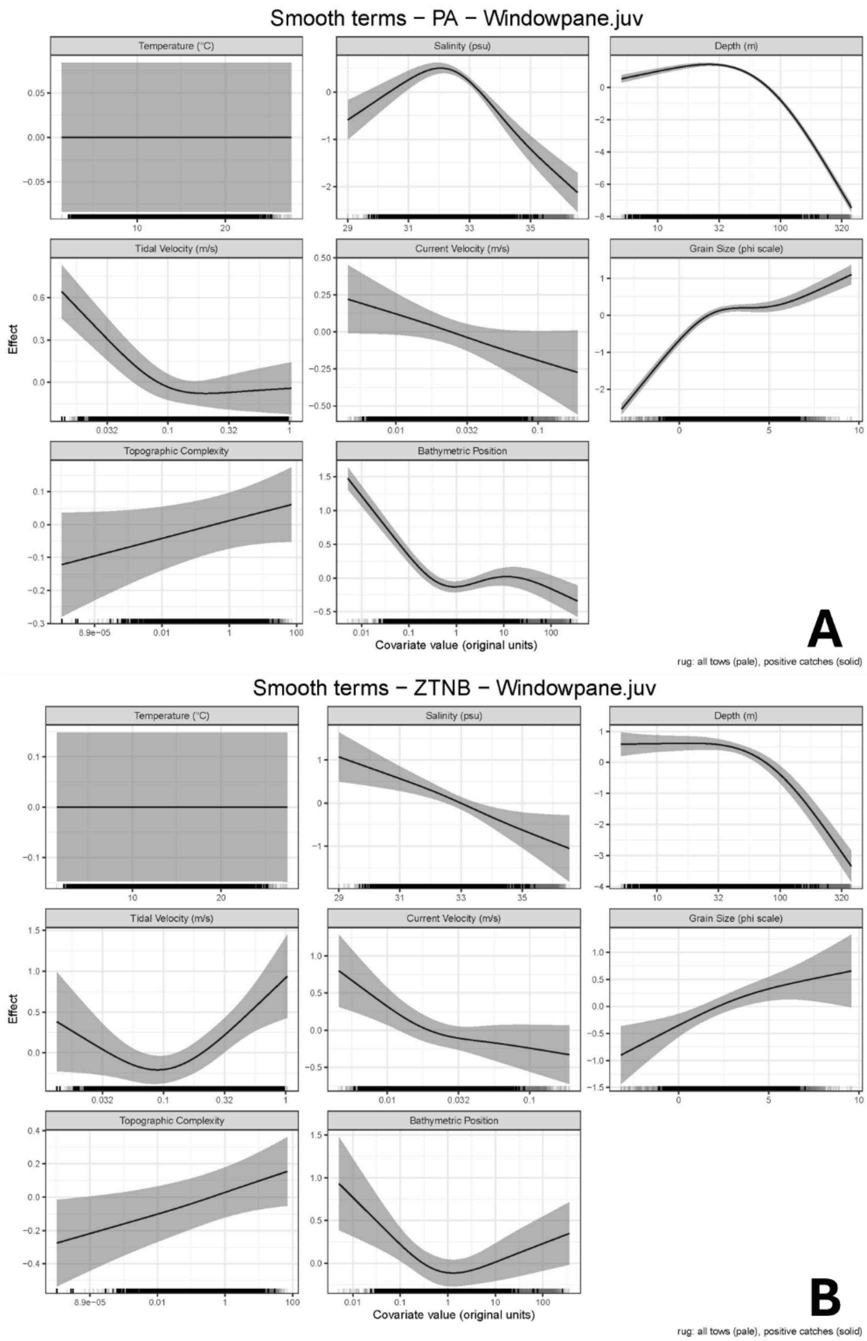

Figure 29. Smooth terms graphs depicting relationships between species counts and individual environmental covariates for adult windowpane flounder (*Scophthalmus aquosus*). (A) Presence-absence component. (B) Zero-truncated negative binomial (count) component of the joint hurdle species distribution model.

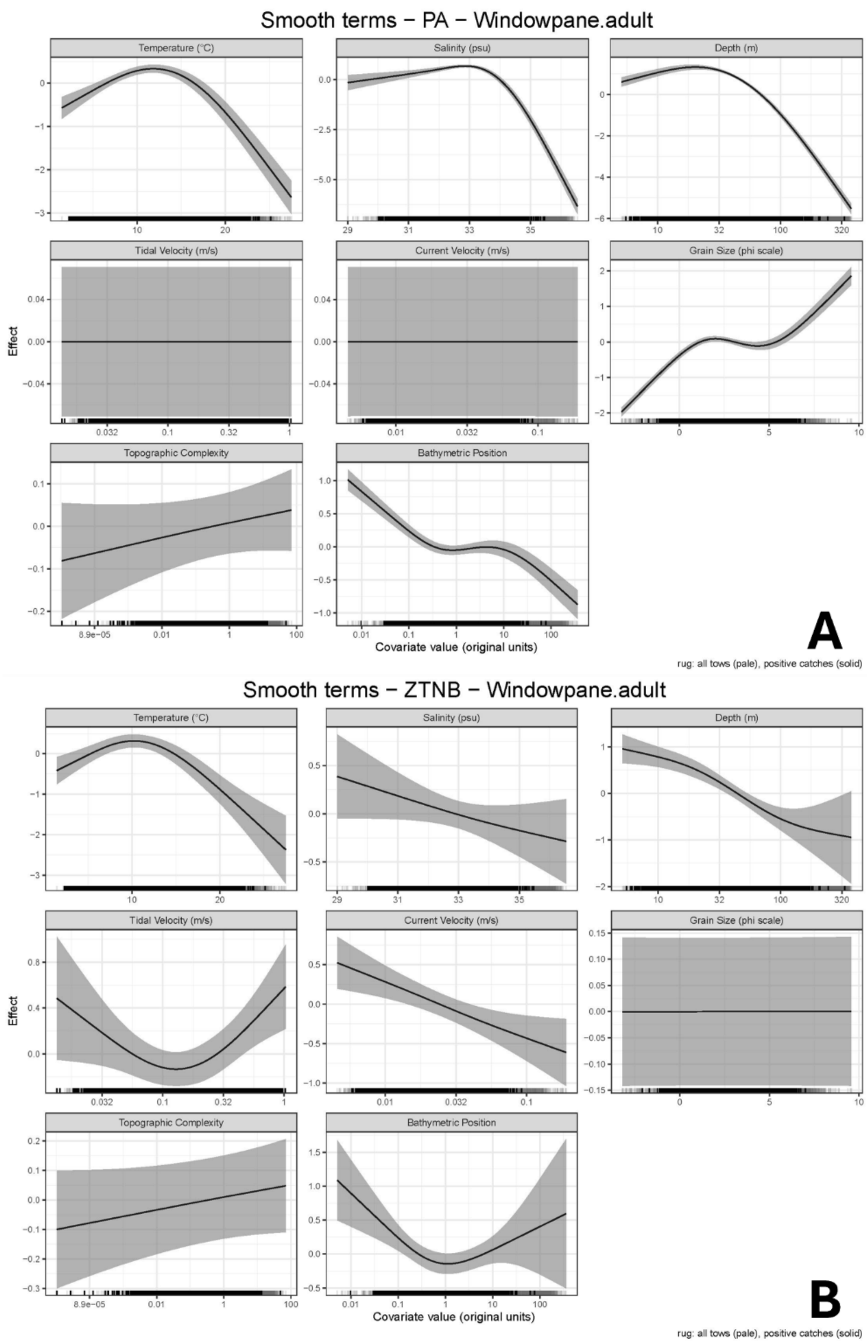

4.2.14 Winter flounder

Figure 30. Smooth terms graphs depicting relationships between species counts and individual environmental covariates for juvenile winter flounder (*Pleuronectes americanus*). (A) Presence-absence component. (B) Zero-truncated negative binomial (count) component of the joint hurdle species distribution model.

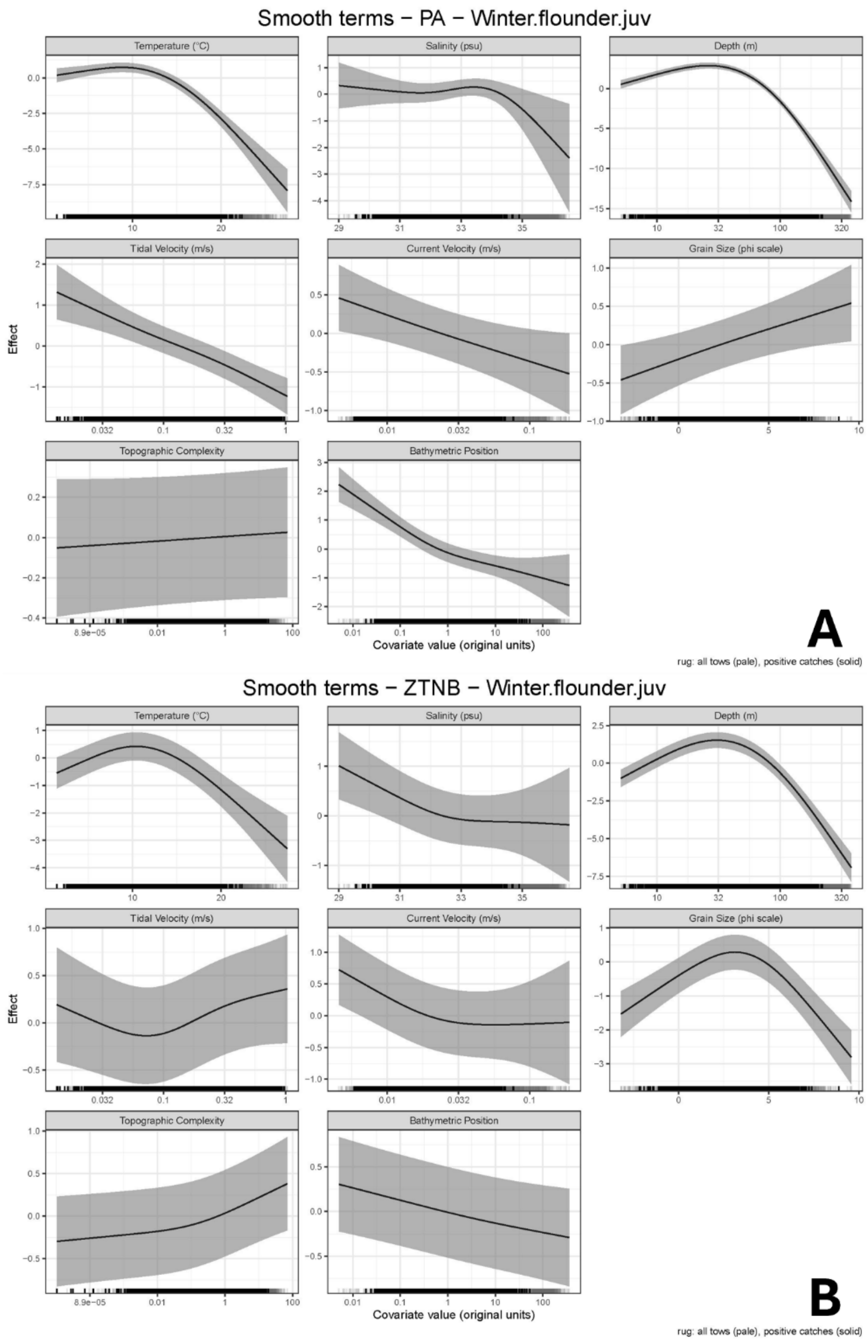

Figure 31. Smooth terms graphs depicting relationships between species counts and individual environmental covariates for adult winter flounder (*Pleuronectes americanus*). (A) Presence-absence component. (B) Zero-truncated negative binomial (count) component of the joint hurdle species distribution model.

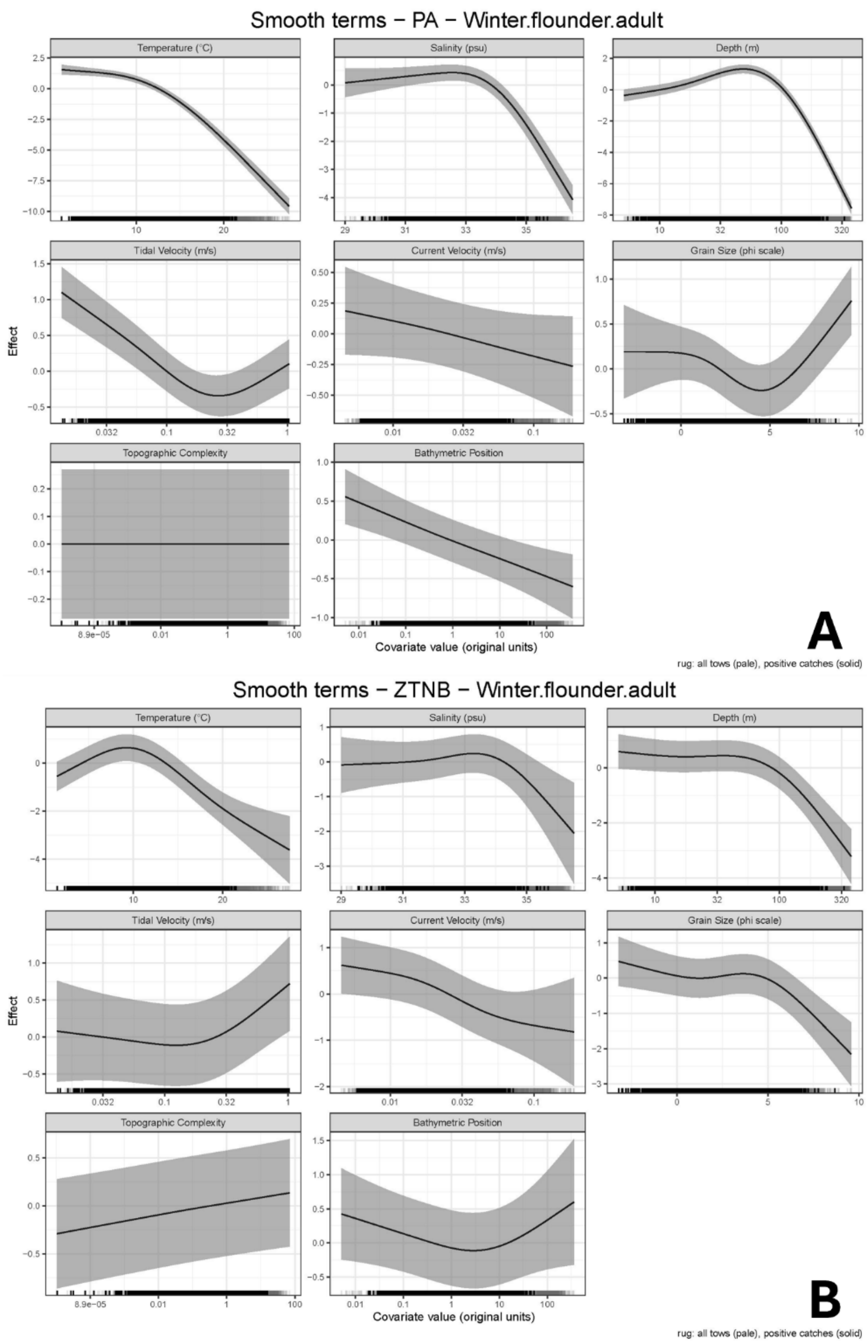

4.2.15 Witch flounder

Figure 32. Smooth terms graphs depicting relationships between species counts and individual environmental covariates for juvenile witch flounder (*Glyptocephalus cynoglossus*). (A) Presence-absence component. (B) Zero-truncated negative binomial (count) component of the joint hurdle species distribution model.

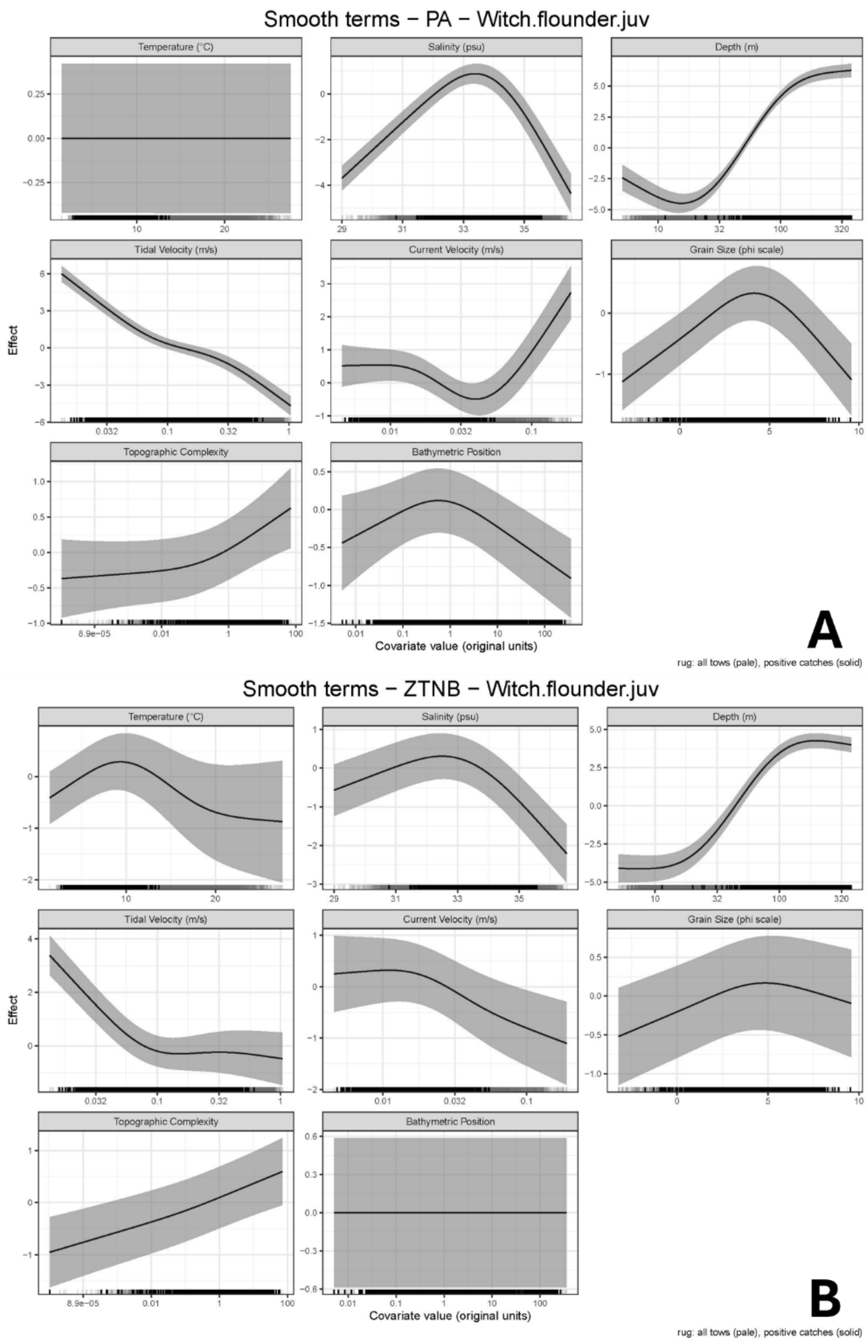

Figure 33. Smooth terms graphs depicting relationships between species counts and individual environmental covariates for adult witch flounder (*Glyptocephalus cynoglossus*). (A) Presence-absence component. (B) Zero-truncated negative binomial (count) component of the joint hurdle species distribution model.

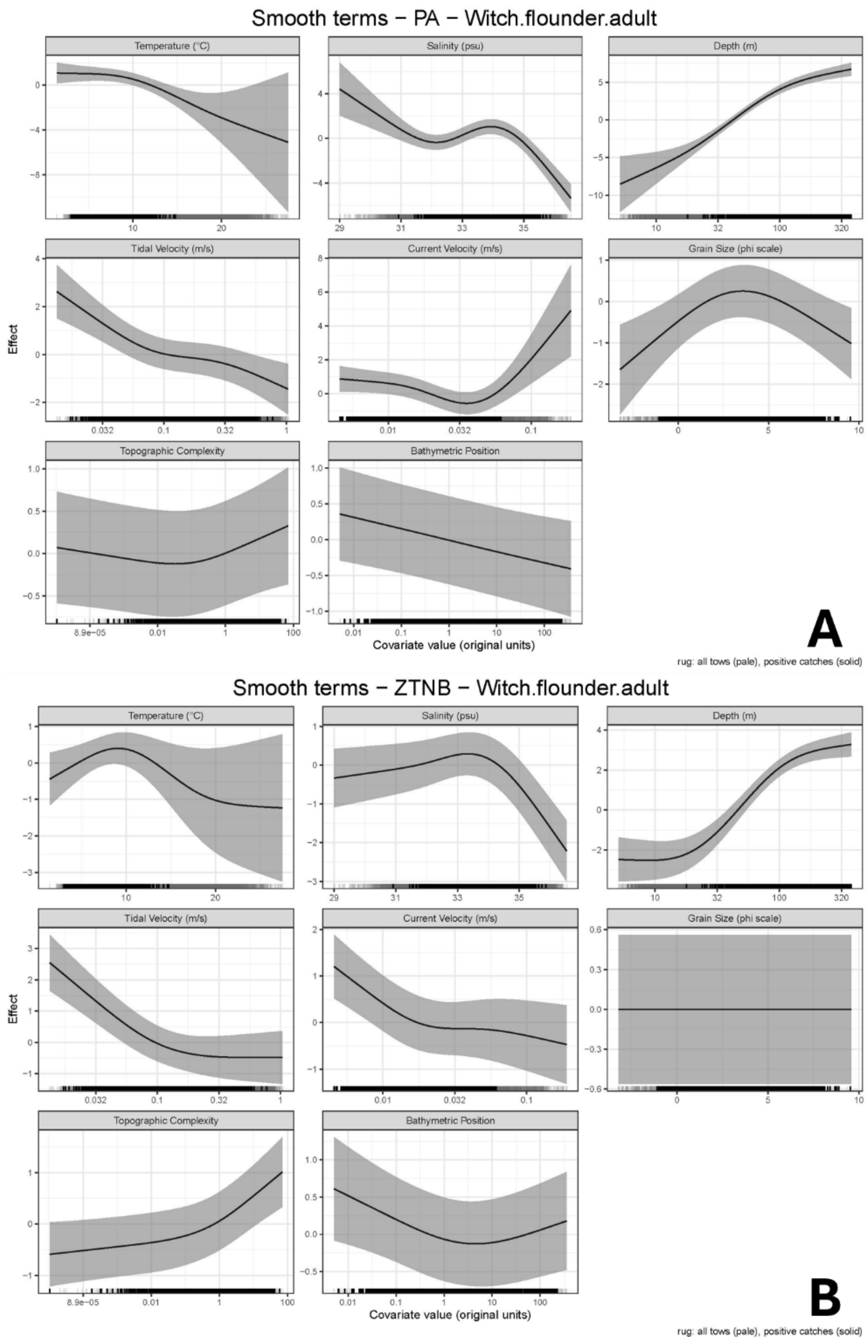

4.2.16 Yellowtail flounder

Figure 34. Smooth terms graphs depicting relationships between species counts and individual environmental covariates for juvenile yellowtail flounder (*Limanda ferruginea*). (A) Presence-absence component. (B) Zero-truncated negative binomial (count) component of the joint hurdle species distribution model.

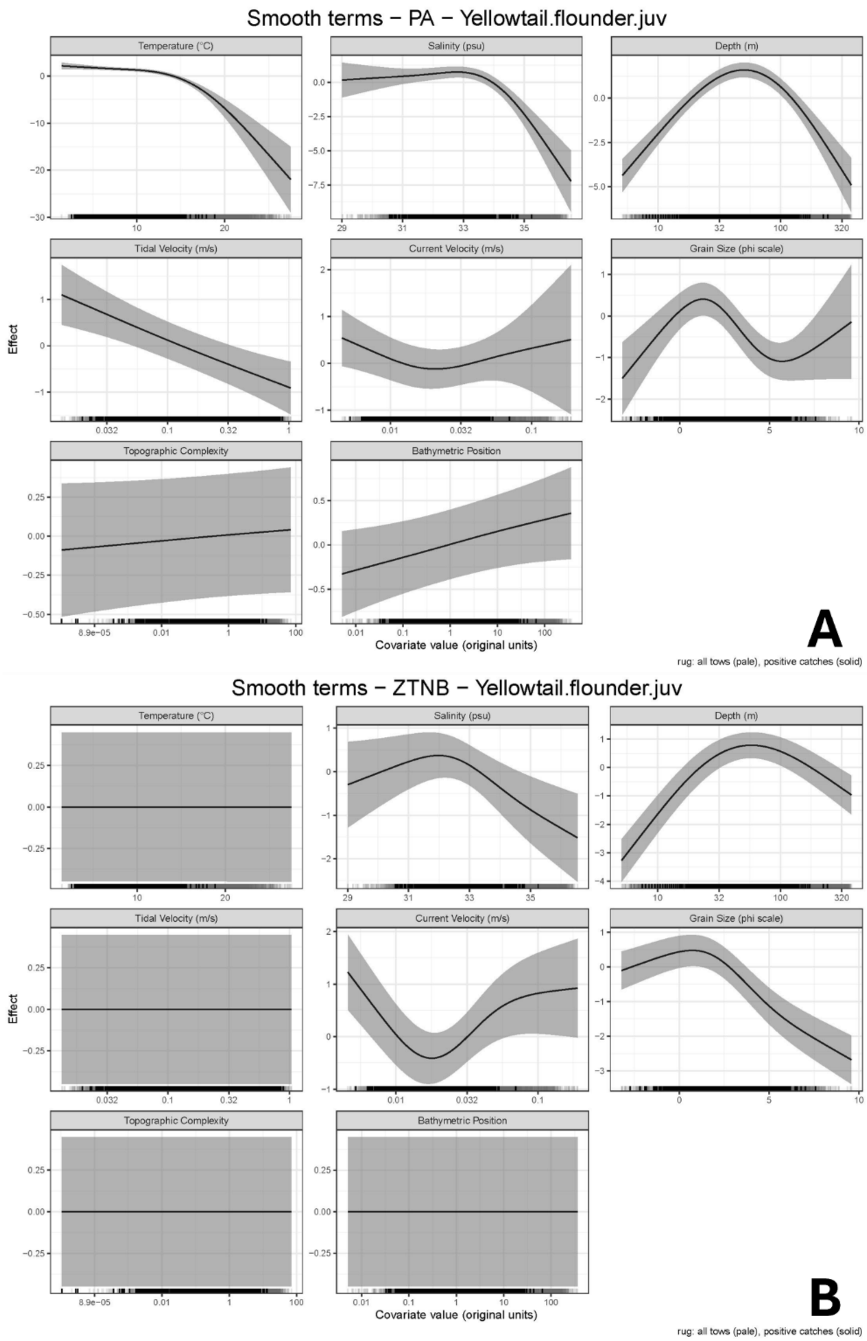

Figure 35. Smooth terms graphs depicting relationships between species counts and individual environmental covariates for adult yellowtail flounder (*Limanda ferruginea*). (A) Presence-absence component. (B) Zero-truncated negative binomial (count) component of the joint hurdle species distribution model.

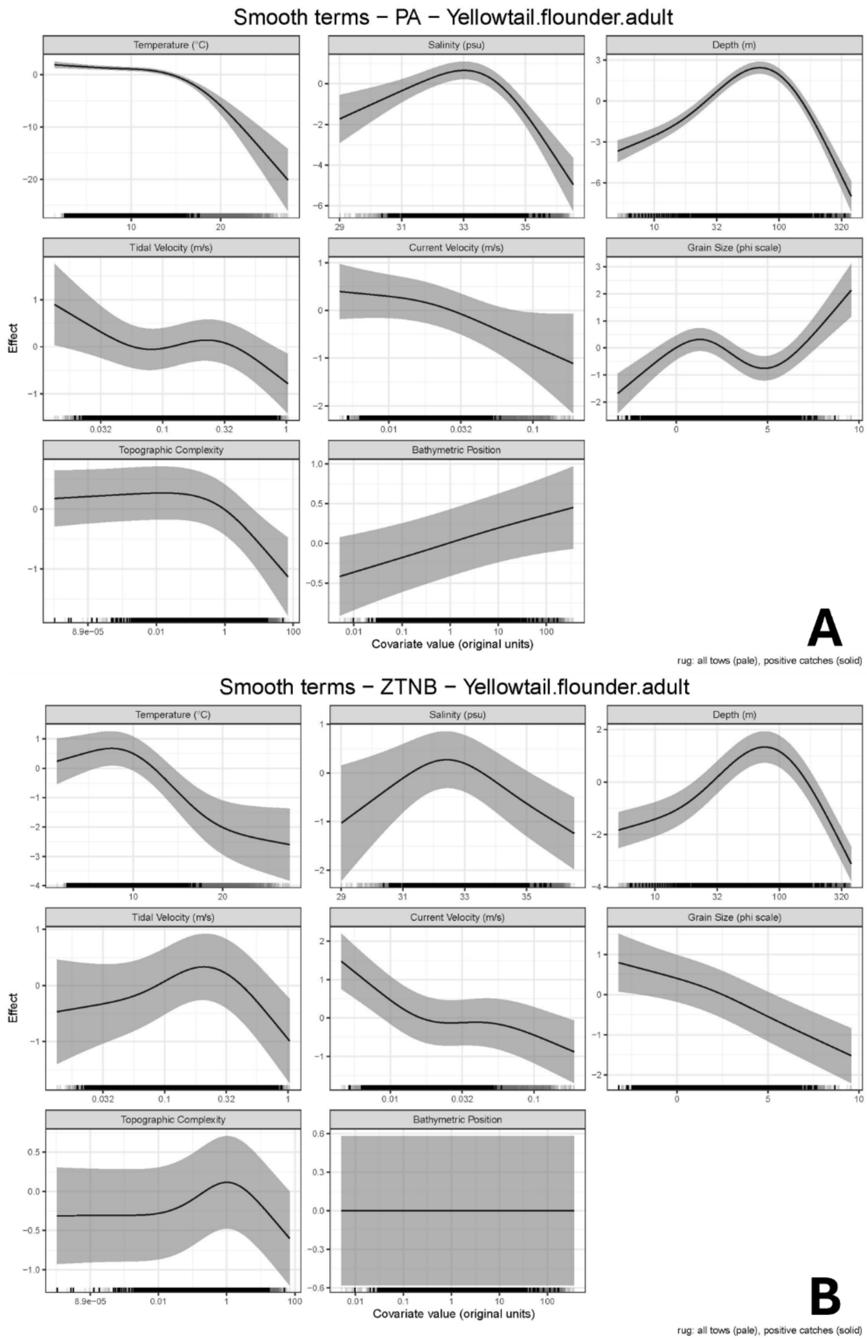

5.0 SPATIAL DISTRIBUTION

In this section, we have included species-specific spatial distribution outputs that complement the updated EFH designation maps. As noted in the Framework document and Appendix E: Detailed EFH Methods, the EFH maps are based on predicted densities from the models, combined with inshore data. Generally, the model outputs are the most important element of the EFH maps given the large extent of the model domain and the inclusion of both inshore and offshore survey data in the models. Inshore fish survey data add estuarine and coastal areas to the EFH maps beyond what is reflected in the maps in this section. Thus, the EFH designation maps may appear different from the plots in this appendix, especially for species that occur in larger numbers inshore.

For each species, both quantile and continuous density plots are shown. First, we show predicted density as four quantiles. The 25%, 50%, and 75% quantiles (yellow, green, and blue) are combined to form the basis of the EFH map, and the 95% quantile (purple) reflects lower density areas. Areas with the lowest 5% of predicted density are not shown. We also provide actual model estimated densities, mapped using a continuous purple to red color ramp. Note that the scale of these continuous maps varies by species (i.e., the redder colors may represent dozens or hundreds of fish per grid cell, depending on the plot).

The densities mapped here reflect a mean/maximum approach. All plots were developed by first calculating the mean density value in each model grid cell across 22 years and then selecting the maximum mean density value across all months or a seasonal subset of months. The larger left-hand panels show the maximum mean value across all six months (March, April, May, September, October, November), and the seasonal spring and fall panels on the upper and lower right-hand side show the maximum mean for spring (March-May) or fall (September-November), respectively. As noted in Appendix E, maximum values within the year are used to provide a conservative estimate of where a species and life stage might be abundant across the seasons. While the six-month plots are generally the basis for the EFH maps, the seasonal products are shown here to reflect the sometimes notable differences in distribution between spring and fall, which may be important for EFH consultation or other applications.

5.1 Acadian redfish

Figure 36. 20-year maximum predicted density (species counts) quantiles for juvenile Acadian redfish (*Sebastes fasciatus*). Maps depict the maximum of the 20-year averages across (A) the full temporal range of the model (six months); (B) spring survey months (March-May); and (C) fall survey months (September-November).

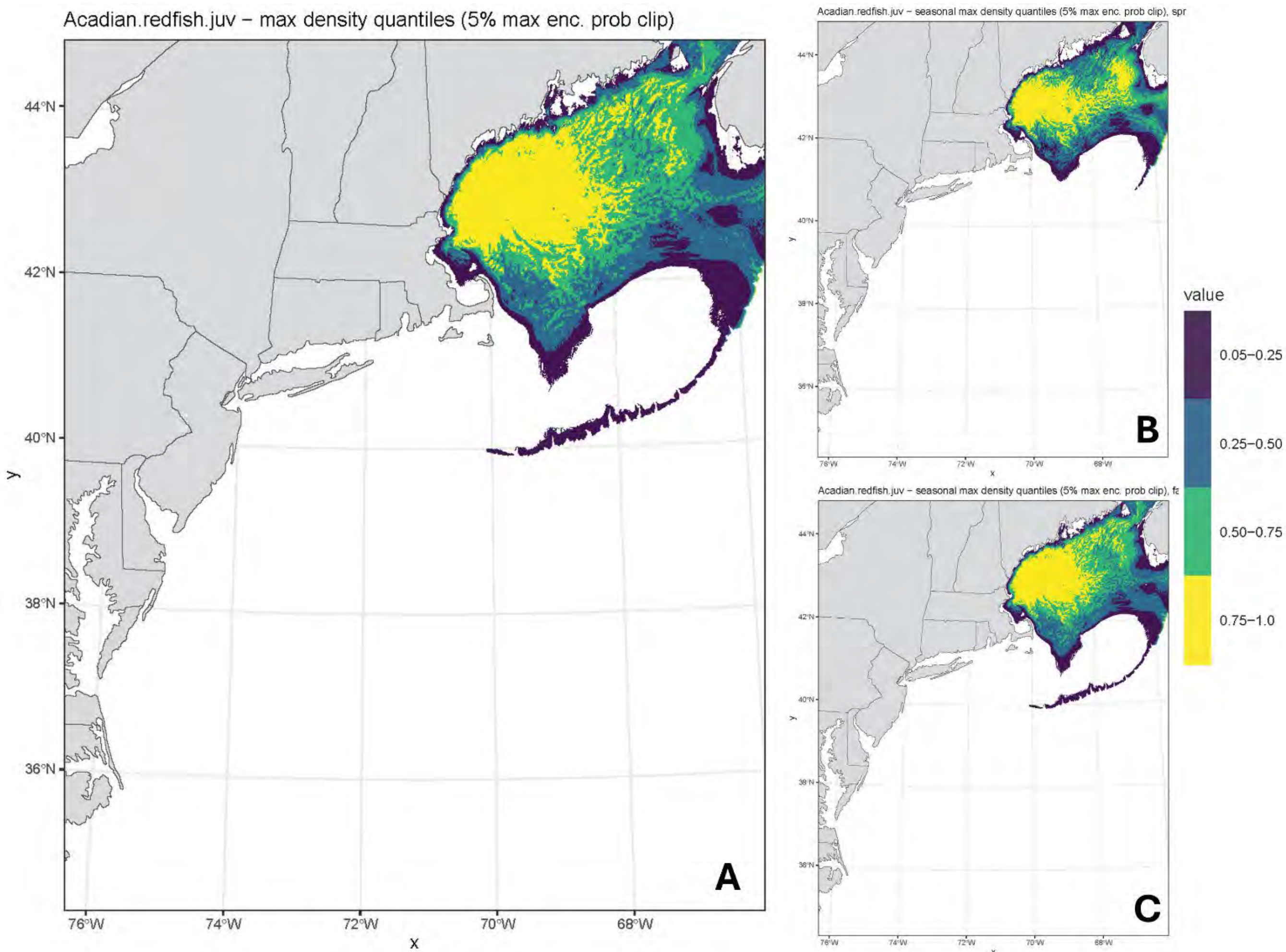

Figure 37. 20-year mean predicted density (species counts) for juvenile Acadian redfish (*Sebastes fasciatus*). Maps depict the maximum of the 20-year averages across (A) the full temporal range of the model (six months); (B) spring survey months (March-May); and (C) fall survey months (September-November).

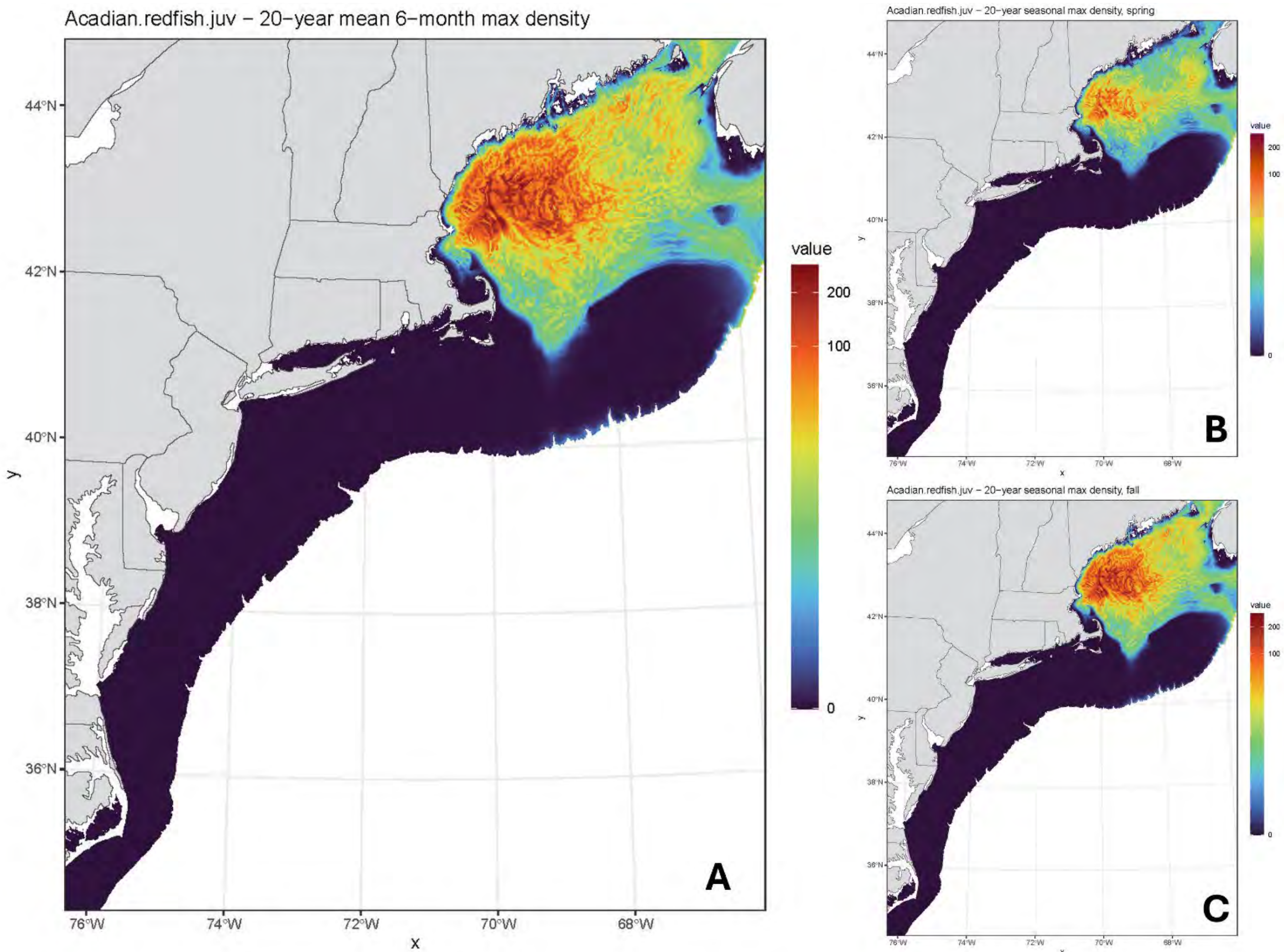

Figure 38. 20-year maximum predicted density (species counts) quantiles for adult Acadian redfish (*Sebastes fasciatus*). Maps depict the maximum of the 20-year averages across (A) the full temporal range of the model (six months); (B) spring survey months (March-May); and (C) fall survey months (September-November).

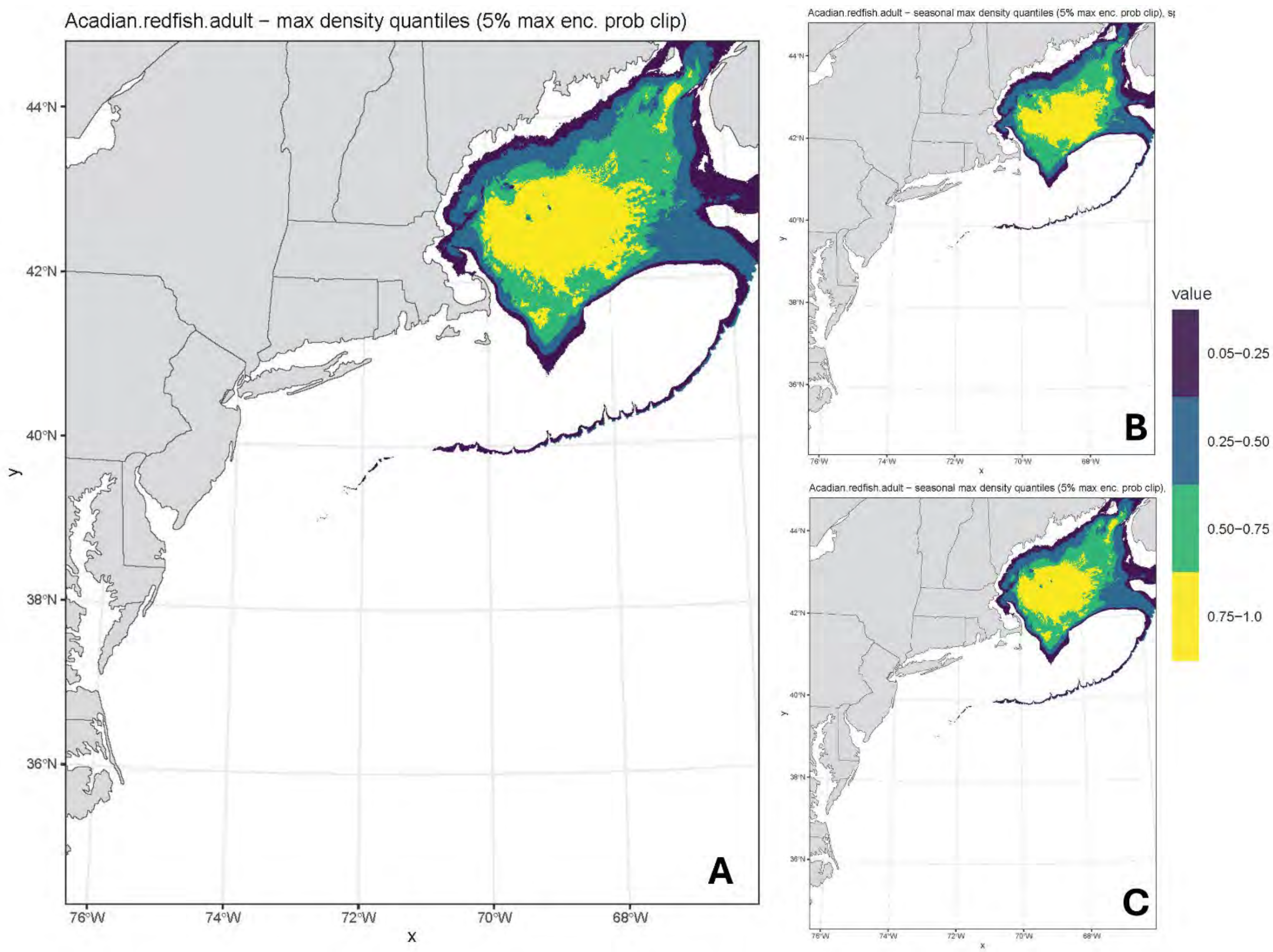

Figure 39. 20-year mean predicted density (species counts) for adult Acadian redfish (*Sebastes fasciatus*). Maps depict the maximum of the 20-year averages across (A) the full temporal range of the model (six months); (B) spring survey months (March-May); and (C) fall survey months (September-November).

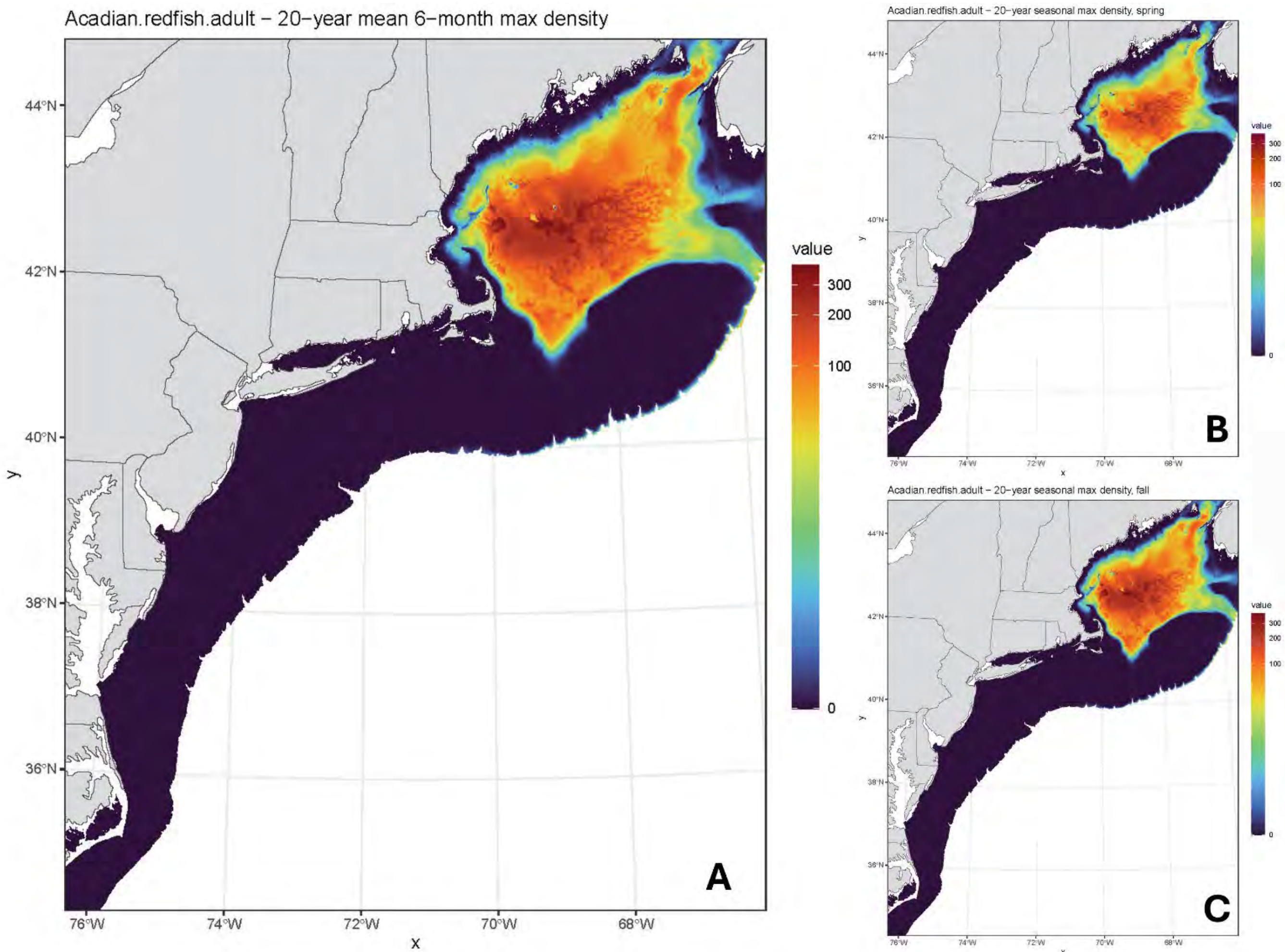

5.2 AMERICAN PLAICE

Figure 40. 20-year maximum predicted density (species counts) quantiles for juvenile American plaice (*Hippoglossoides platessoides*). Maps depict the maximum of the 20-year averages across (A) the full temporal range of the model (six months); (B) spring survey months (March-May); and (C) fall survey months (September-November).

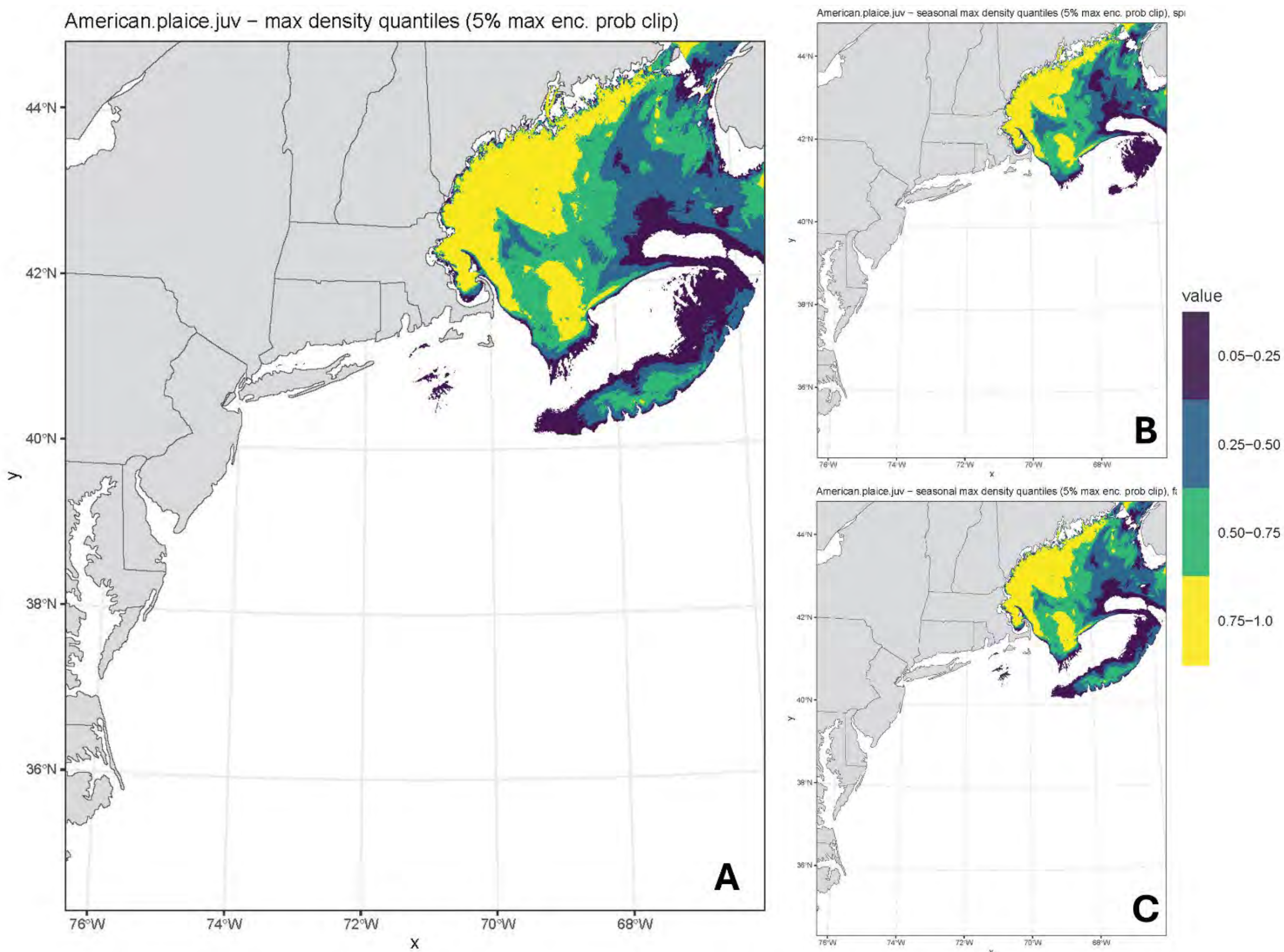

Figure 41. 20-year mean predicted density (species counts) for juvenile American plaice (*Hippoglossoides platessoides*). Maps depict the maximum of the 20-year averages across (A) the full temporal range of the model (six months); (B) spring survey months (March-May); and (C) fall survey months (September-November).

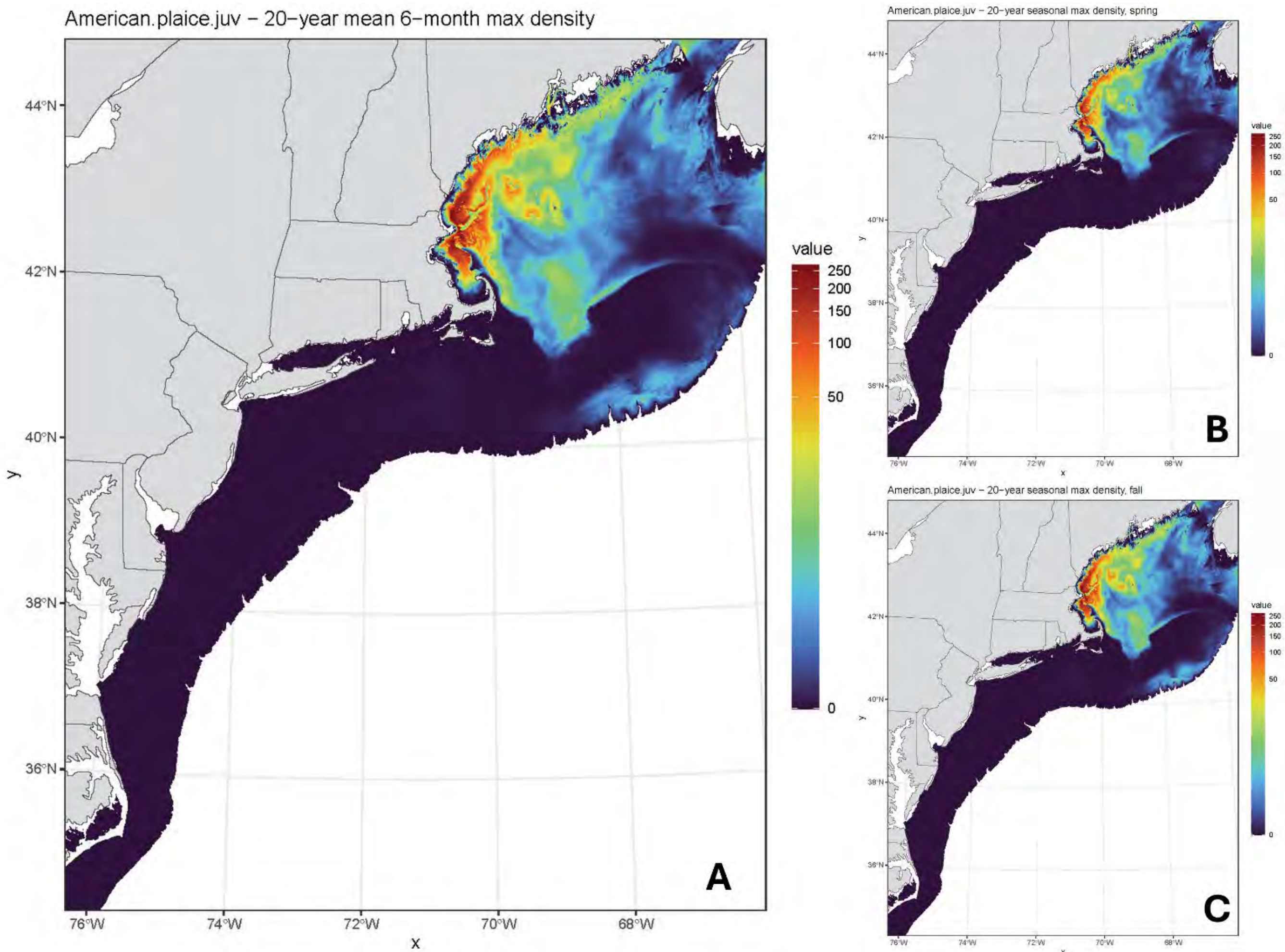

Figure 42. 20-year maximum predicted density (species counts) quantiles for adult American plaice (*Hippoglossoides platessoides*). Maps depict the maximum of the 20-year averages across (A) the full temporal range of the model (six months); (B) spring survey months (March-May); and (C) fall survey months (September-November).

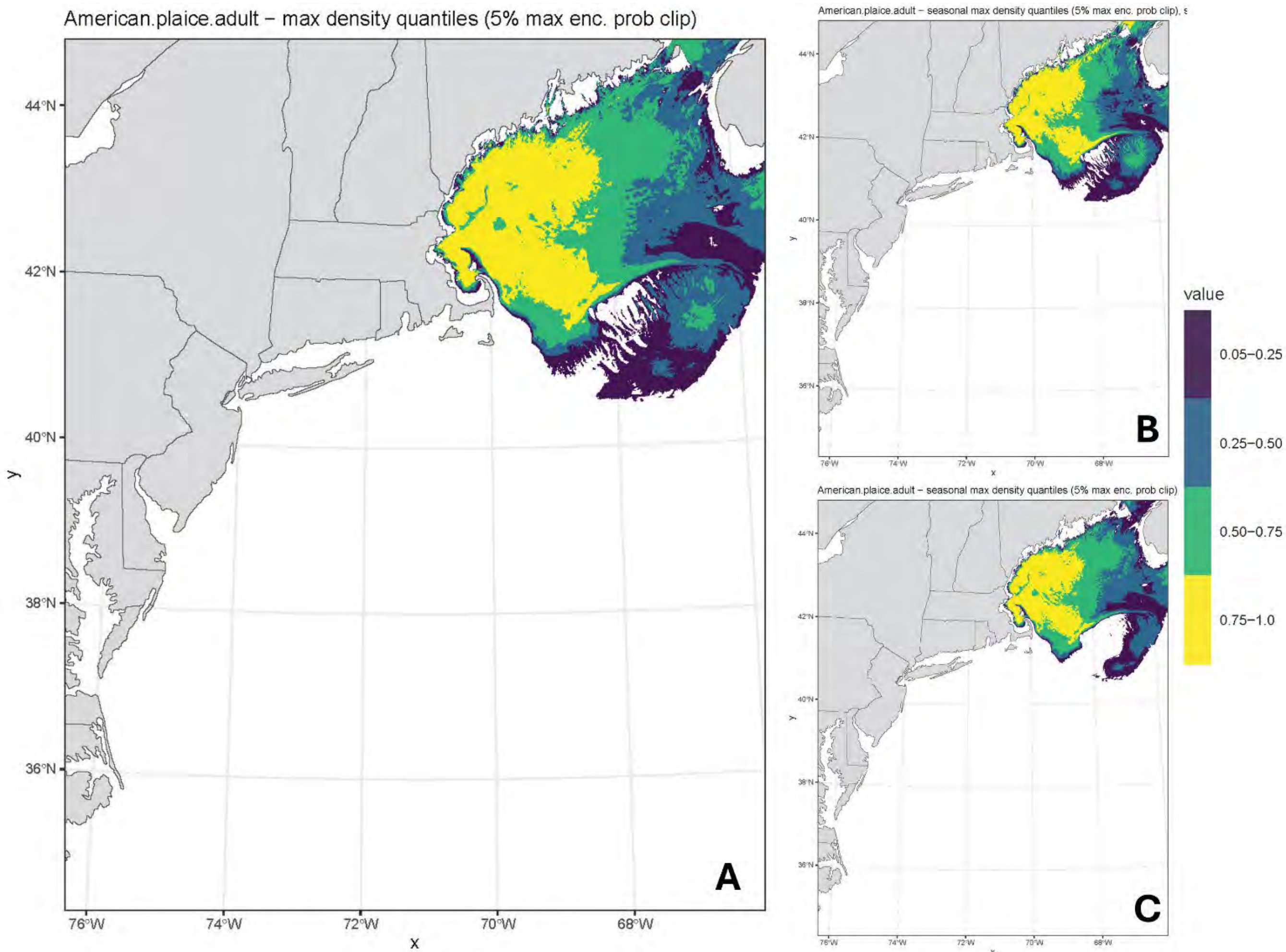

Figure 43. 20-year mean predicted density (species counts) for adult American plaice (*Hippoglossoides platessoides*). Maps depict the maximum of the 20-year averages across (A) the full temporal range of the model (six months); (B) spring survey months (March-May); and (C) fall survey months (September-November).

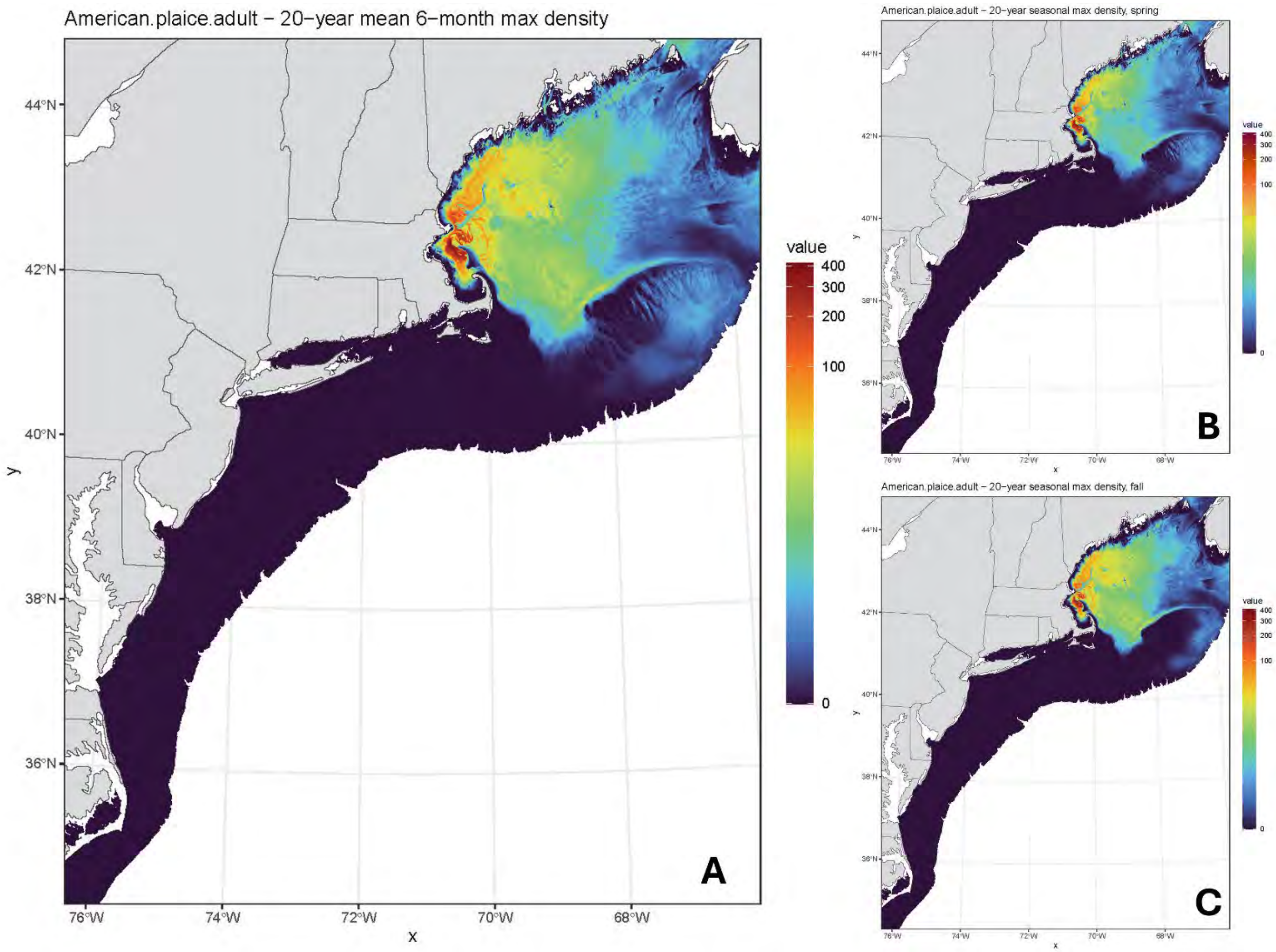

5.3 ATLANTIC HALIBUT

Figure 44. 20-year maximum predicted density (species counts) quantiles for juvenile Atlantic halibut (*Hippoglossus hippoglossus*). Maps depict the maximum of the 20-year averages across (A) the full temporal range of the model (six months); (B) spring survey months (March-May); and (C) fall survey months (September-November).

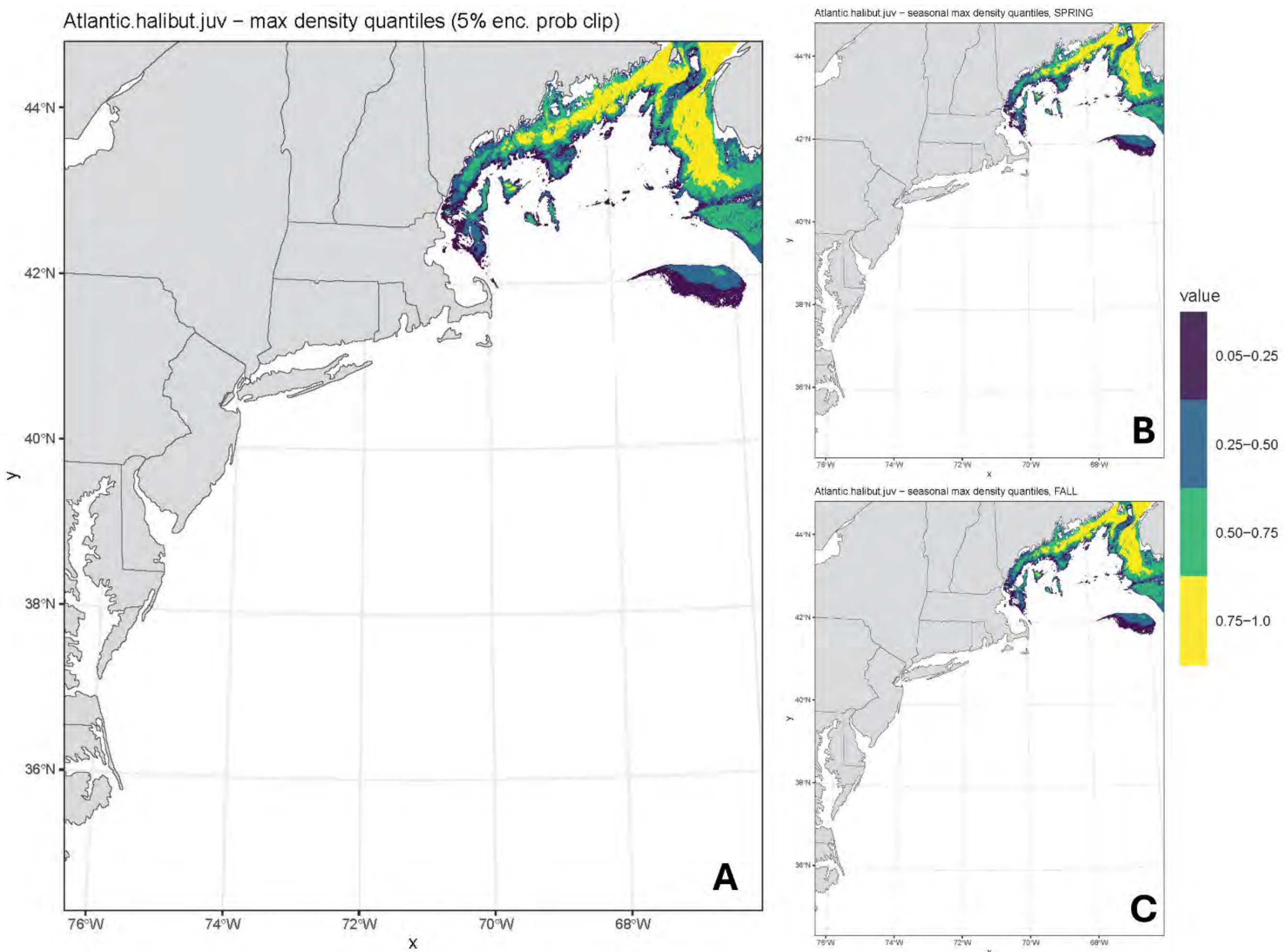

Figure 45. 20-year mean predicted density (species counts) for juvenile Atlantic halibut (*Hippoglossus hippoglossus*). Maps depict the maximum of the 20-year averages across (A) the full temporal range of the model (six months); (B) spring survey months (March-May); and (C) fall survey months (September-November).

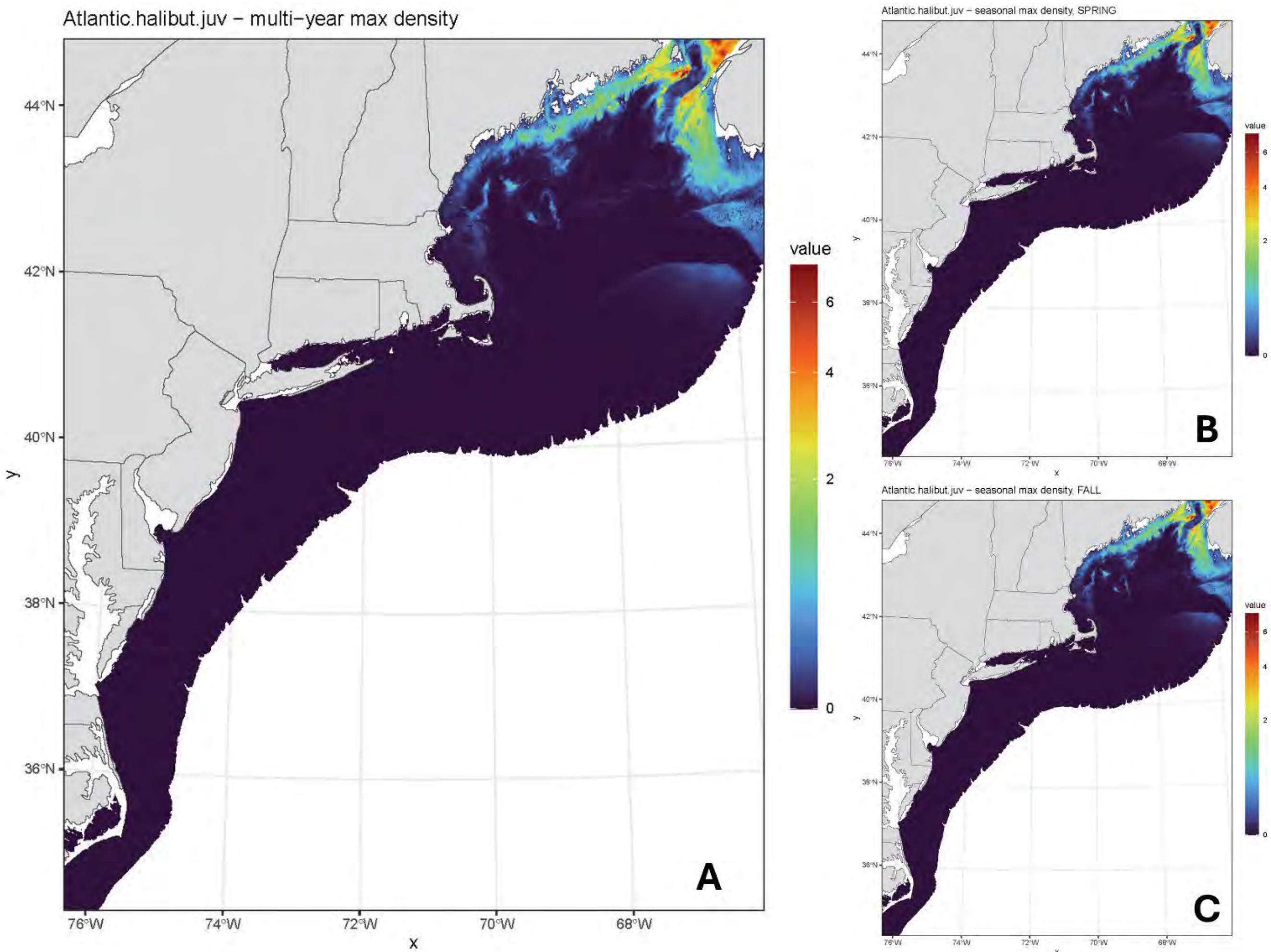

Figure 46. 20-year maximum predicted density (species counts) quantiles for adult Atlantic halibut (*Hippoglossus hippoglossus*). Maps depict the maximum of the 20-year averages across (A) the full temporal range of the model (six months); (B) spring survey months (March-May); and (C) fall survey months (September-November).

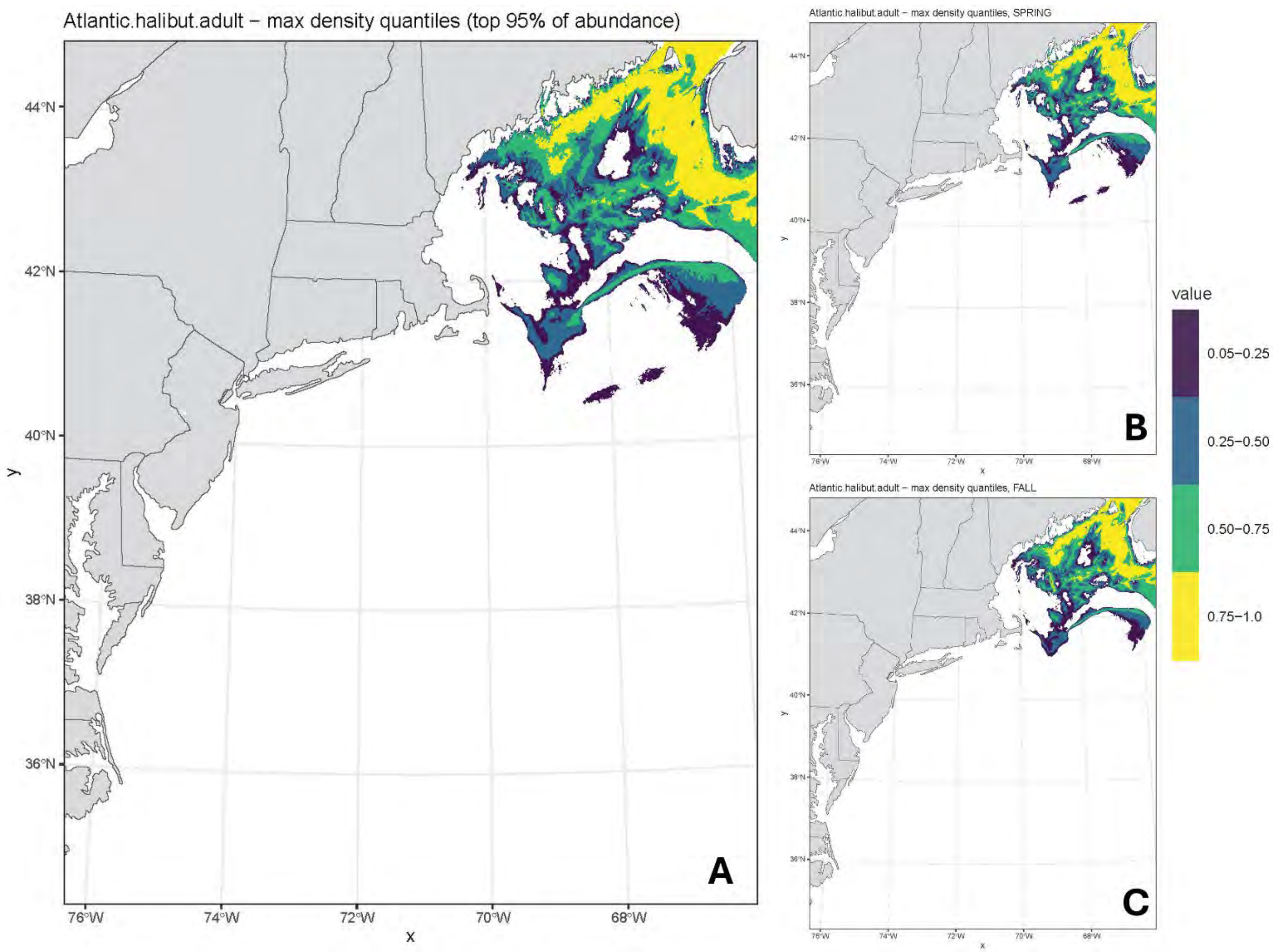

Figure 47. 20-year mean predicted density (species counts) for adult Atlantic halibut (*Hippoglossus hippoglossus*). Maps depict the maximum of the 20-year averages across (A) the full temporal range of the model (six months); (B) spring survey months (March-May); and (C) fall survey months (September-November).

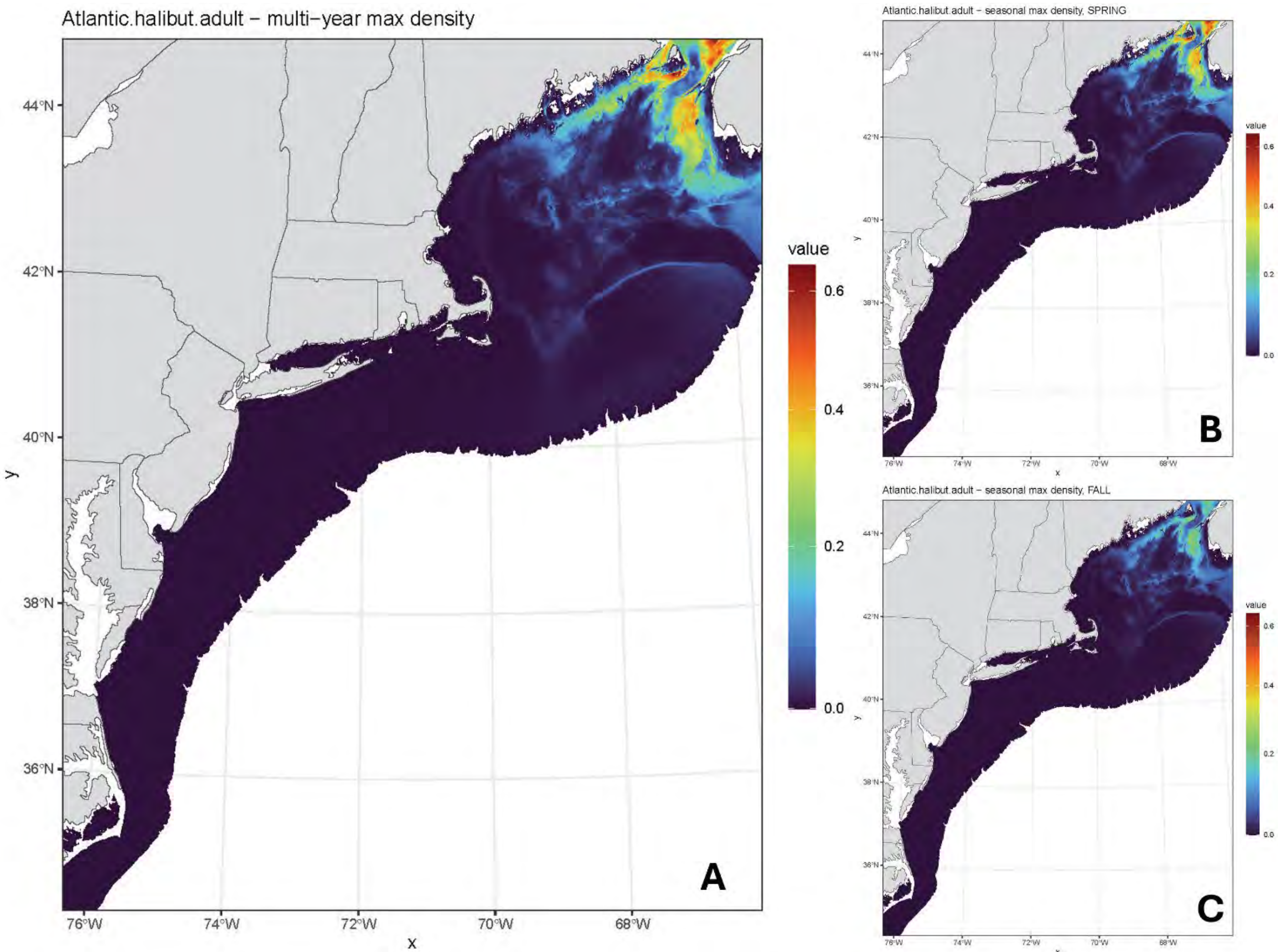

5.4 ATLANTIC SEA SCALLOP

Figure 48. 20-year mean predicted density (species counts) quantiles for pooled juvenile and adult Atlantic sea scallop (*Placopecten magellanicus*). Maps depict the mean of the 20-year averages across the full temporal range of the dredge-trawl integrated model.

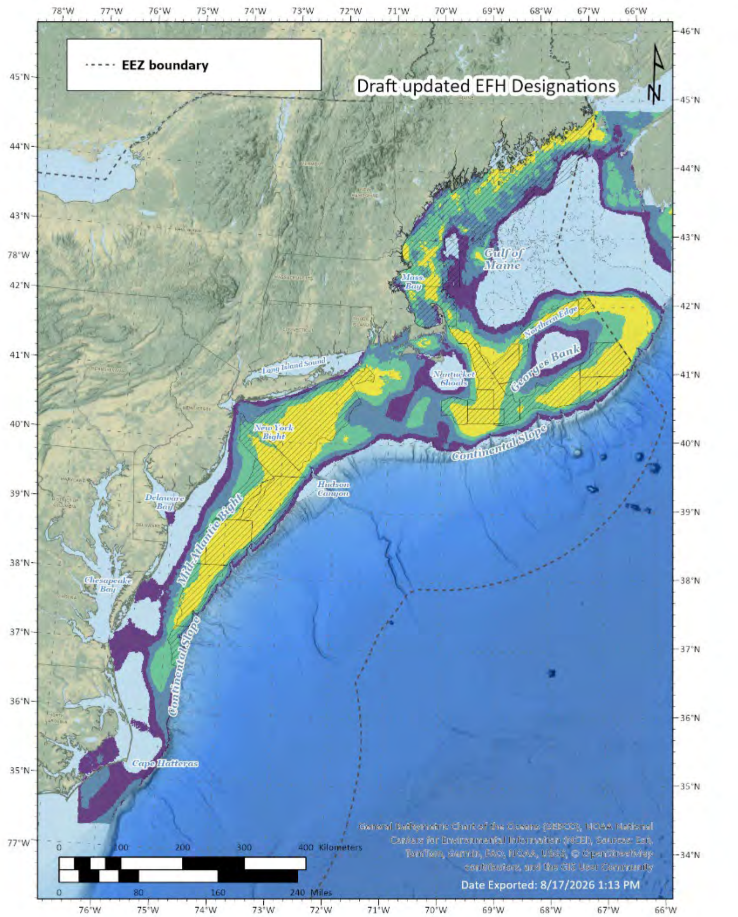

Figure 49. 20-year mean predicted density (species counts) for pooled juvenile and adult Atlantic sea scallop (*Placopecten magellanicus*). Maps depict the mean of the 20-year averages across the full temporal range of the dredge-trawl integrated model.

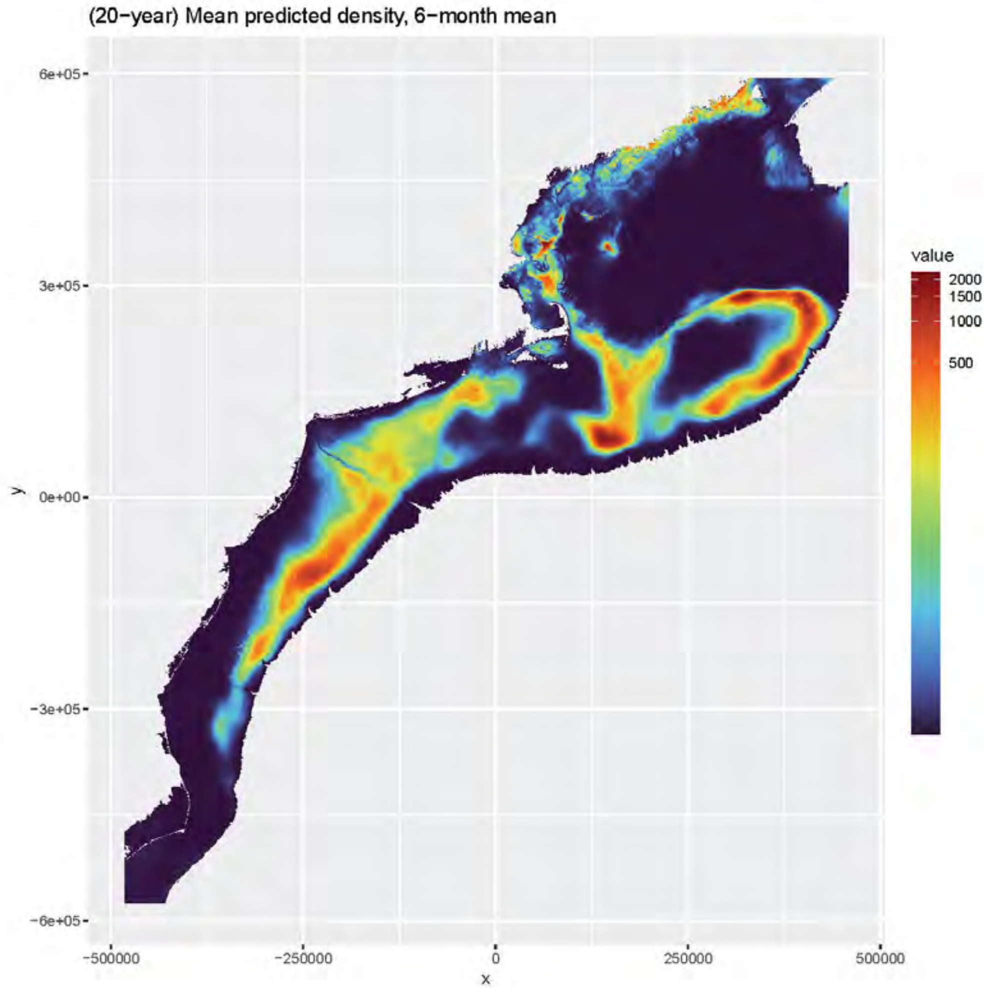

5.5 ATLANTIC WOLFFISH

Figure 50. 20-year maximum predicted density (species counts) quantiles for juvenile Atlantic wolffish (*Anarhichas lupus*). Maps depict the maximum of the 20-year averages across (A) the full temporal range of the model (six months); (B) spring survey months (March-May); and (C) fall survey months (September-November). Note that while the EFH designation extends into the South-Atlantic (from non-modeled, nearshore areas), model predictions do not.

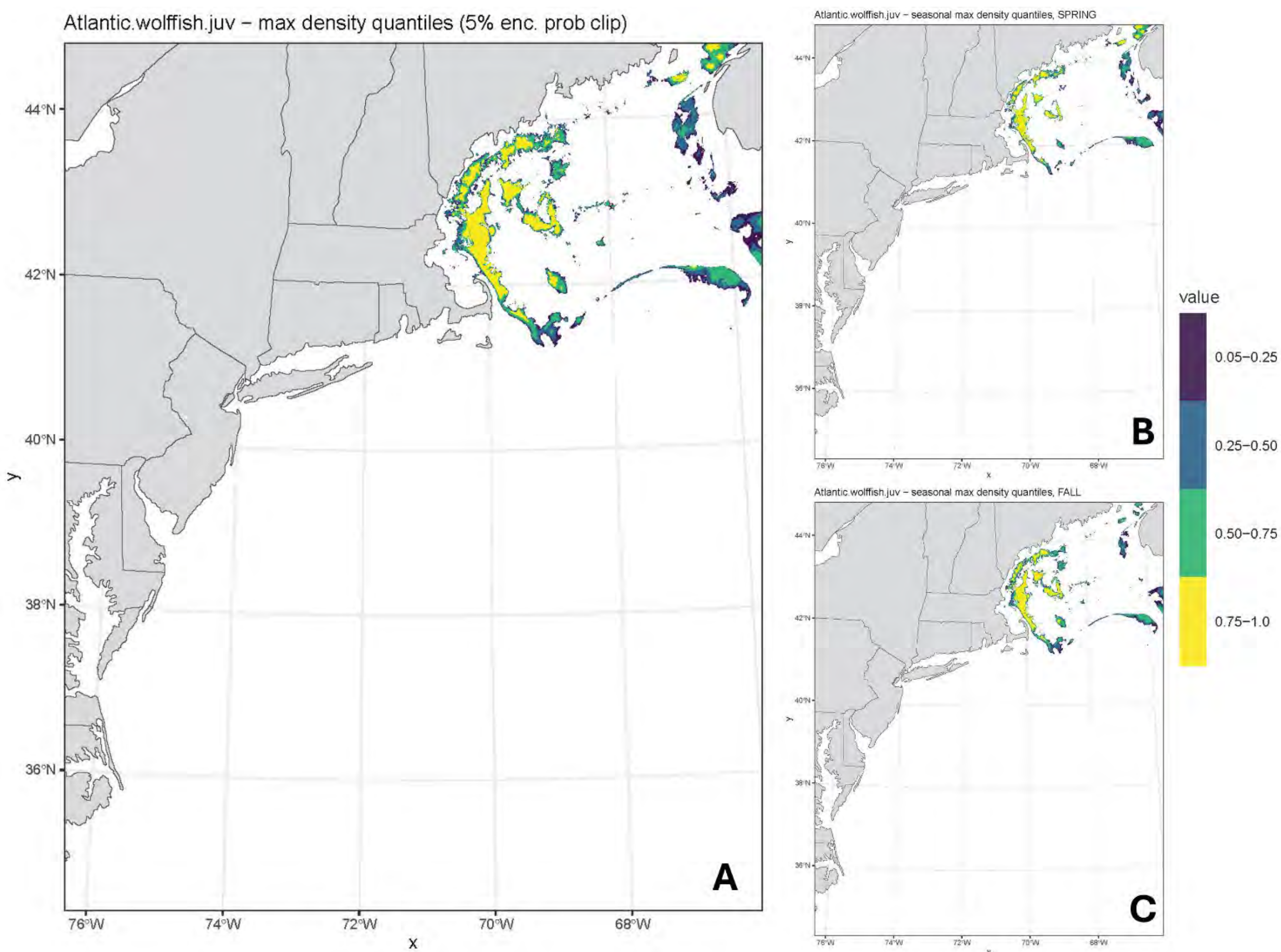

Figure 51. 20-year mean predicted density (species counts) for juvenile Atlantic wolffish (*Anarhichas lupus*). Maps depict the maximum of the 20-year averages across (A) the full temporal range of the model (six months); and (C) fall survey months (September-November). Note that while the EFH designation extends into the South-Atlantic (from non-modeled, nearshore areas), model predictions do not.

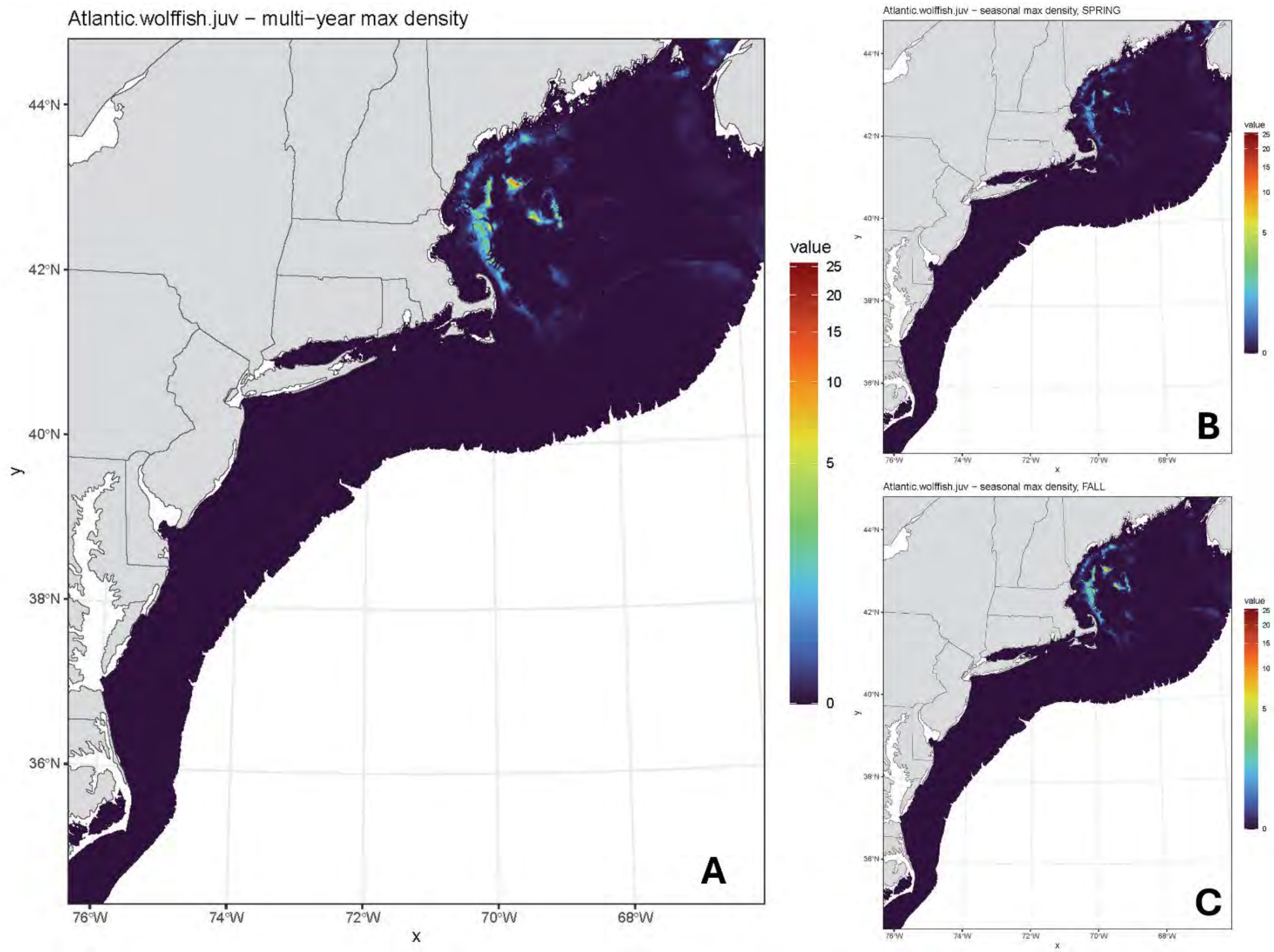

Figure 52. 20-year maximum predicted density (species counts) quantiles for adult Atlantic wolffish (*Anarhichas lupus*). Maps depict the maximum of the 20-year averages across (A) the full temporal range of the model (six months); and (C) fall survey months (September-November). Note that while the EFH designation extends into the South-Atlantic (from non-modeled, nearshore areas), model predictions do not.

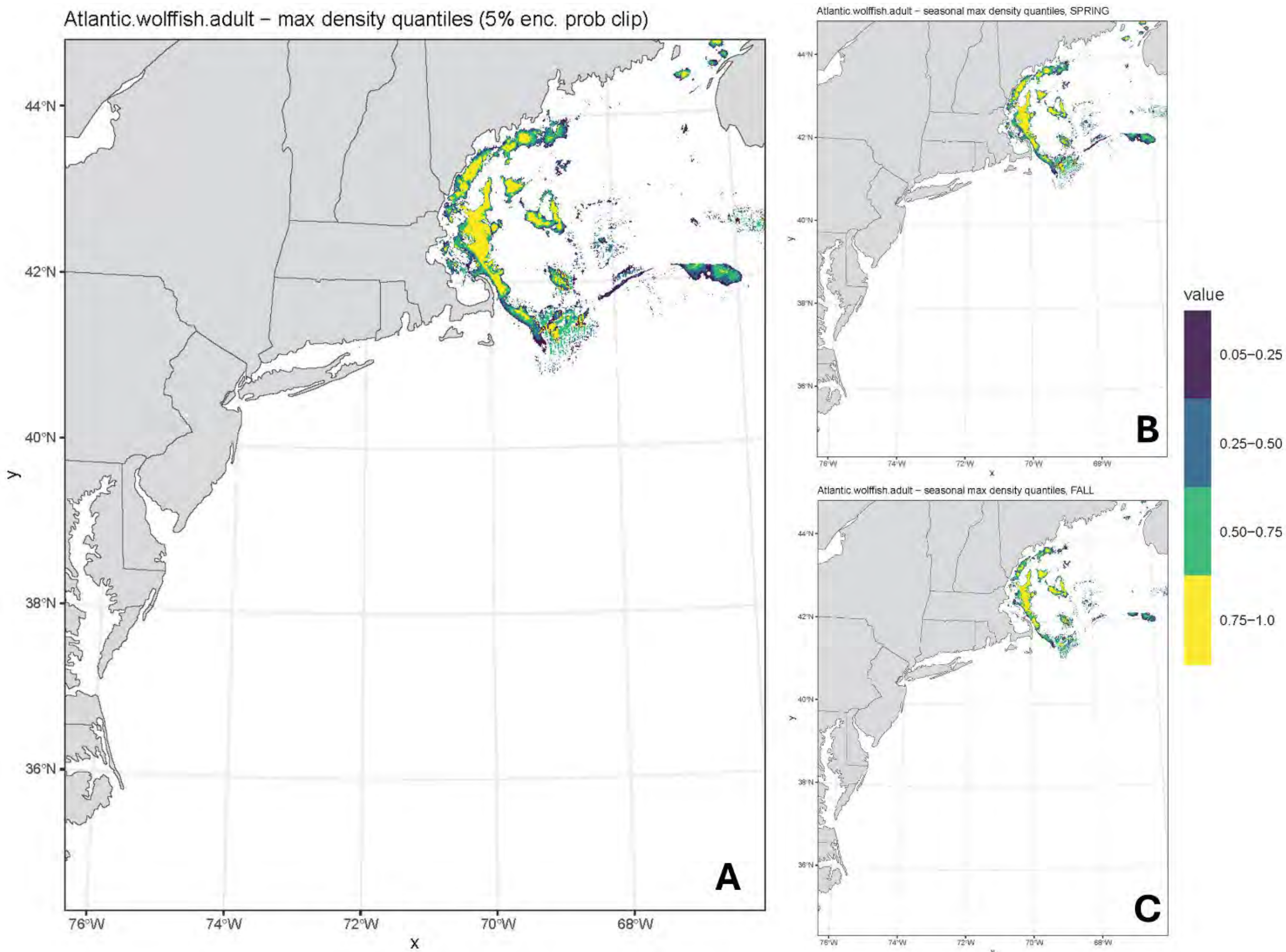

Figure 53. 20-year mean predicted density (species counts) for adult Atlantic wolffish (*Anarhichas lupus*). Maps depict the maximum of the 20-year averages across (A) the full temporal range of the model (six months); and (C) fall survey months (September-November). Note that while the EFH designation extends into the South-Atlantic (from non-modeled, nearshore areas), model predictions do not.

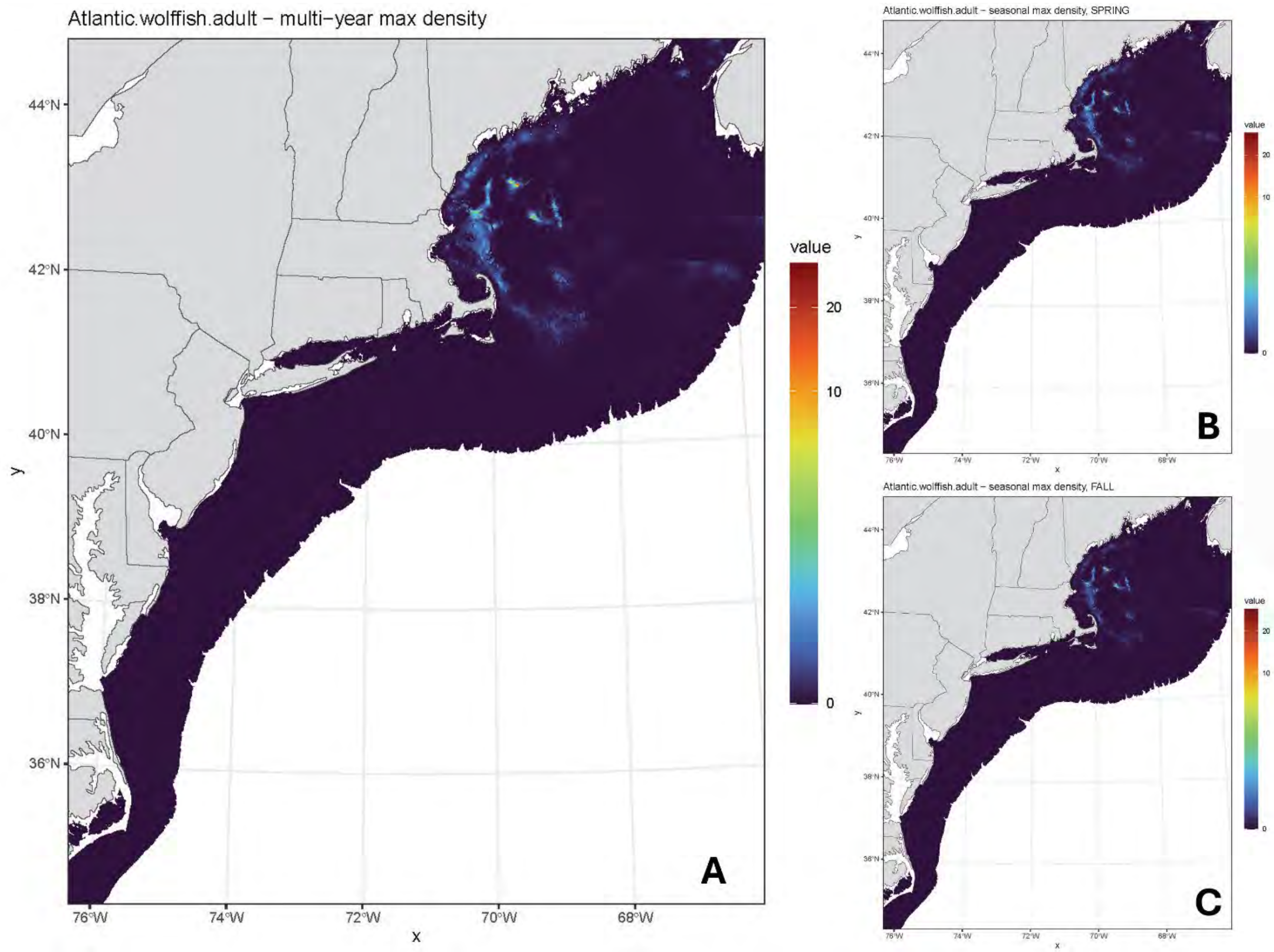

5.6 Haddock

Figure 54. 20-year maximum predicted density (species counts) quantiles for juvenile haddock (*Melanogrammus aeglefinus*). Maps depict the maximum of the 20-year averages across (A) the full temporal range of the model (six months); (B) spring survey months (March-May); and (C) fall survey months (September-November).

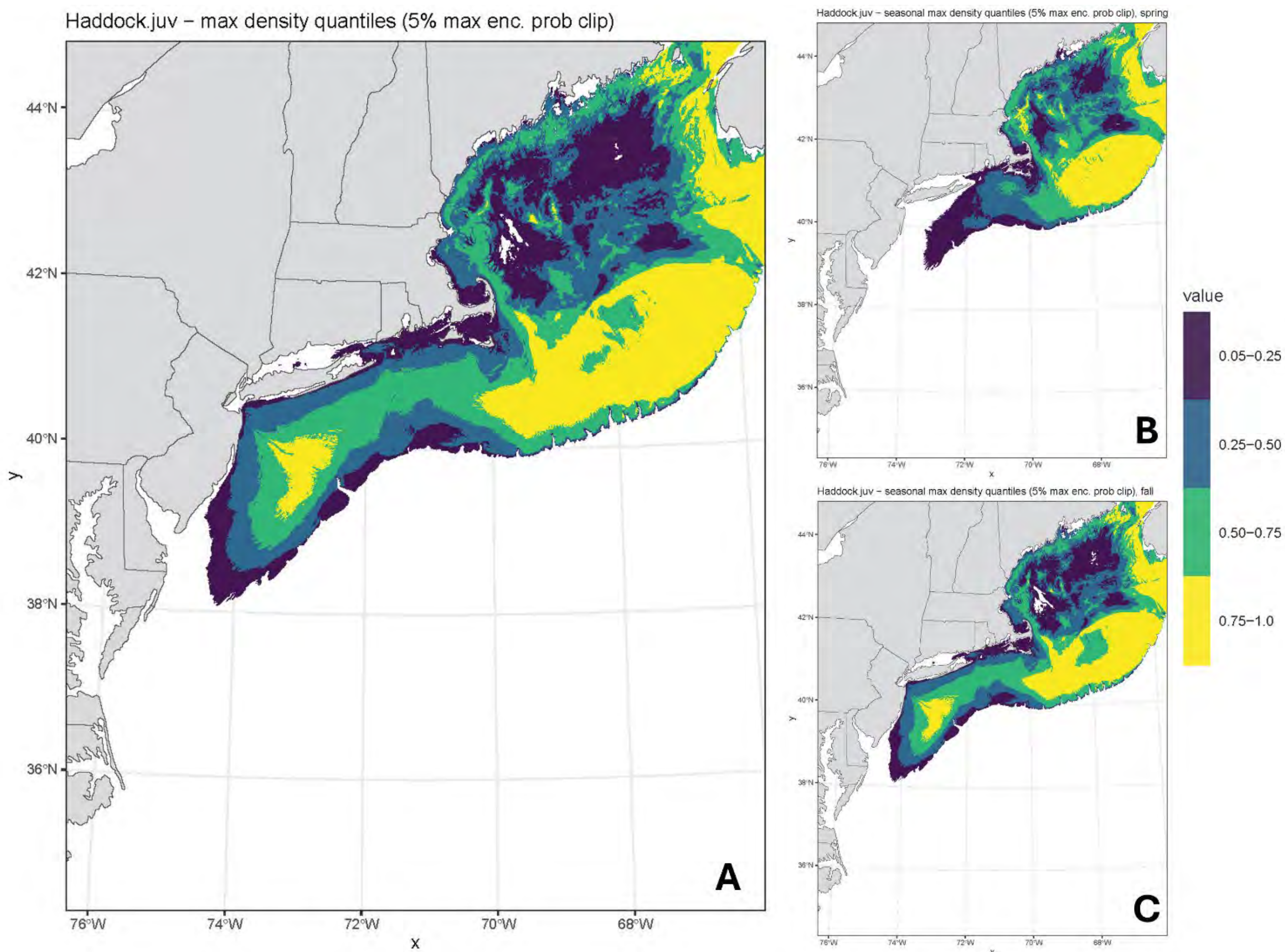

Figure 55. 20-year mean predicted density (species counts) for juvenile haddock (*Melanogrammus aeglefinus*). Maps depict the maximum of the 20-year averages across (A) the full temporal range of the model (six months); (B) spring survey months (March-May); and (C) fall survey months (September-November).

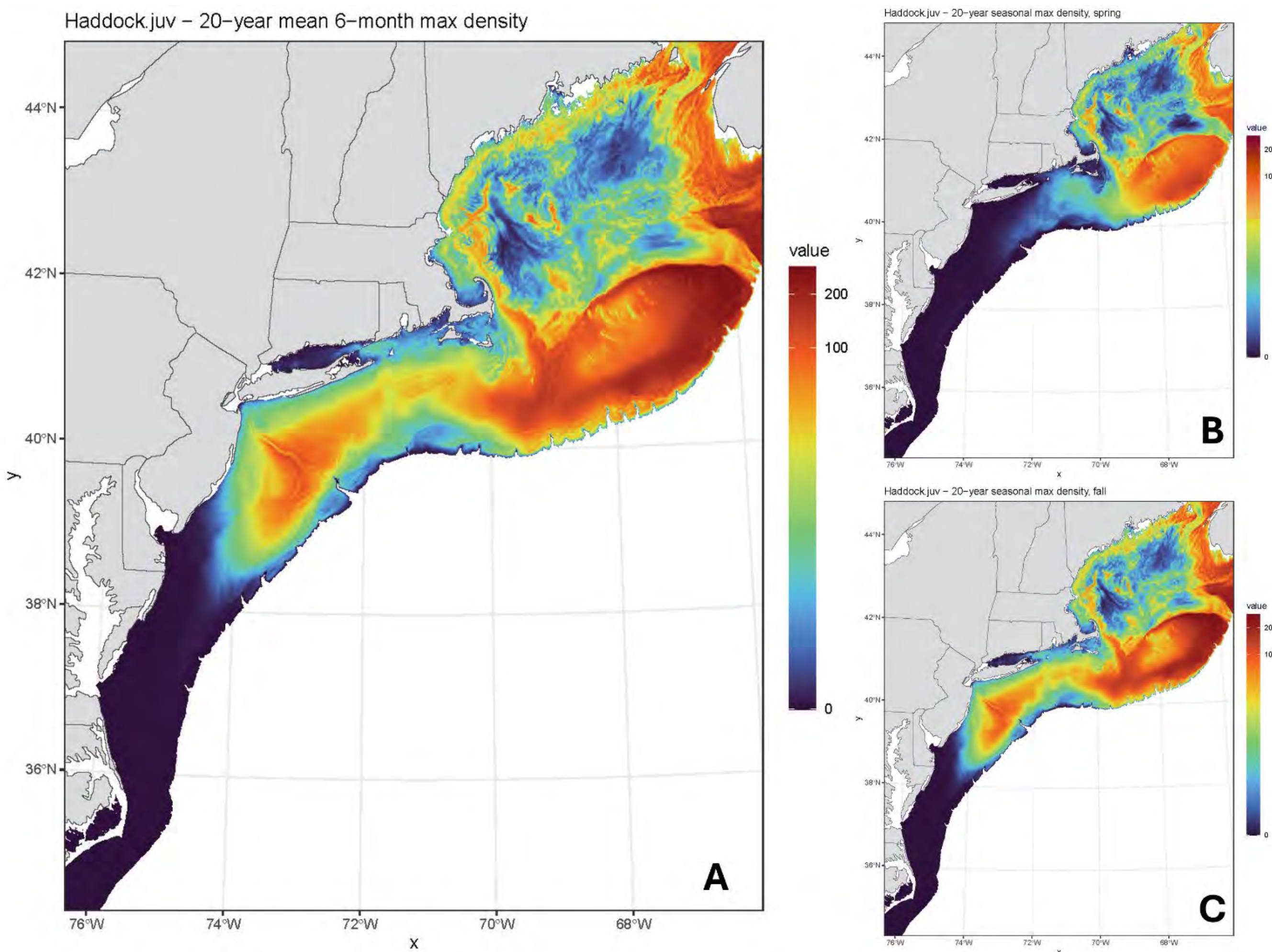

Figure 56. 20-year maximum predicted density (species counts) quantiles for adult haddock (*Melanogrammus aeglefinus*). Maps depict the maximum of the 20-year averages across (A) the full temporal range of the model (six months); (B) spring survey months (March-May); and (C) fall survey months (September-November).

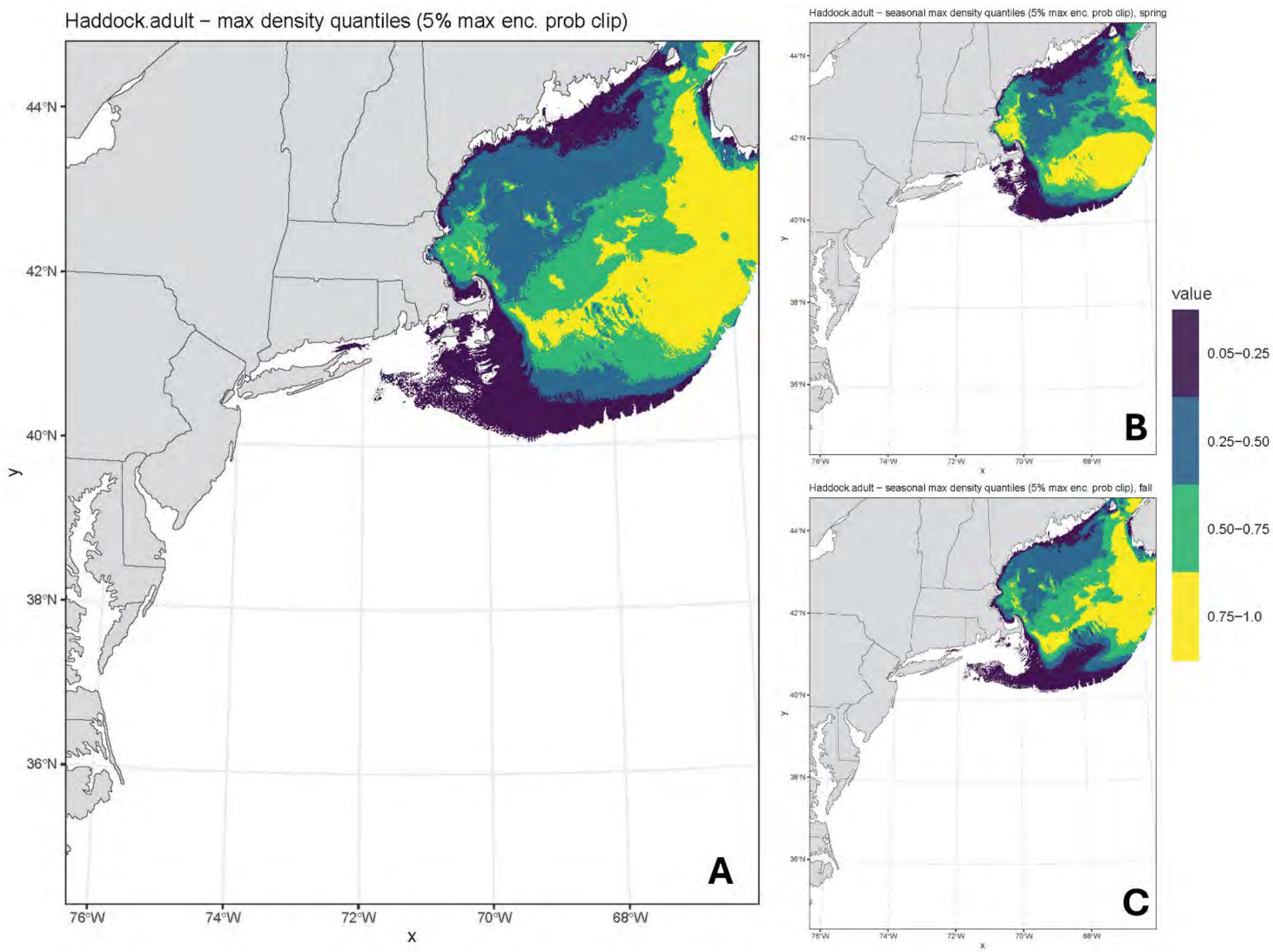

Figure 57. 20-year mean predicted density (species counts) for adult haddock (*Melanogrammus aeglefinus*). Maps depict the maximum of the 20-year averages across (A) the full temporal range of the model (six months); (B) spring survey months (March-May); and (C) fall survey months (September-November).

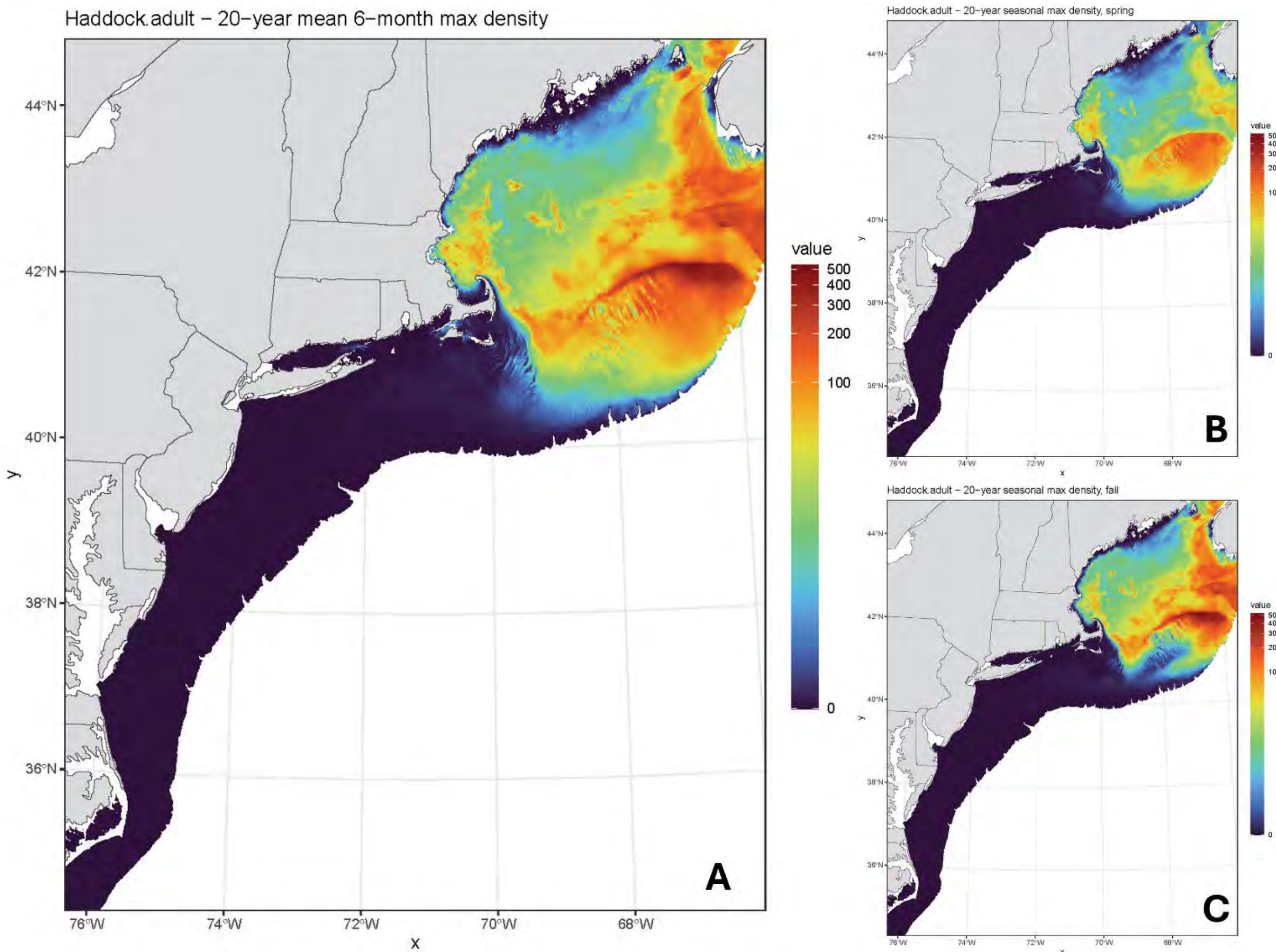

5.7 OCEAN POUT

Figure 58. 20-year maximum predicted density (species counts) quantiles for pooled juvenile ocean pout (*Macrozoarces americanus*). Maps depict the maximum of the 20-year averages across (A) the full temporal range of the model (six months); (B) spring survey months (March-May); and (C) fall survey months (September-November).

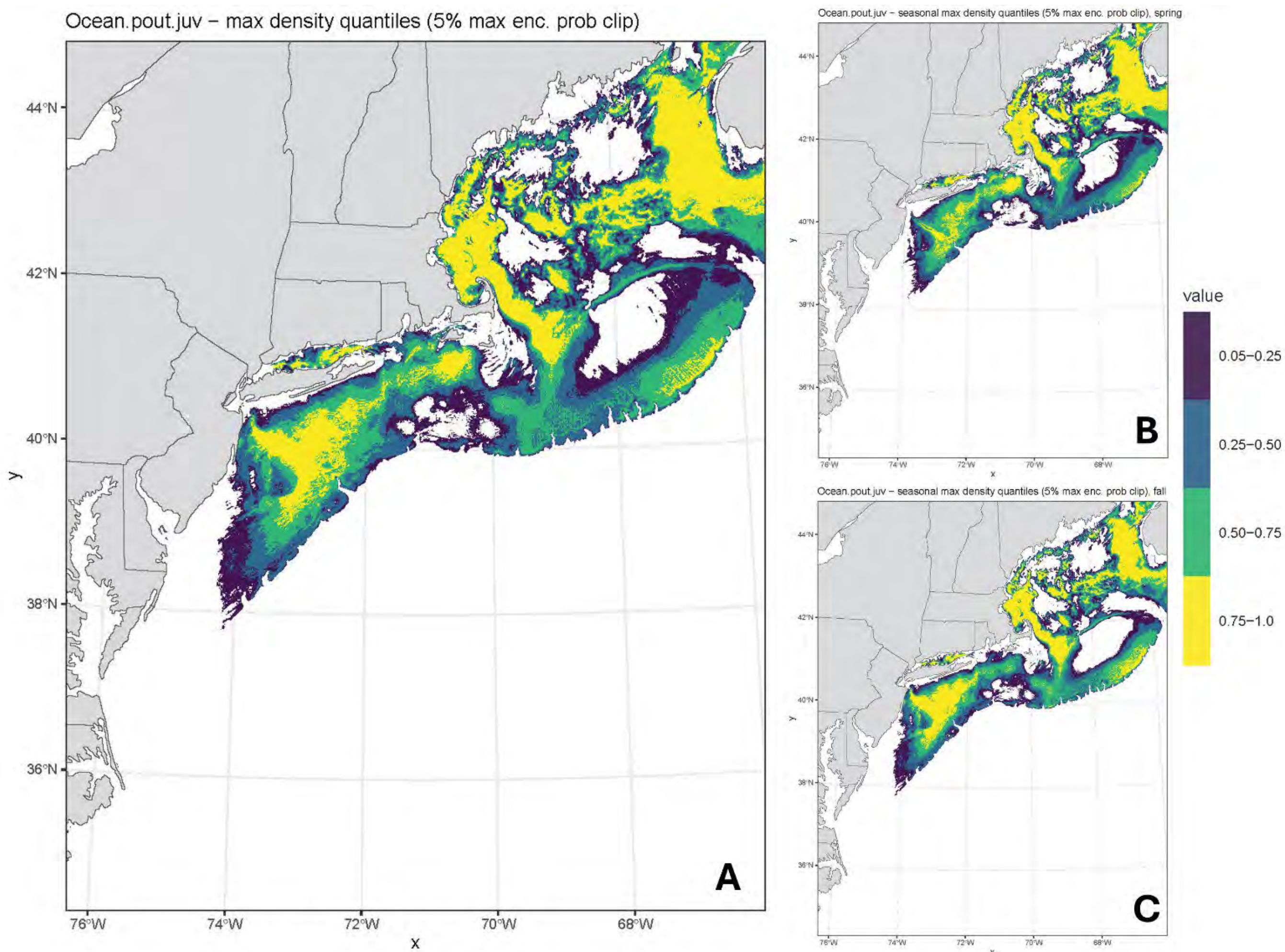

Figure 59. 20-year mean predicted density (species counts) for pooled juvenile ocean pout (*Macrozoarces americanus*). Maps depict the maximum of the 20-year averages across (A) the full temporal range of the model (six months); (B) spring survey months (March-May); and (C) fall survey months (September-November).

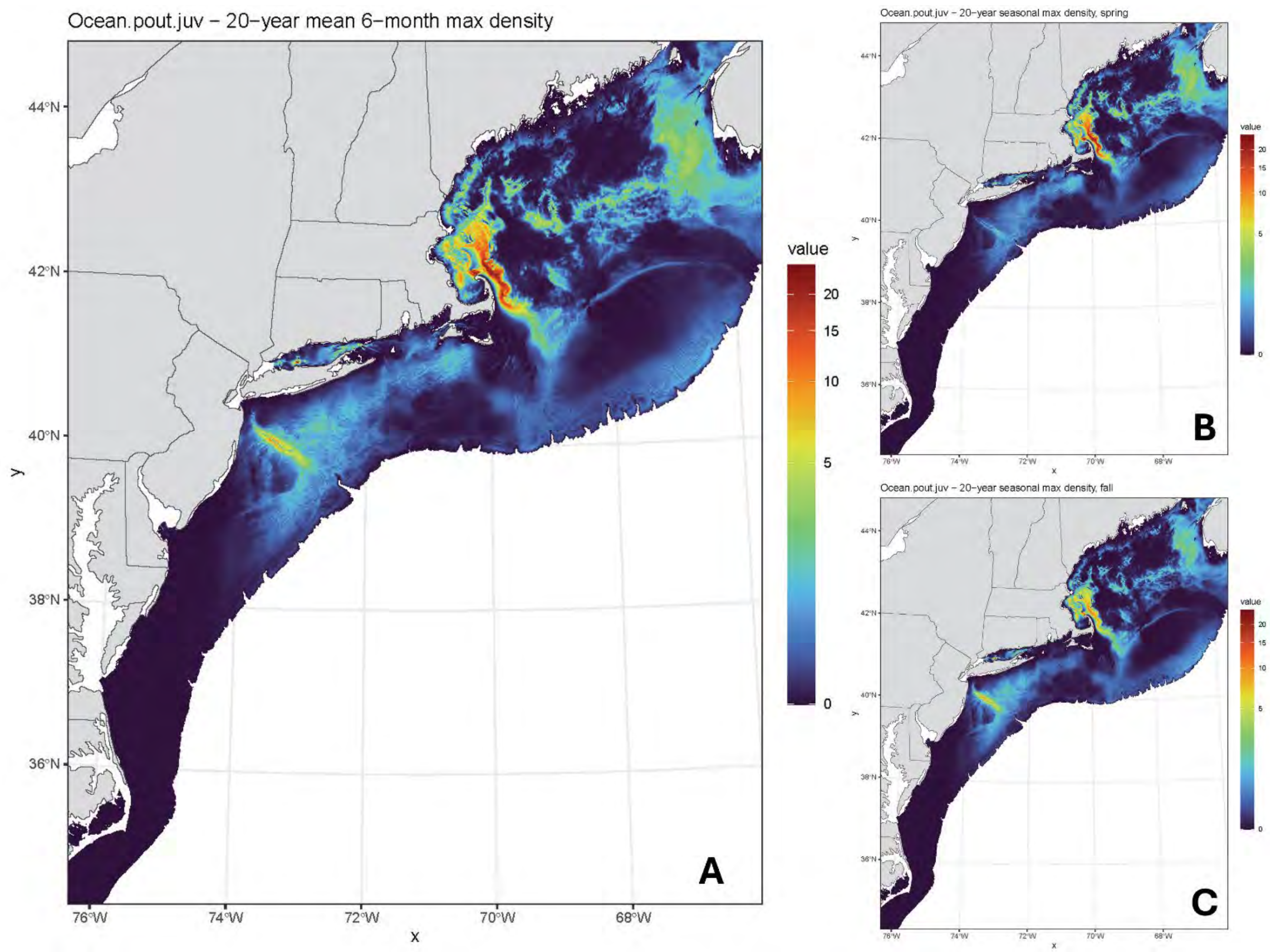

Figure 60. 20-year maximum predicted density (species counts) quantiles for pooled adult ocean pout (*Macrozoarces americanus*). Maps depict the maximum of the 20-year averages across (A) the full temporal range of the model (six months); (B) spring survey months (March-May); and (C) fall survey months (September-November).

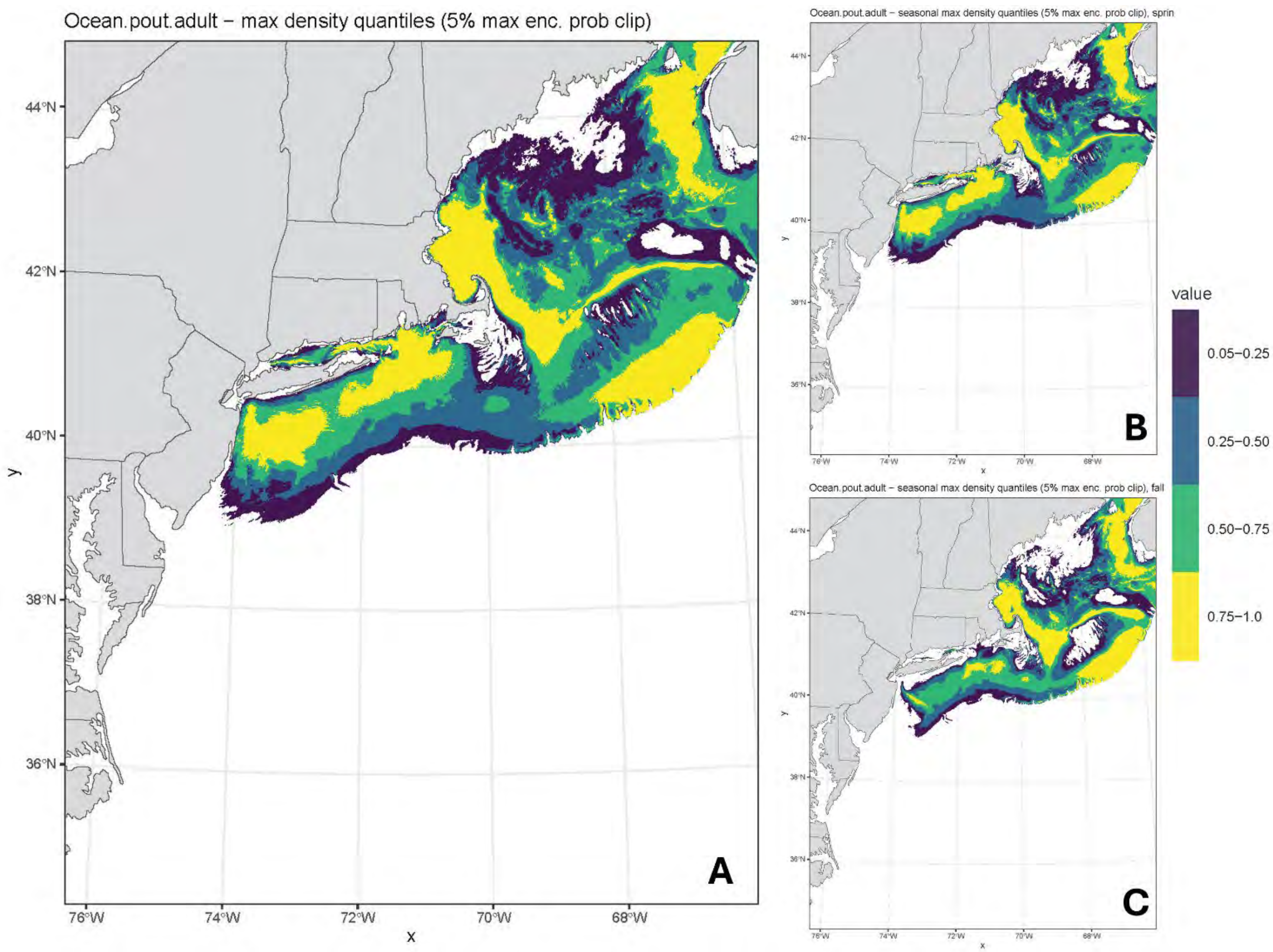

Figure 61. 20-year mean predicted density (species counts) for pooled adult ocean pout (*Macrozoarces americanus*). Maps depict the maximum of the 20-year averages across (A) the full temporal range of the model (six months); (B) spring survey months (March-May); and (C) fall survey months (September-November).

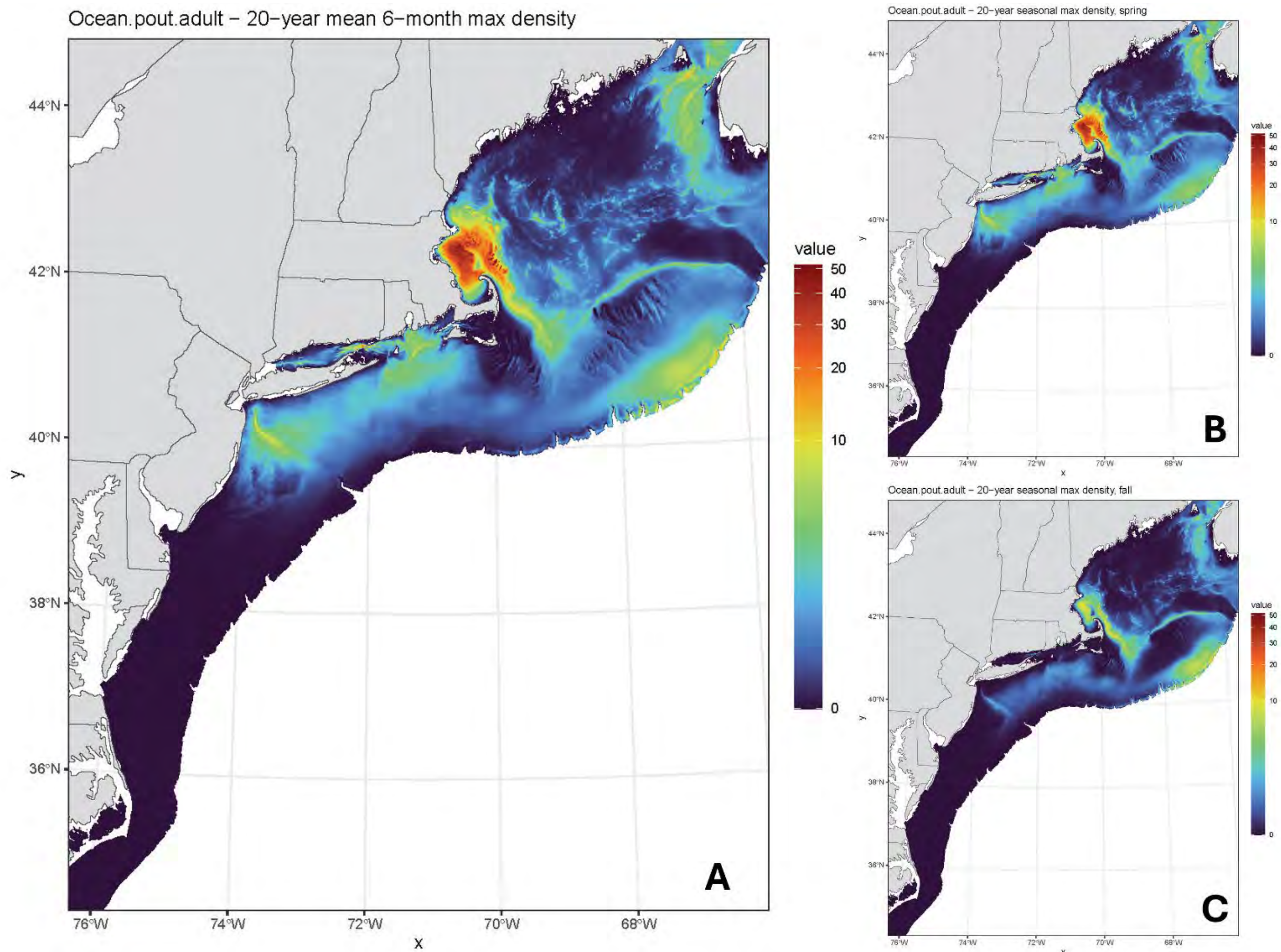

5.8 Offshore hake

Figure 62. 20-year maximum predicted density (species counts) quantiles for juvenile offshore hake (*Merluccius albidus*). Maps depict the maximum of the 20-year averages across (A) the full temporal range of the model (six months); (B) spring survey months (March-May); and (C) fall survey months (September-November).

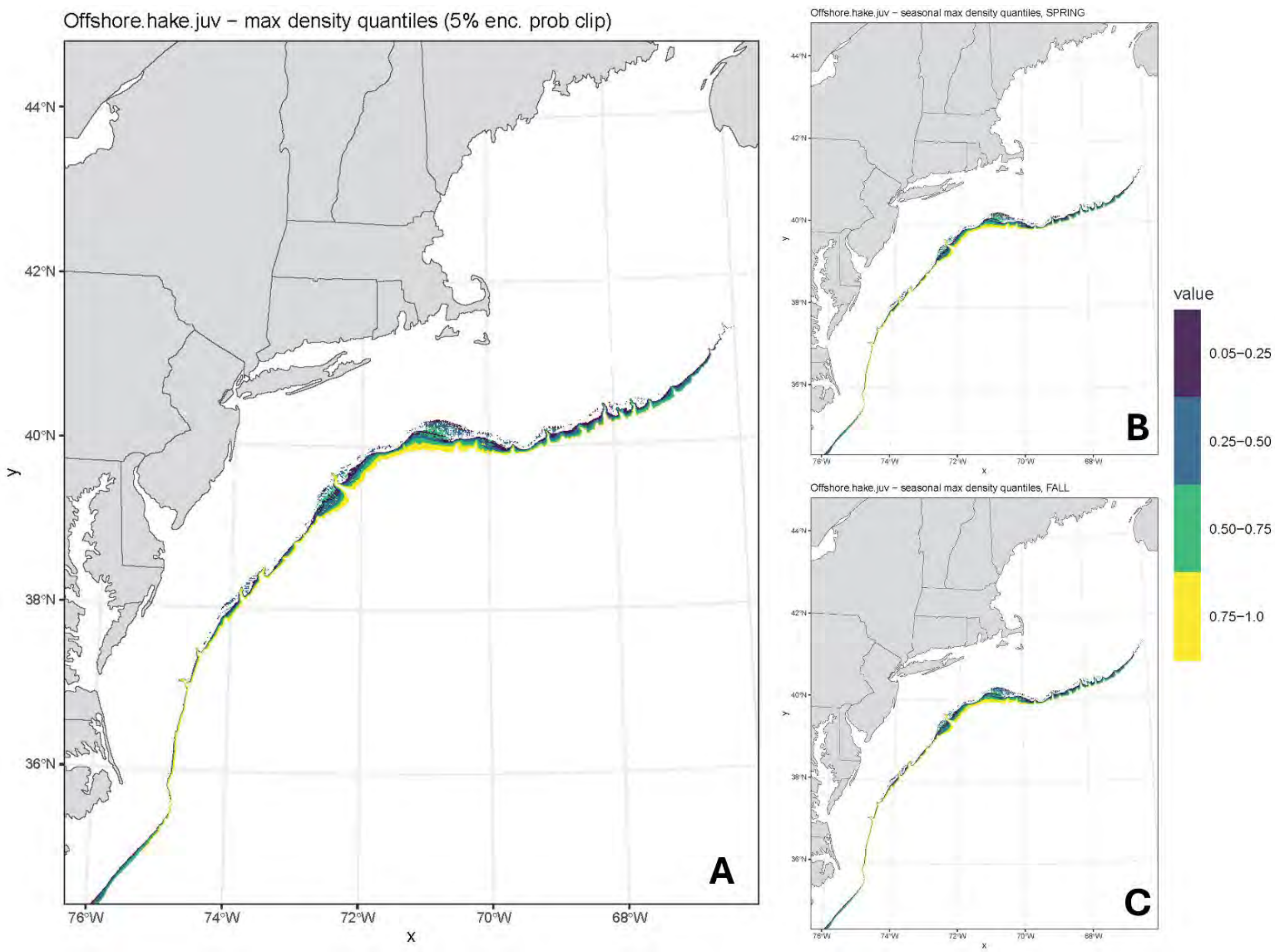

Figure 63. 20-year mean predicted density (species counts) for juvenile offshore hake (*Merluccius albidus*). Maps depict the maximum of the 20-year averages across (A) the full temporal range of the model (six months); (B) spring survey months (March-May); and (C) fall survey months (September-November).

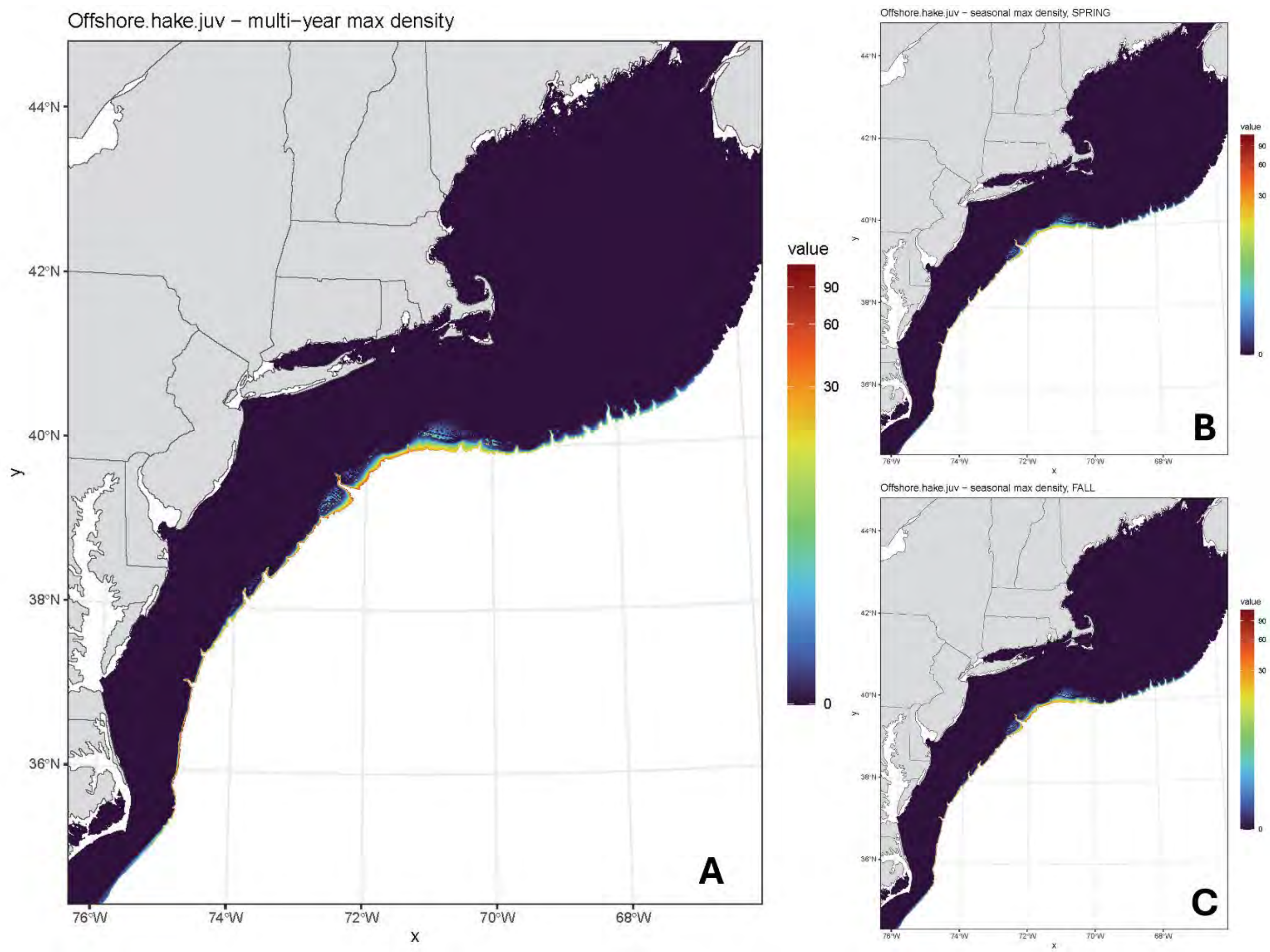

Figure 64. 20-year maximum predicted density (species counts) quantiles for adult offshore hake (*Merluccius albidus*). Maps depict the maximum of the 20-year averages across (A) the full temporal range of the model (six months); (B) spring survey months (March-May); and (C) fall survey months (September-November).

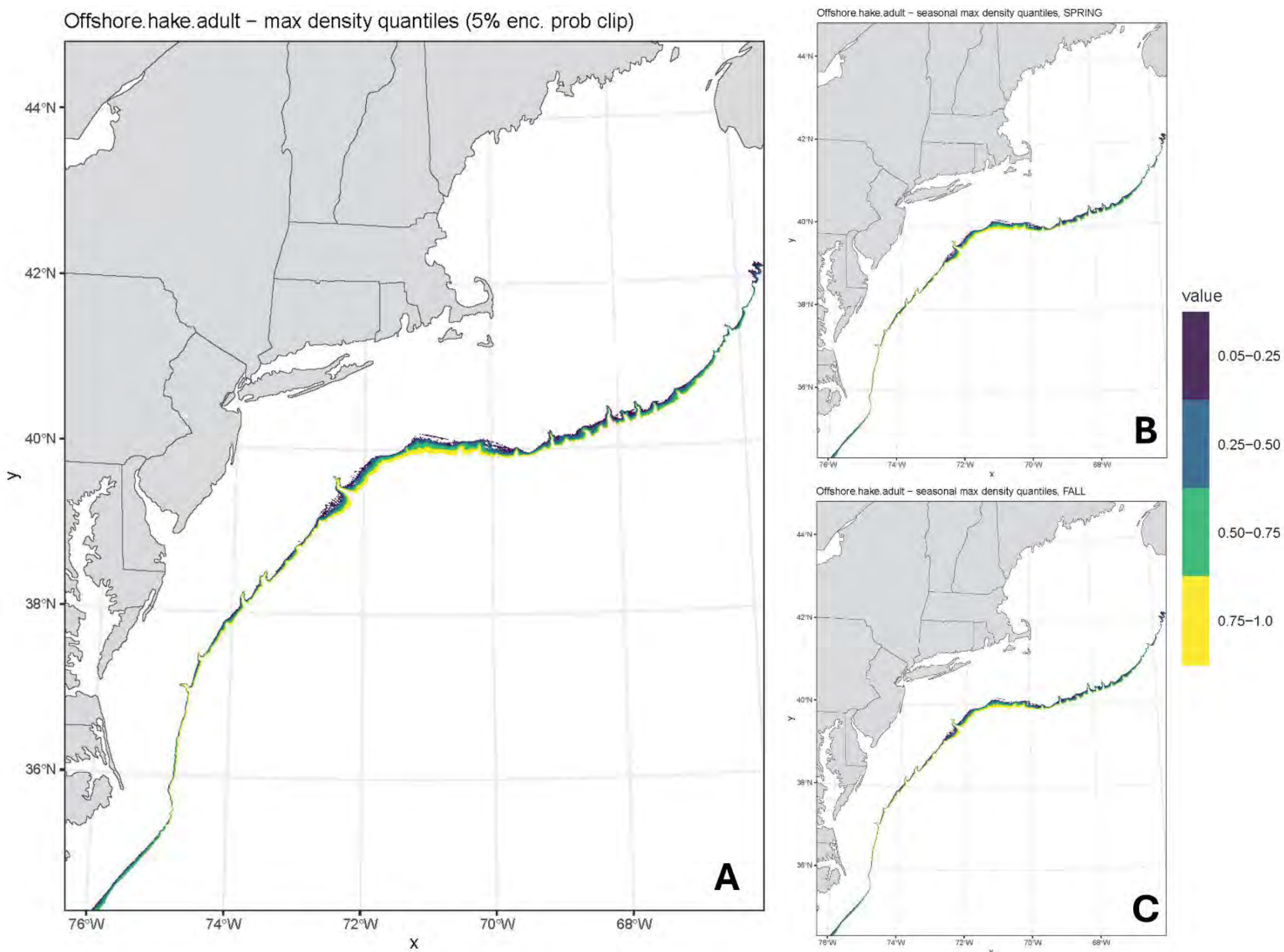

Figure 65. 20-year mean predicted density (species counts) for adult offshore hake (*Merluccius albidus*). Maps depict the maximum of the 20-year averages across (A) the full temporal range of the model (six months); (B) spring survey months (March-May); and (C) fall survey months (September-November).

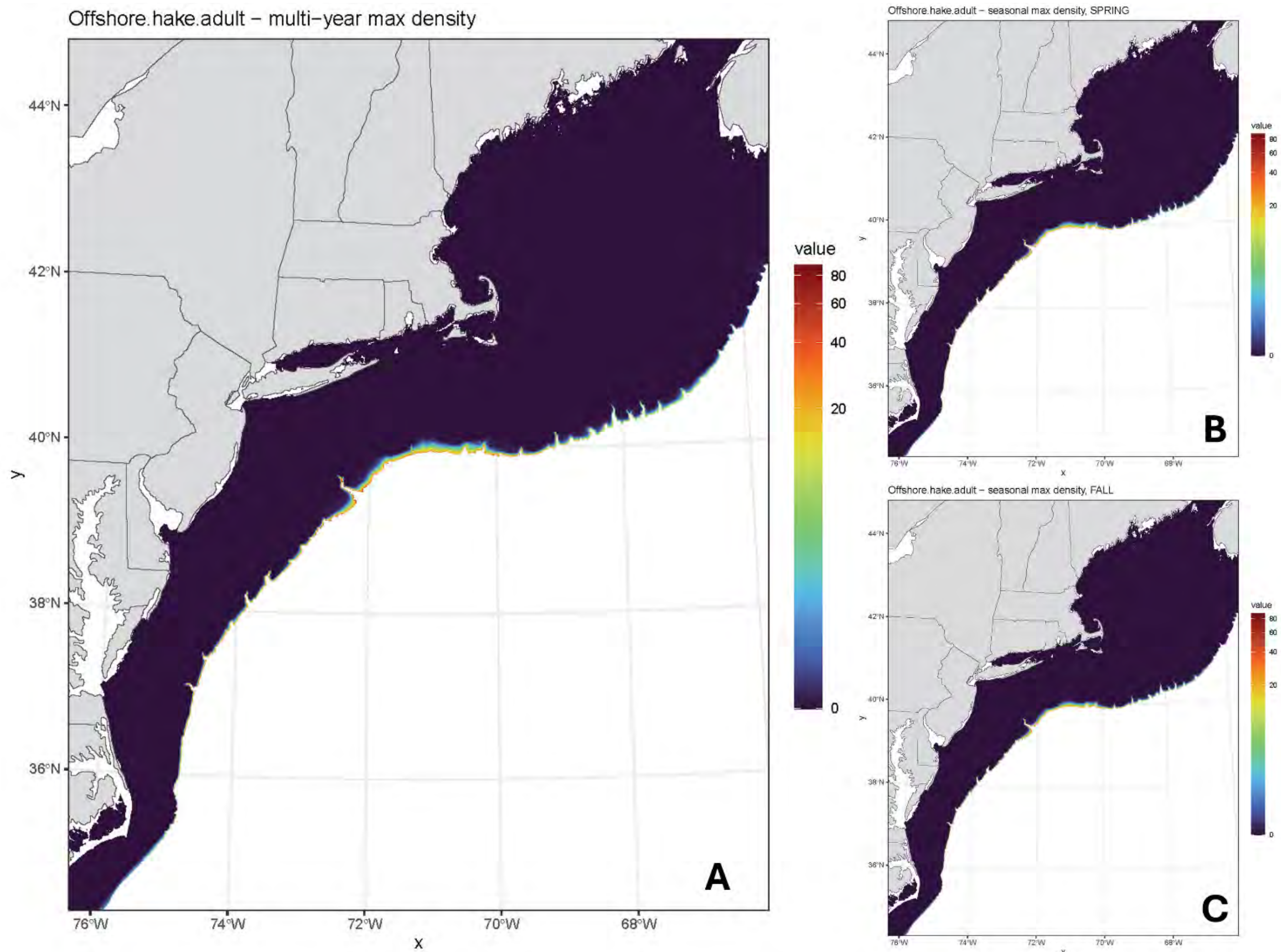

5.9 Pollock

Figure 66. 20-year maximum predicted density (species counts) quantiles for juvenile pollock (*Pollachius virens*). Maps depict the maximum of the 20-year averages across (A) the full temporal range of the model (six months); (B) spring survey months (March-May); and (C) fall survey months (September-November).

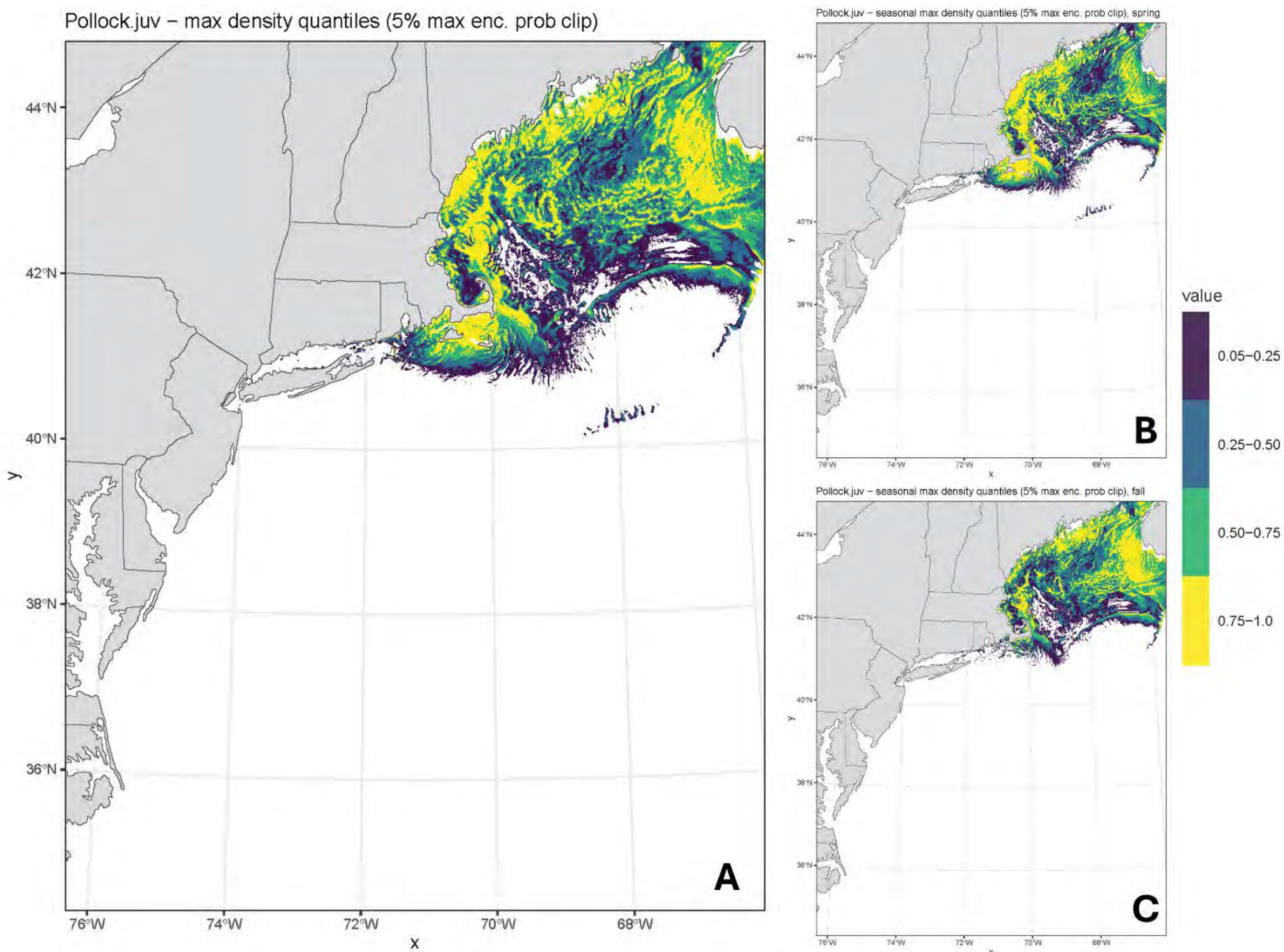

Figure 67. 20-year mean predicted density (species counts) for juvenile pollock (*Pollachius virens*). Maps depict the maximum of the 20-year averages across (A) the full temporal range of the model (six months); (B) spring survey months (March-May); and (C) fall survey months (September-November).

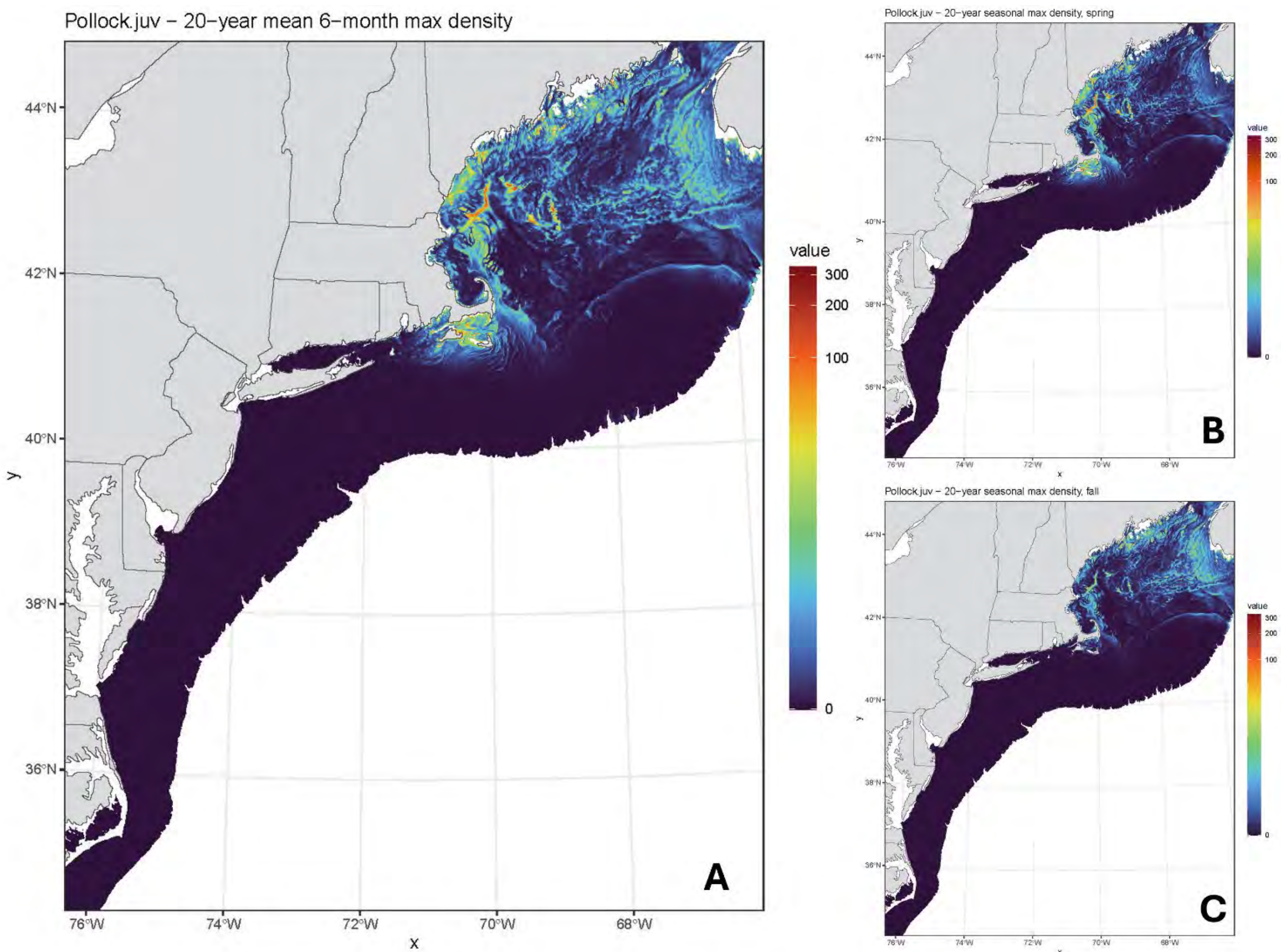

Figure 68. 20-year maximum predicted density (species counts) quantiles for adult pollock (*Pollachius virens*). Maps depict the maximum of the 20-year averages across (A) the full temporal range of the model (six months); (B) spring survey months (March-May); and (C) fall survey months (September-November).

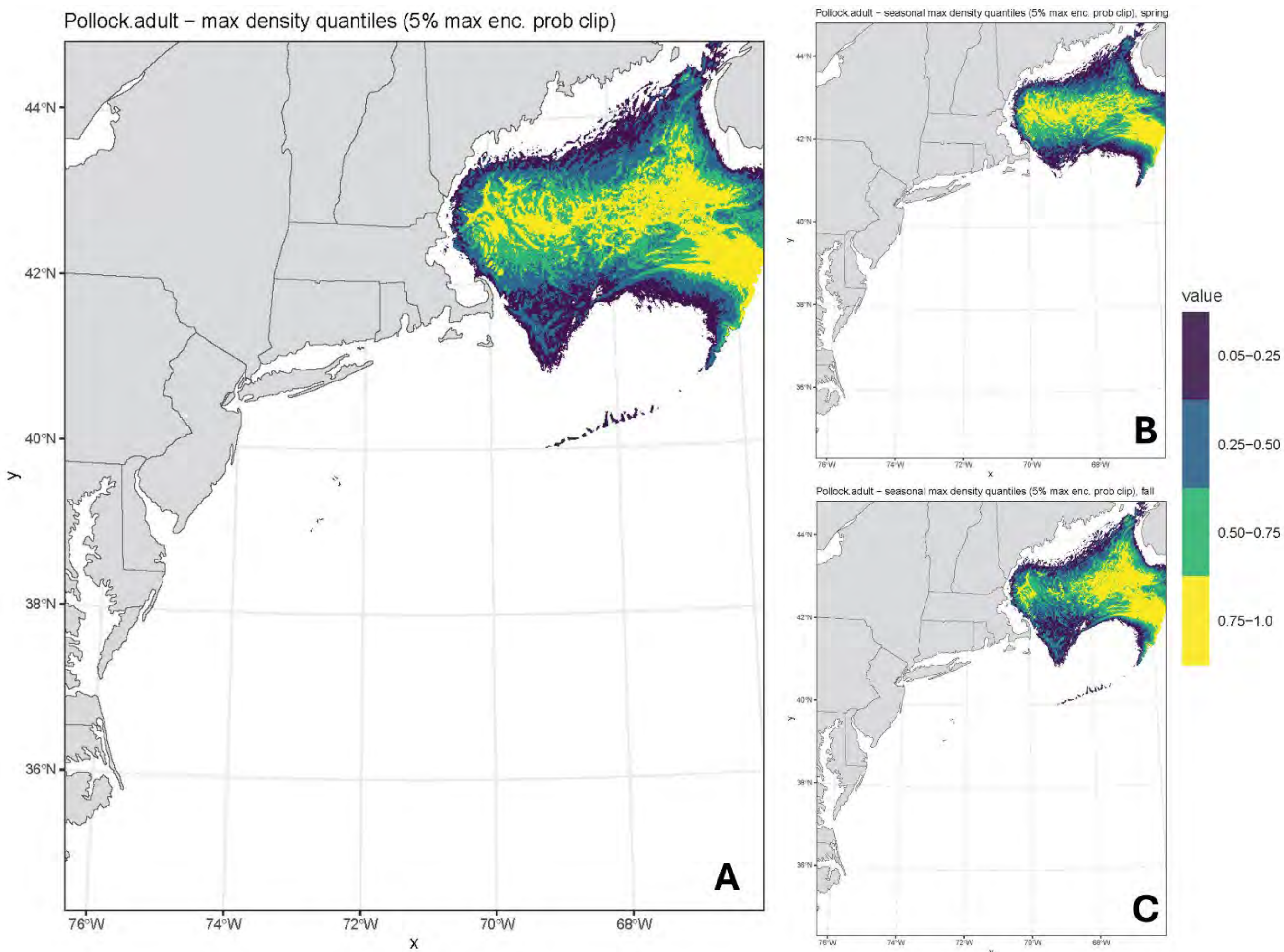

Figure 69. 20-year mean predicted density (species counts) for adult pollock (*Pollachius virens*). Maps depict the maximum of the 20-year averages across (A) the full temporal range of the model (six months); (B) spring survey months (March-May); and (C) fall survey months (September-November).

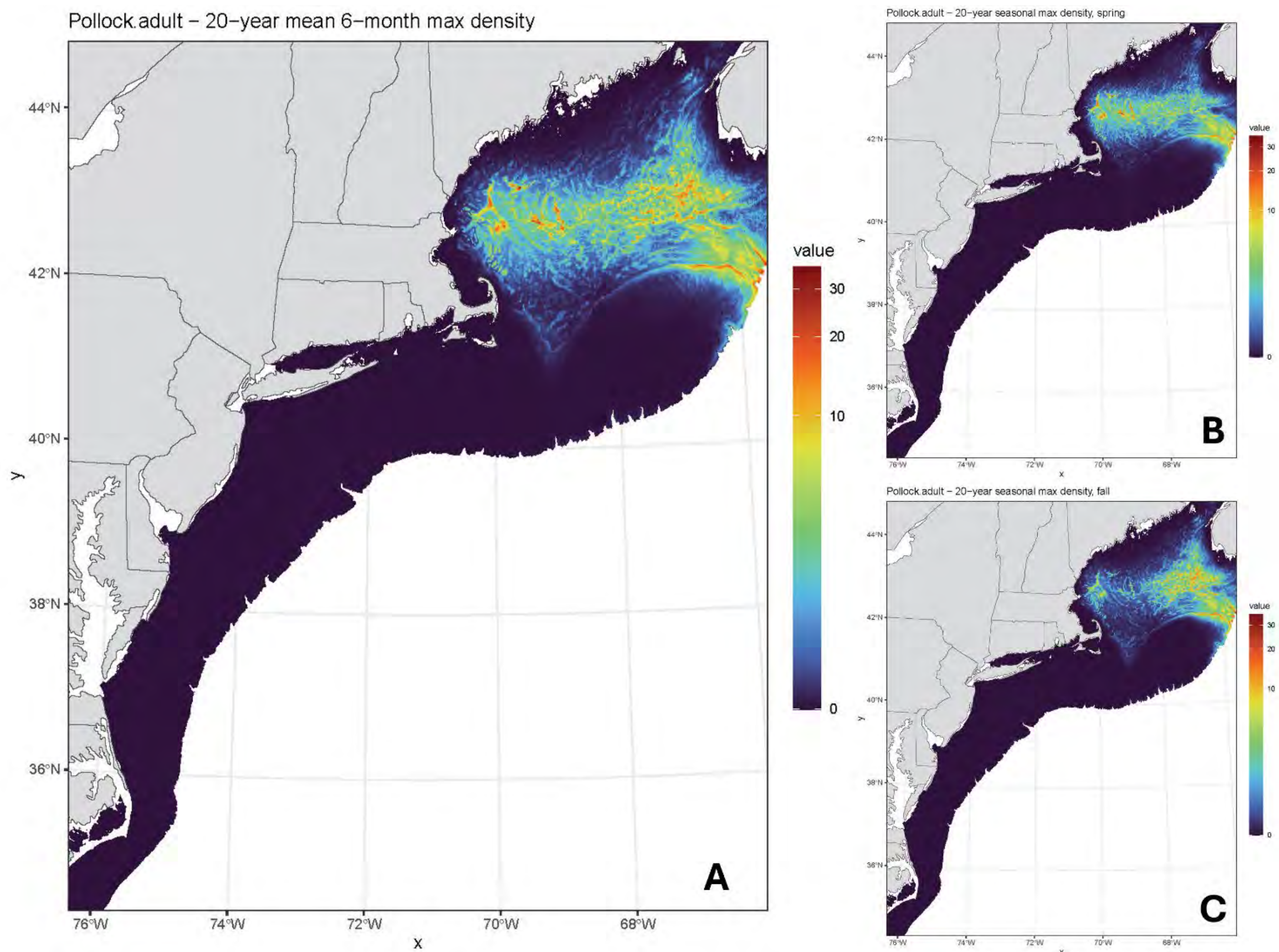

5.10 Red hake

Figure 70. 20-year maximum predicted density (species counts) quantiles for juvenile red hake (*Urophycis chuss*). Maps depict the maximum of the 20-year averages across (A) the full temporal range of the model (six months); (B) spring survey months (March-May); and (C) fall survey months (September-November).

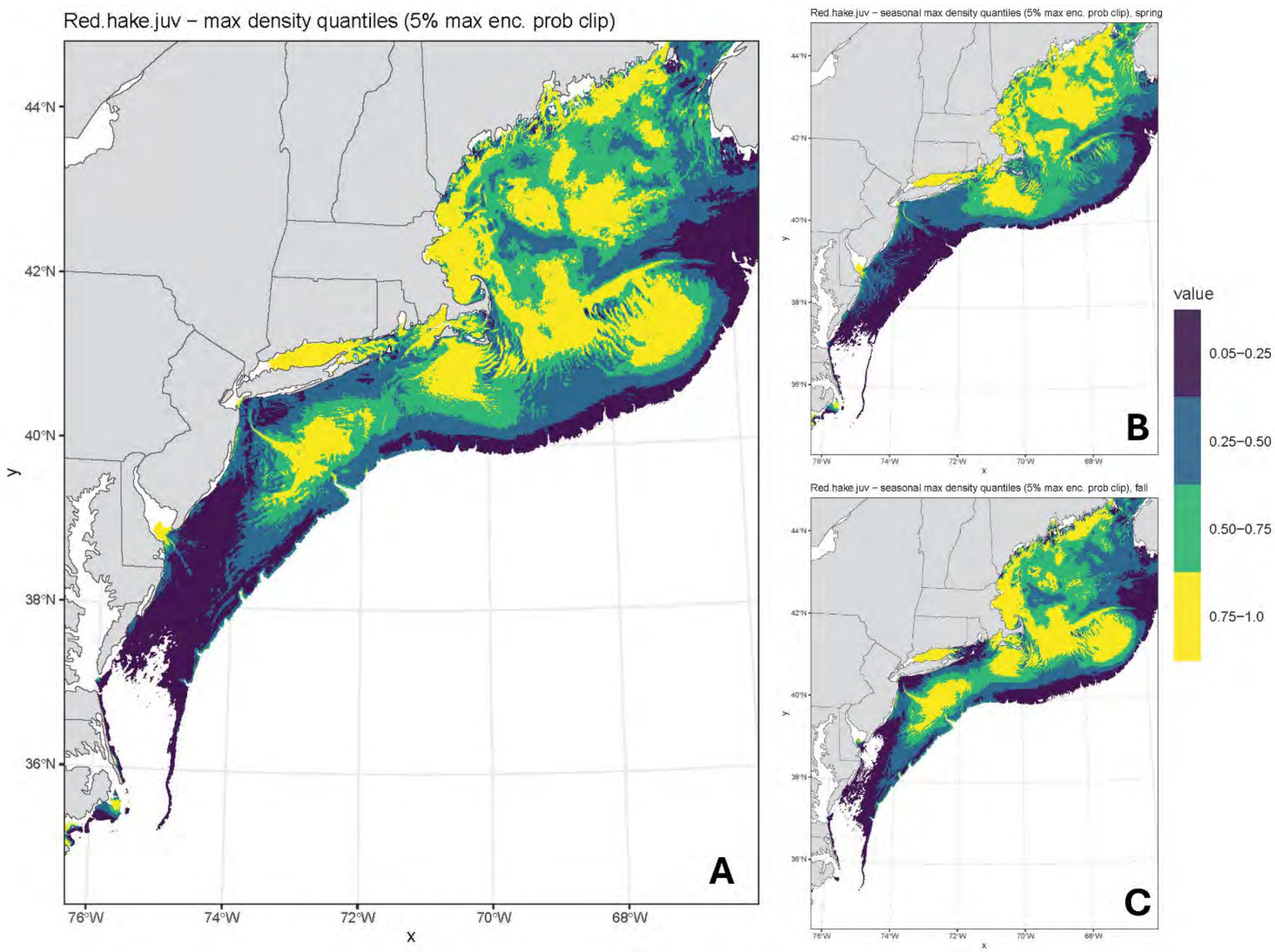

Figure 71. 20-year mean predicted density (species counts) for juvenile red hake (*Urophycis chuss*). Maps depict the maximum of the 20-year averages across (A) the full temporal range of the model (six months); (B) spring survey months (March-May); and (C) fall survey months (September-November).

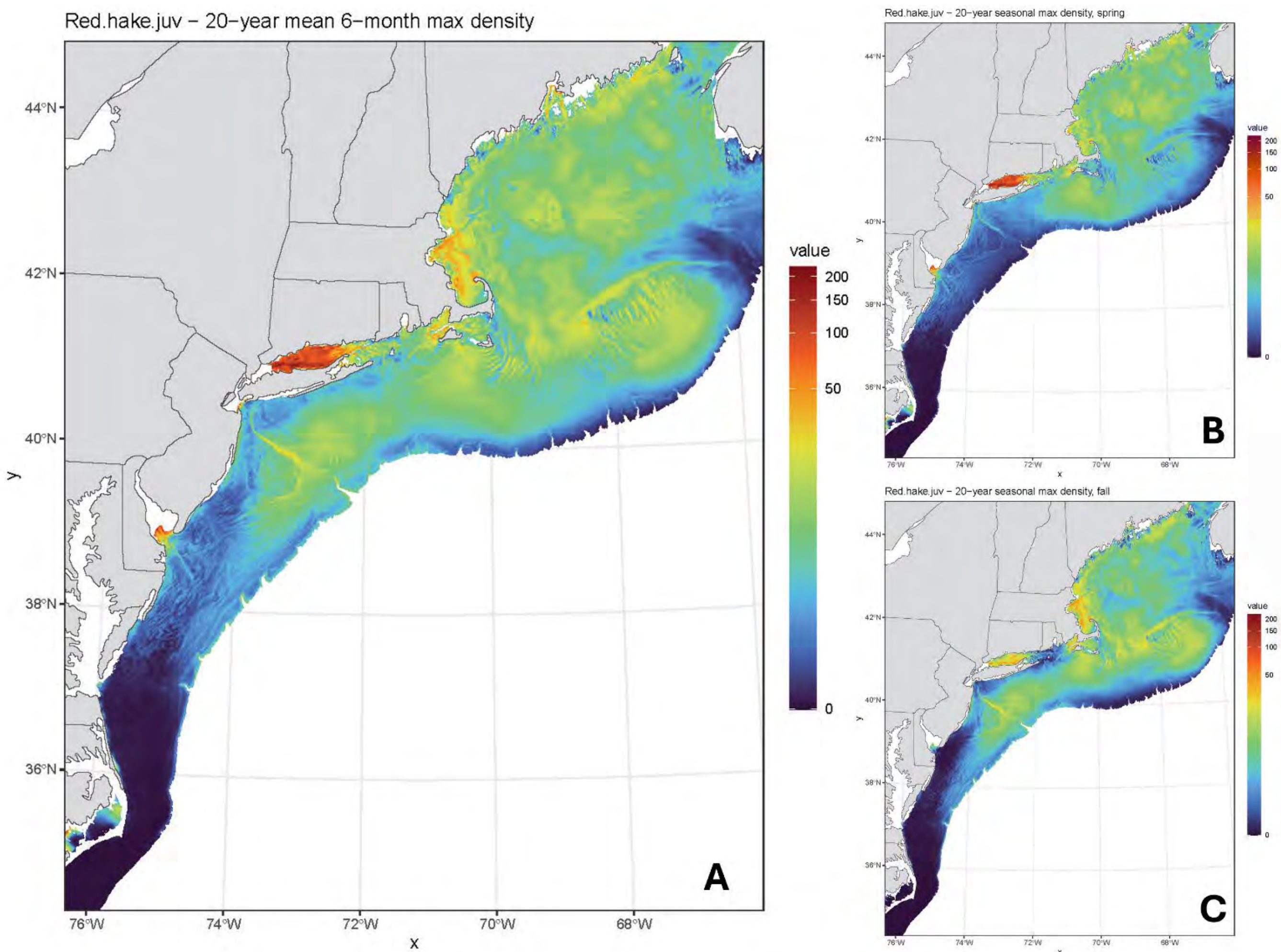

Figure 72. 20-year maximum predicted density (species counts) quantiles for adult red hake (*Urophycis chuss*). Maps depict the maximum of the 20-year averages across (A) the full temporal range of the model (six months); (B) spring survey months (March-May); and (C) fall survey months (September-November).

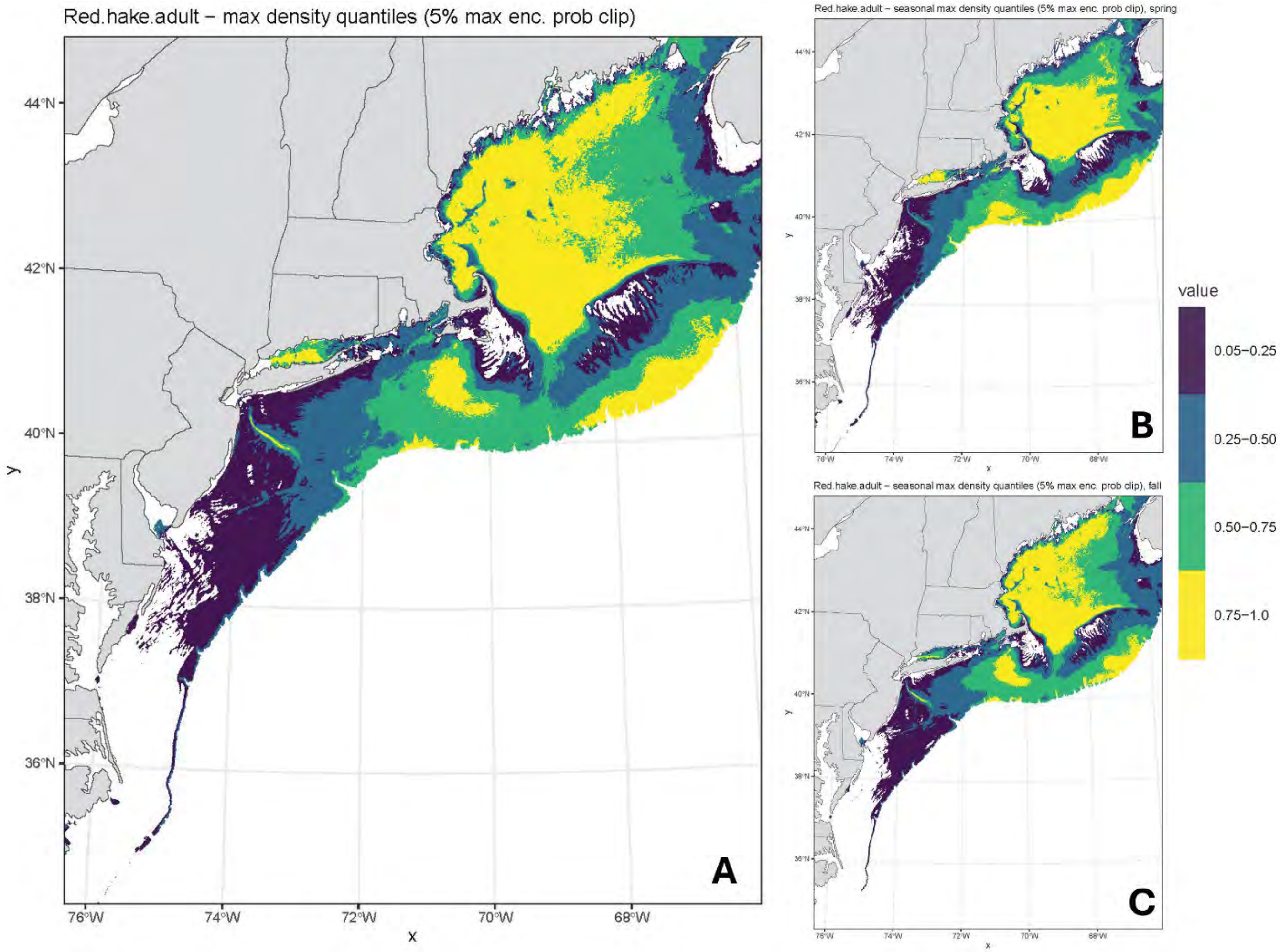

Figure 73. 20-year mean predicted density (species counts) for adult red hake (*Urophycis chuss*). Maps depict the maximum of the 20-year averages across (A) the full temporal range of the model (six months); (B) spring survey months (March-May); and (C) fall survey months (September-November).

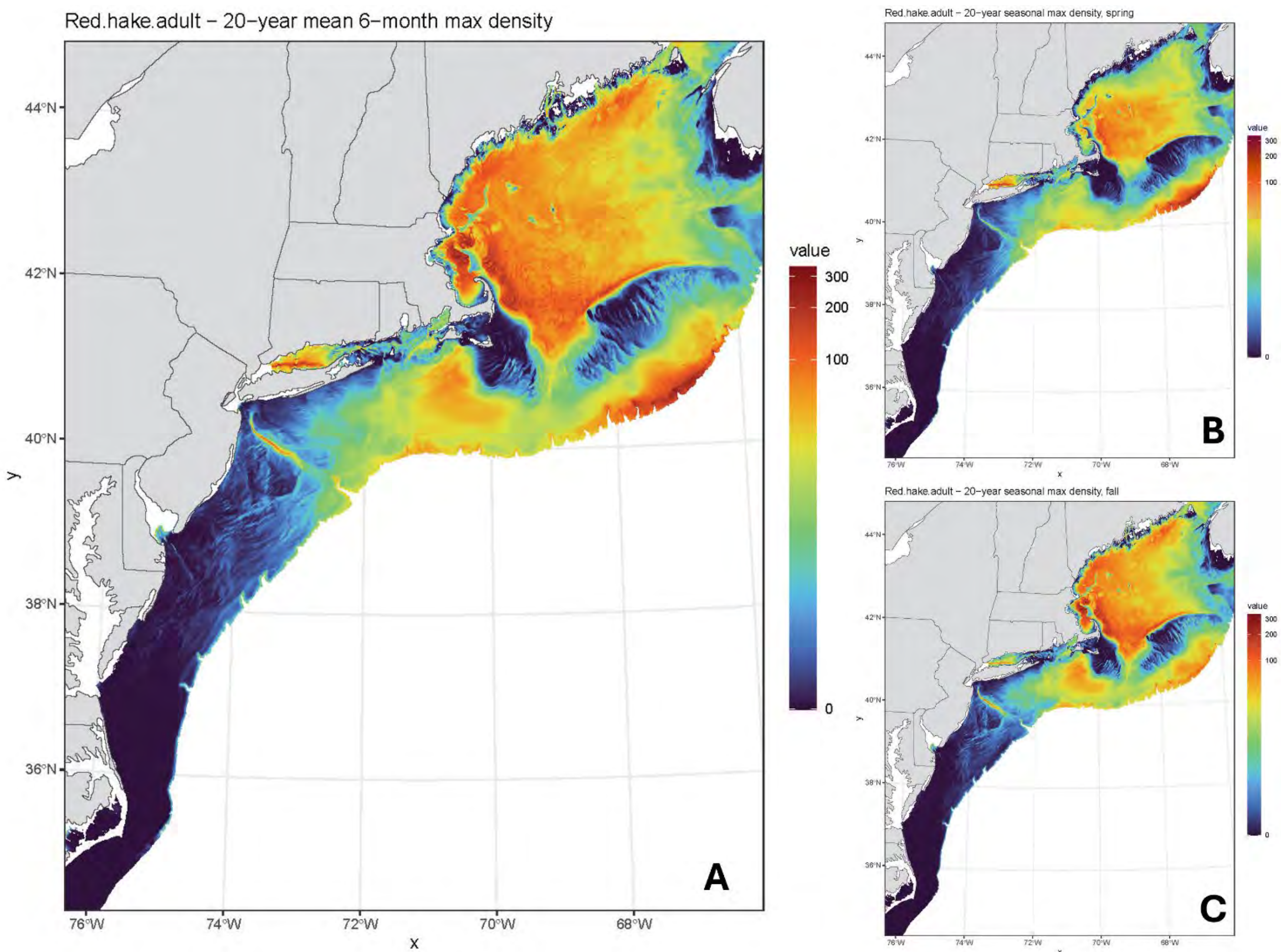

5.11 Silver Hake

Figure 74. 20-year maximum predicted density (species counts) quantiles for juvenile silver hake (*Merluccius bilinearis*). Maps depict the maximum of the 20-year averages across (A) the full temporal range of the model (six months); (B) spring survey months (March-May); and (C) fall survey months (September-November).

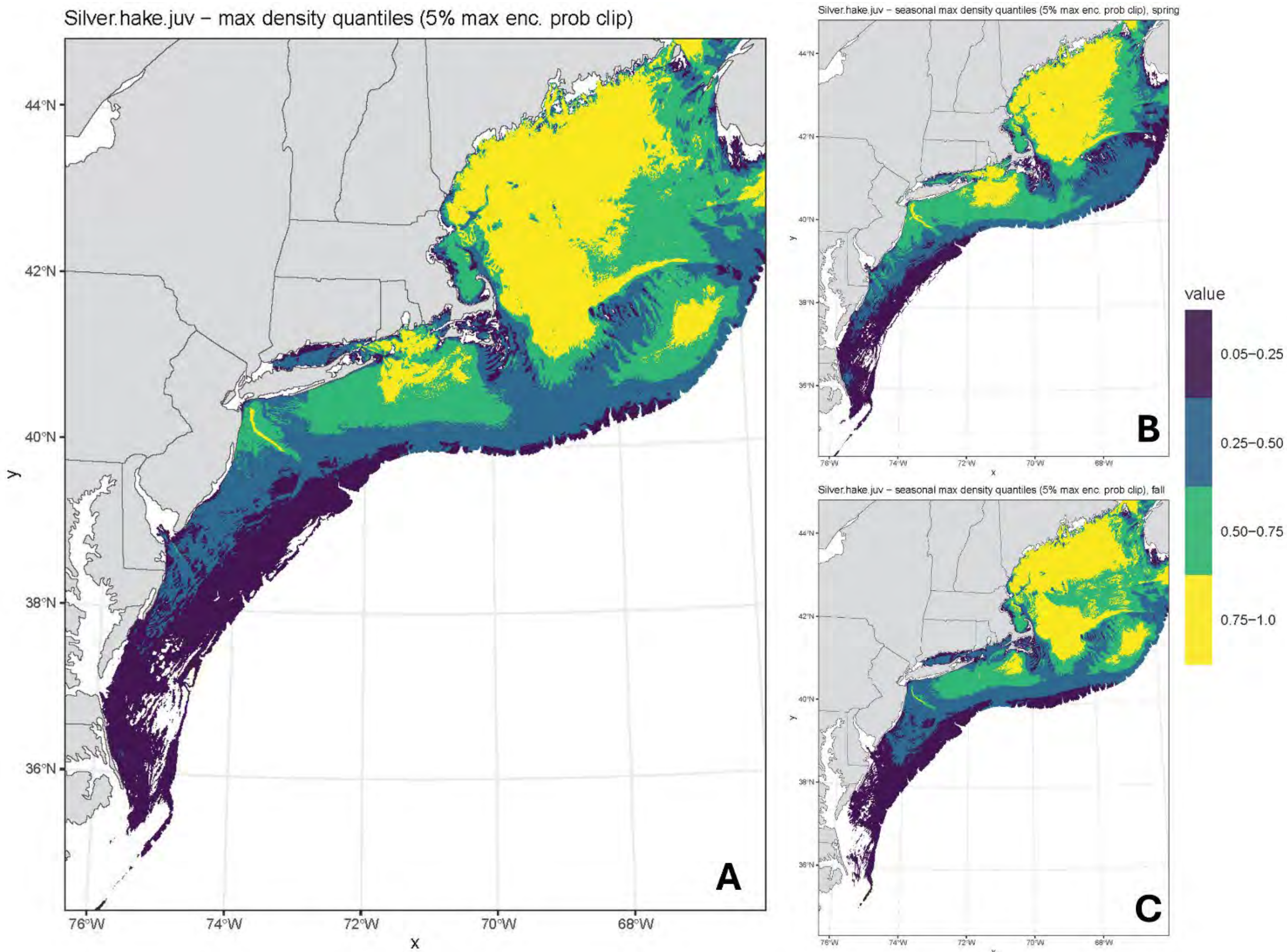

Figure 75. 20-year mean predicted density (species counts) for juvenile silver hake (*Merluccius bilinearis*). Maps depict the maximum of the 20-year averages across (A) the full temporal range of the model (six months); (B) spring survey months (March-May); and (C) fall survey months (September-November).

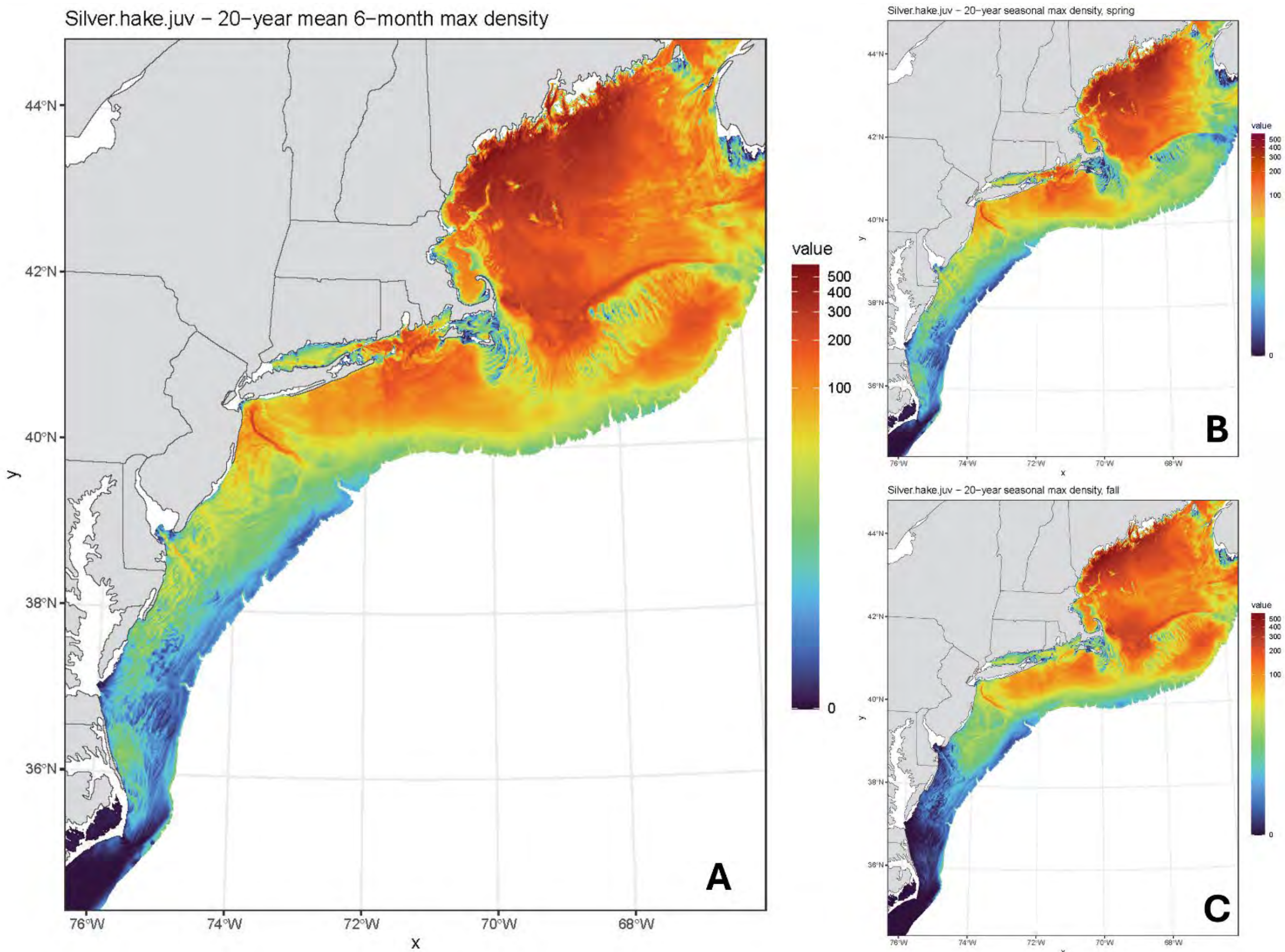

Figure 76. 20-year maximum predicted density (species counts) quantiles for adult silver hake (*Merluccius bilinearis*). Maps depict the maximum of the 20-year averages across (A) the full temporal range of the model (six months); (B) spring survey months (March-May); and (C) fall survey months (September-November).

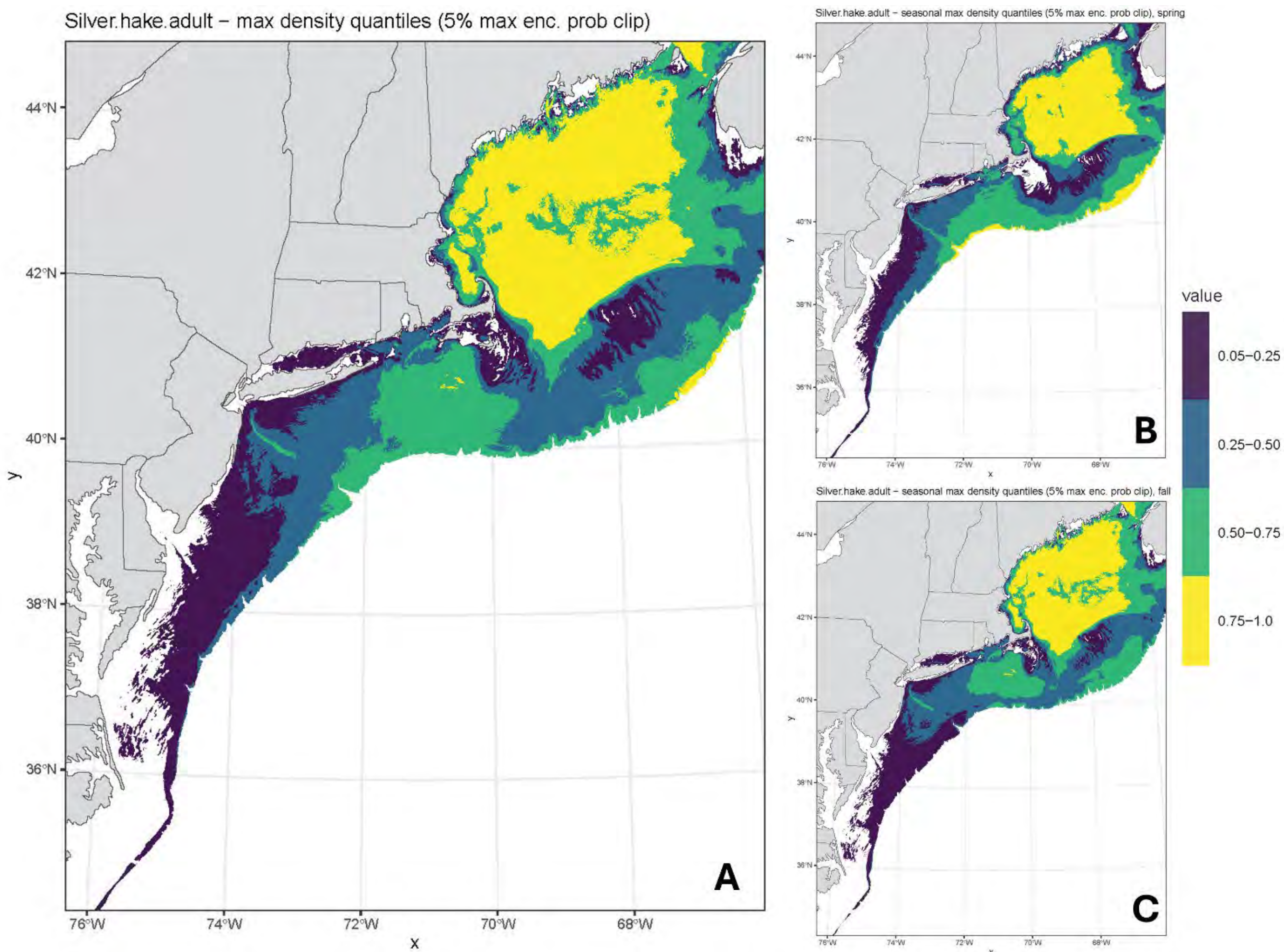

Figure 77. 20-year mean predicted density (species counts) for adult silver hake (*Merluccius bilinearis*). Maps depict the maximum of the 20-year averages across (A) the full temporal range of the model (six months); (B) spring survey months (March-May); and (C) fall survey months (September-November).

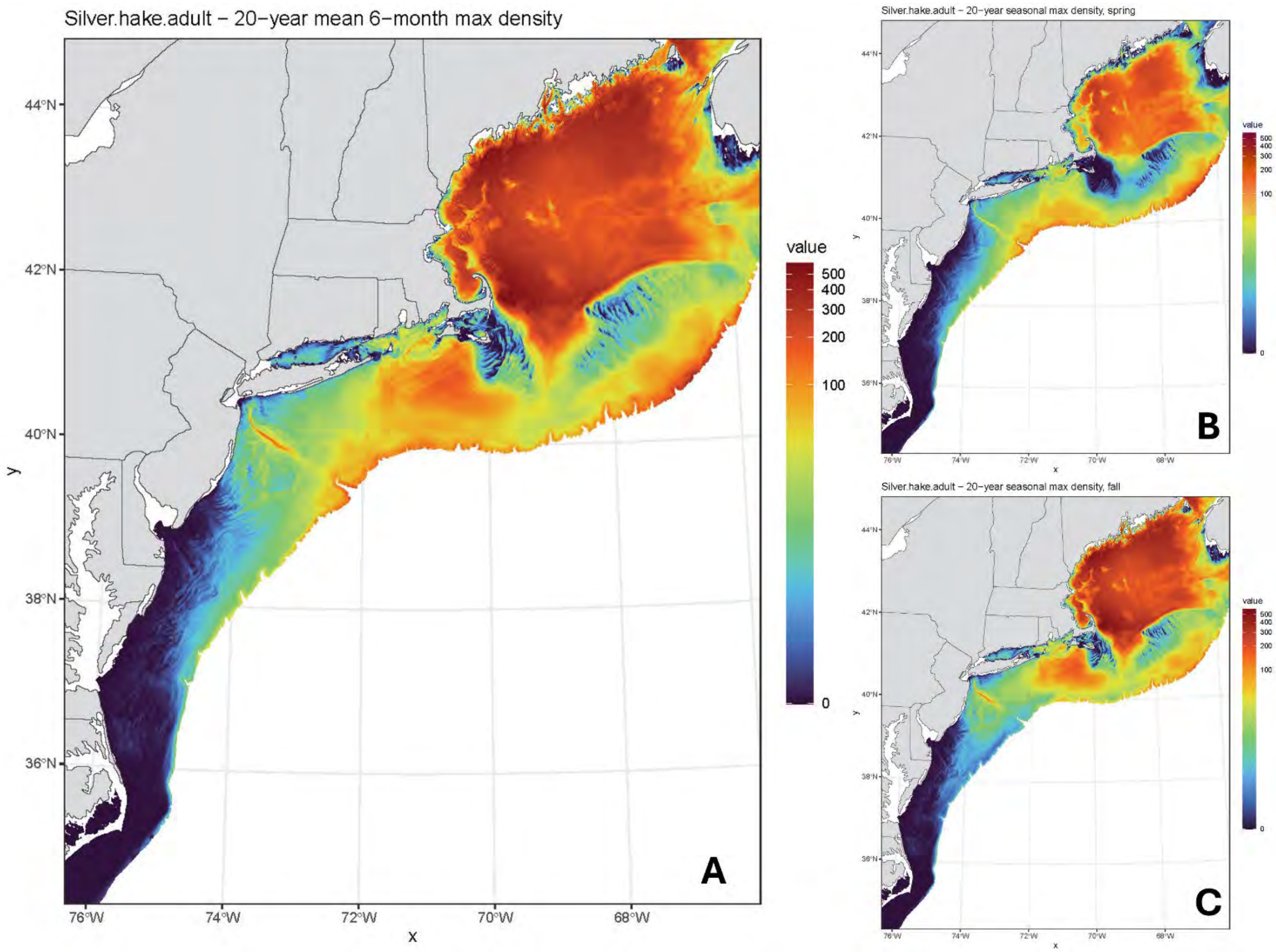

5.12 White hake

Figure 78. 20-year maximum predicted density (species counts) quantiles for juvenile white hake (*Urophycis tenuis*). Maps depict the maximum of the 20-year averages across (A) the full temporal range of the model (six months); (B) spring survey months (March-May); and (C) fall survey months (September-November).

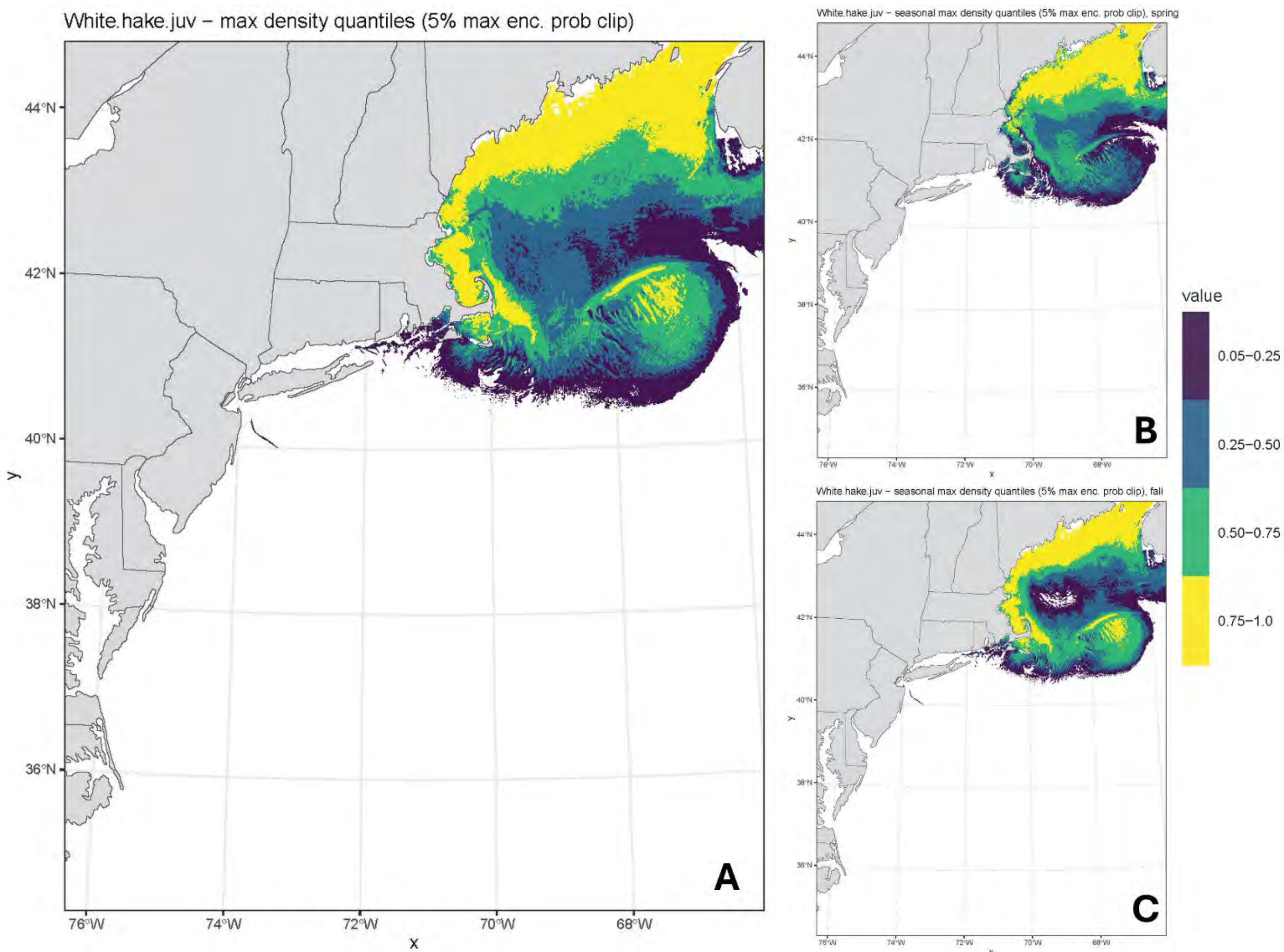

Figure 79. 20-year mean predicted density (species counts) for juvenile white hake (*Urophycis tenuis*). Maps depict the maximum of the 20-year averages across (A) the full temporal range of the model (six months); (B) spring survey months (March-May); and (C) fall survey months (September-November).

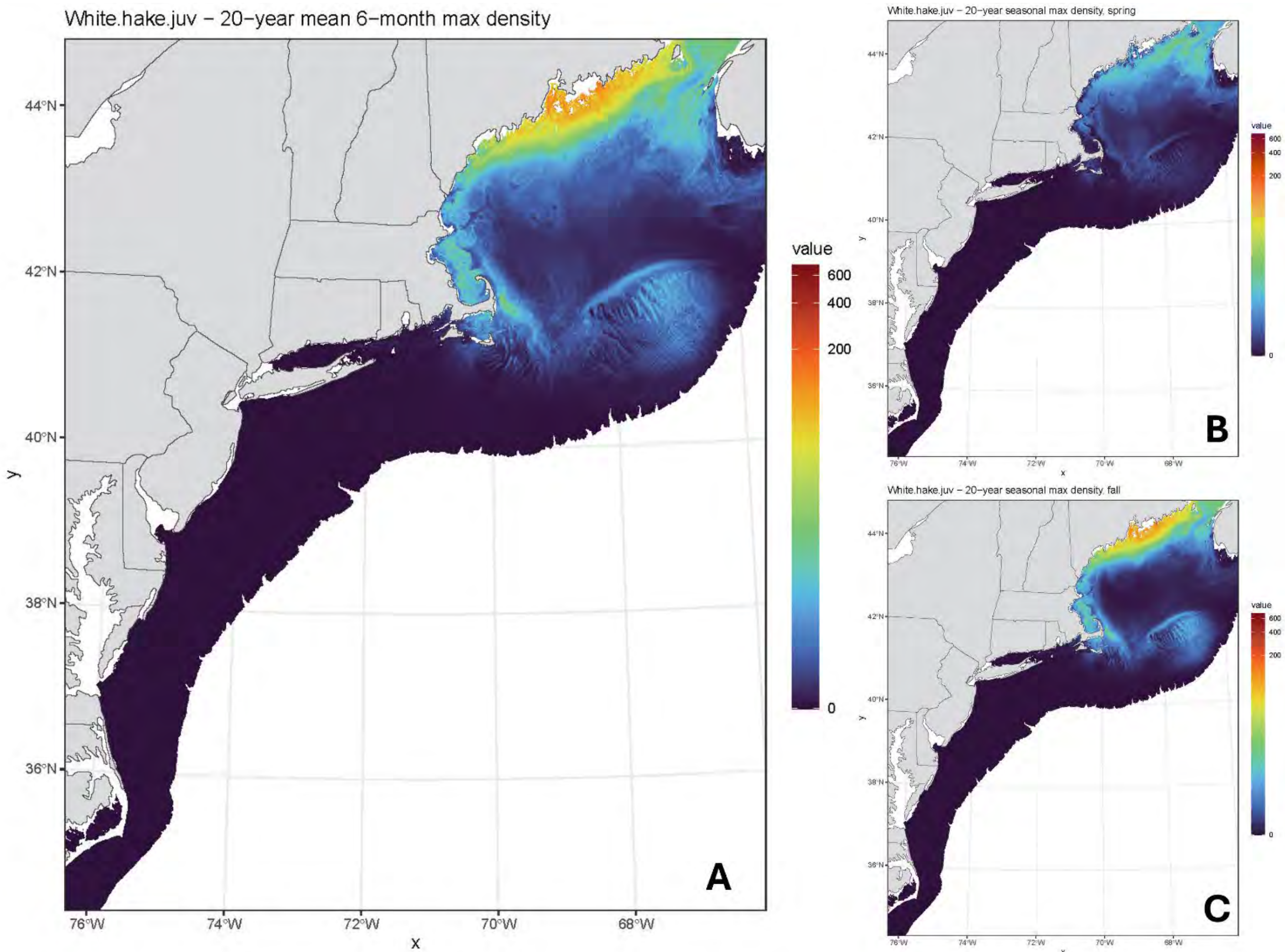

Figure 80. 20-year maximum predicted density (species counts) quantiles for adult white hake (*Urophycis tenuis*). Maps depict the maximum of the 20-year averages across (A) the full temporal range of the model (six months); (B) spring survey months (March-May); and (C) fall survey months (September-November).

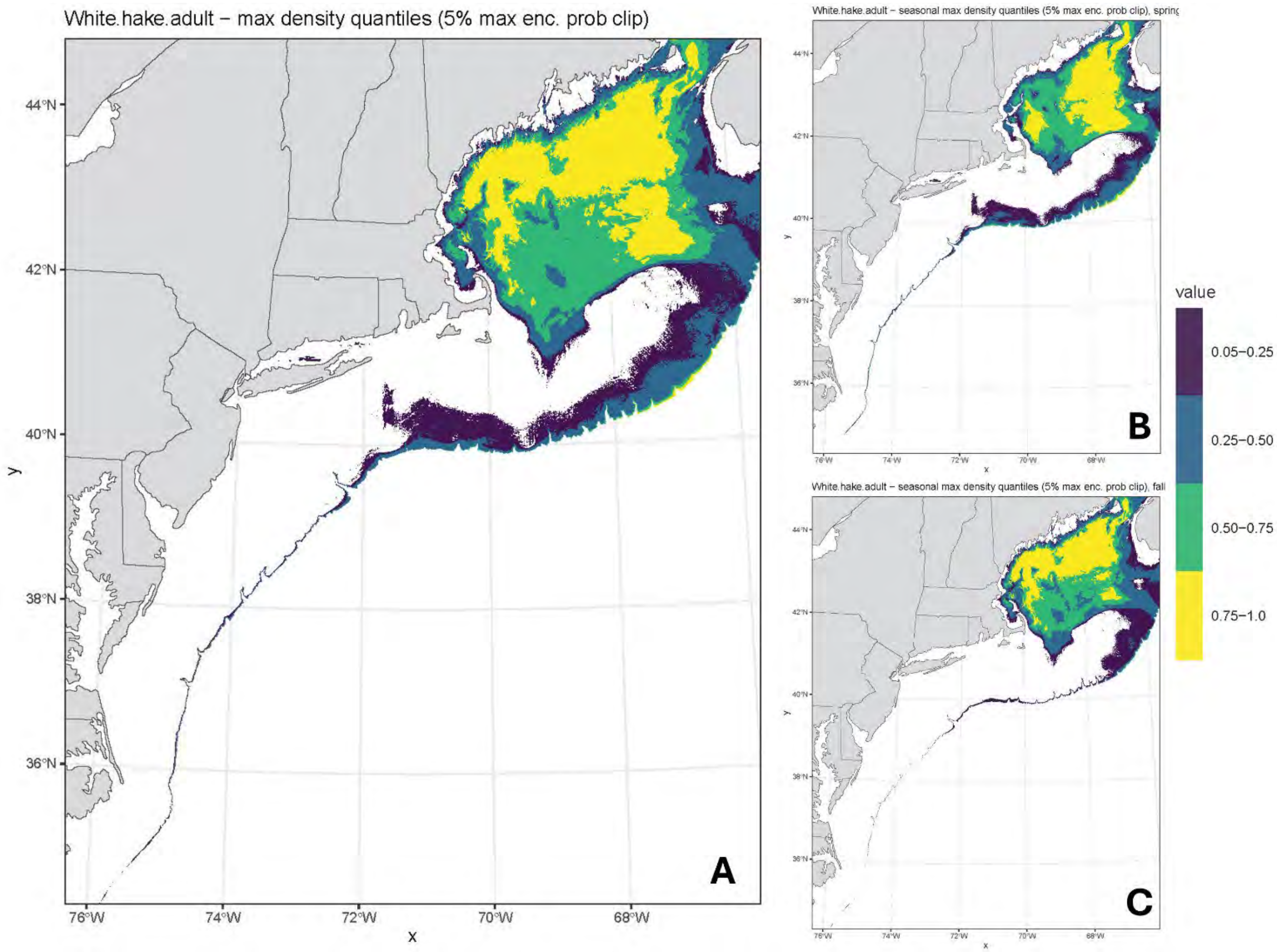

Figure 81. 20-year mean predicted density (species counts) for adult white hake (*Urophycis tenuis*). Maps depict the maximum of the 20-year averages across (A) the full temporal range of the model (six months); (B) spring survey months (March-May); and (C) fall survey months (September-November).

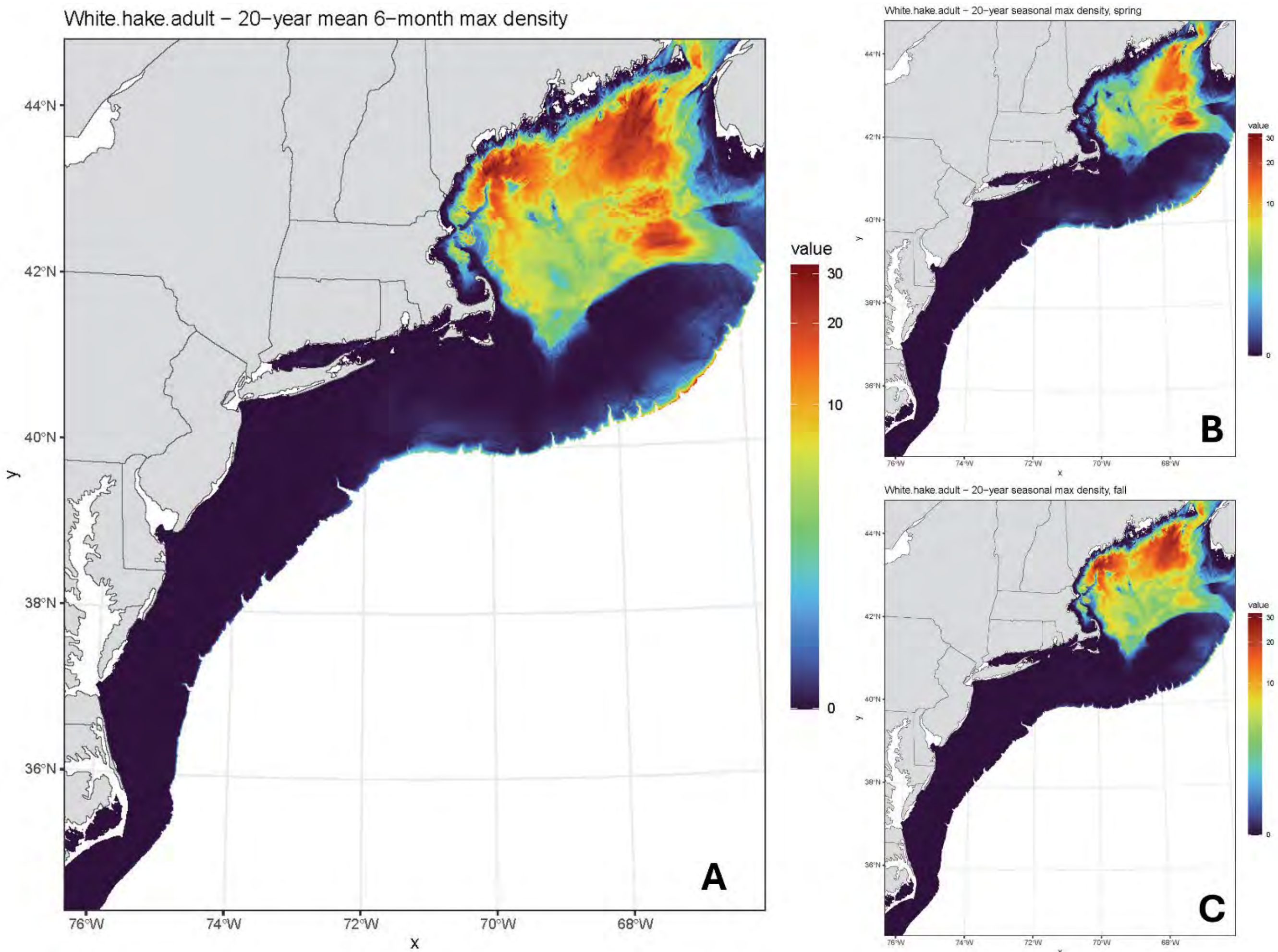

5.13 WINDOWPANE FLOUNDER

Figure 82. 20-year maximum predicted density (species counts) quantiles for juvenile windowpane flounder (*Scophthalmus aquosus*). Maps depict the maximum of the 20-year averages across (A) the full temporal range of the model (six months); (B) spring survey months (March-May); and (C) fall survey months (September-November).

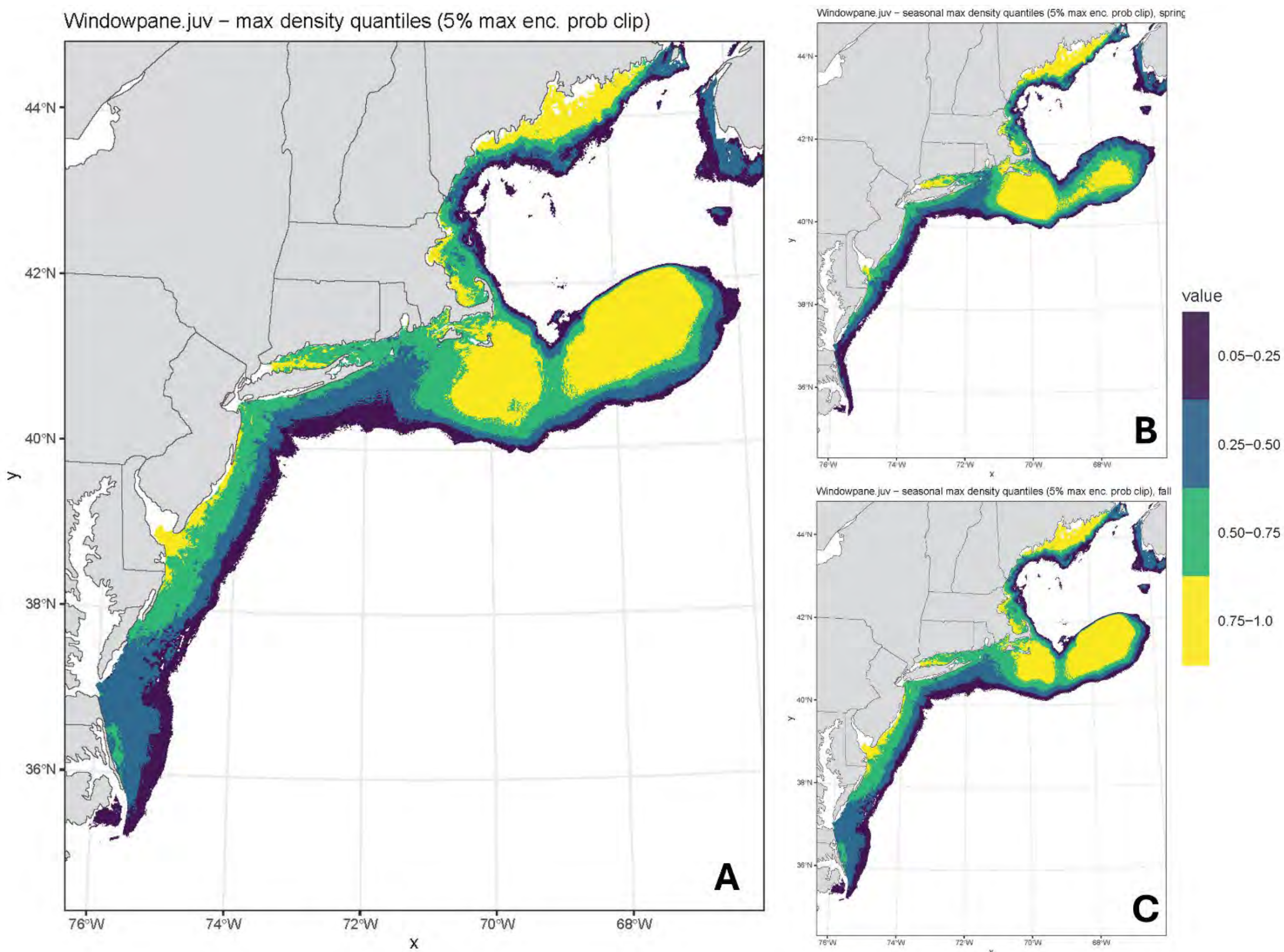

Figure 83. 20-year mean predicted density (species counts) for juvenile windowpane flounder (*Scophthalmus aquosus*). Maps depict the maximum of the 20-year averages across (A) the full temporal range of the model (six months); (B) spring survey months (March-May); and (C) fall survey months (September-November).

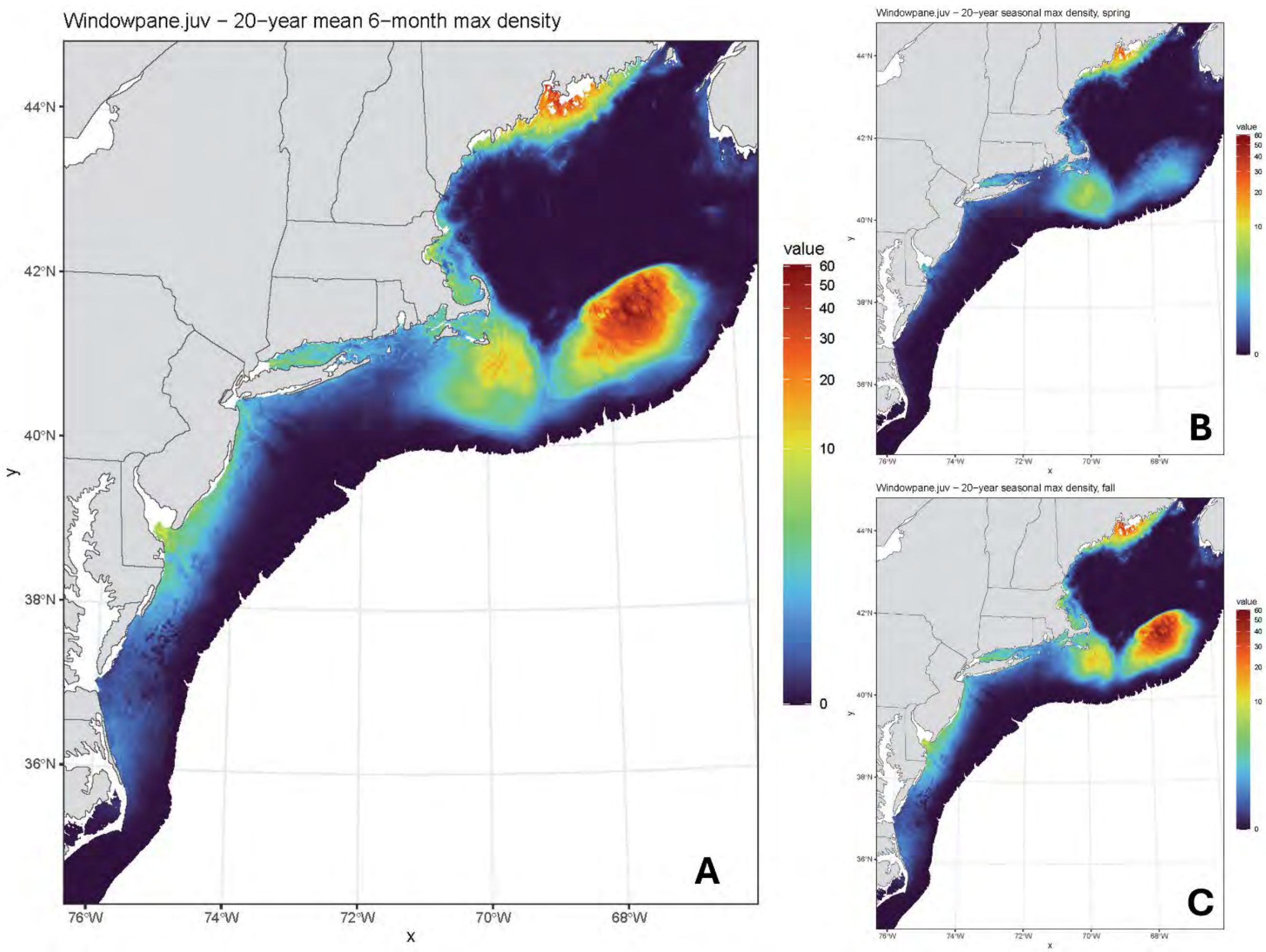

Figure 84. 20-year maximum predicted density (species counts) quantiles for adult windowpane flounder (*Scophthalmus aquosus*). Maps depict the maximum of the 20-year averages across (A) the full temporal range of the model (six months); (B) spring survey months (March-May); and (C) fall survey months (September-November).

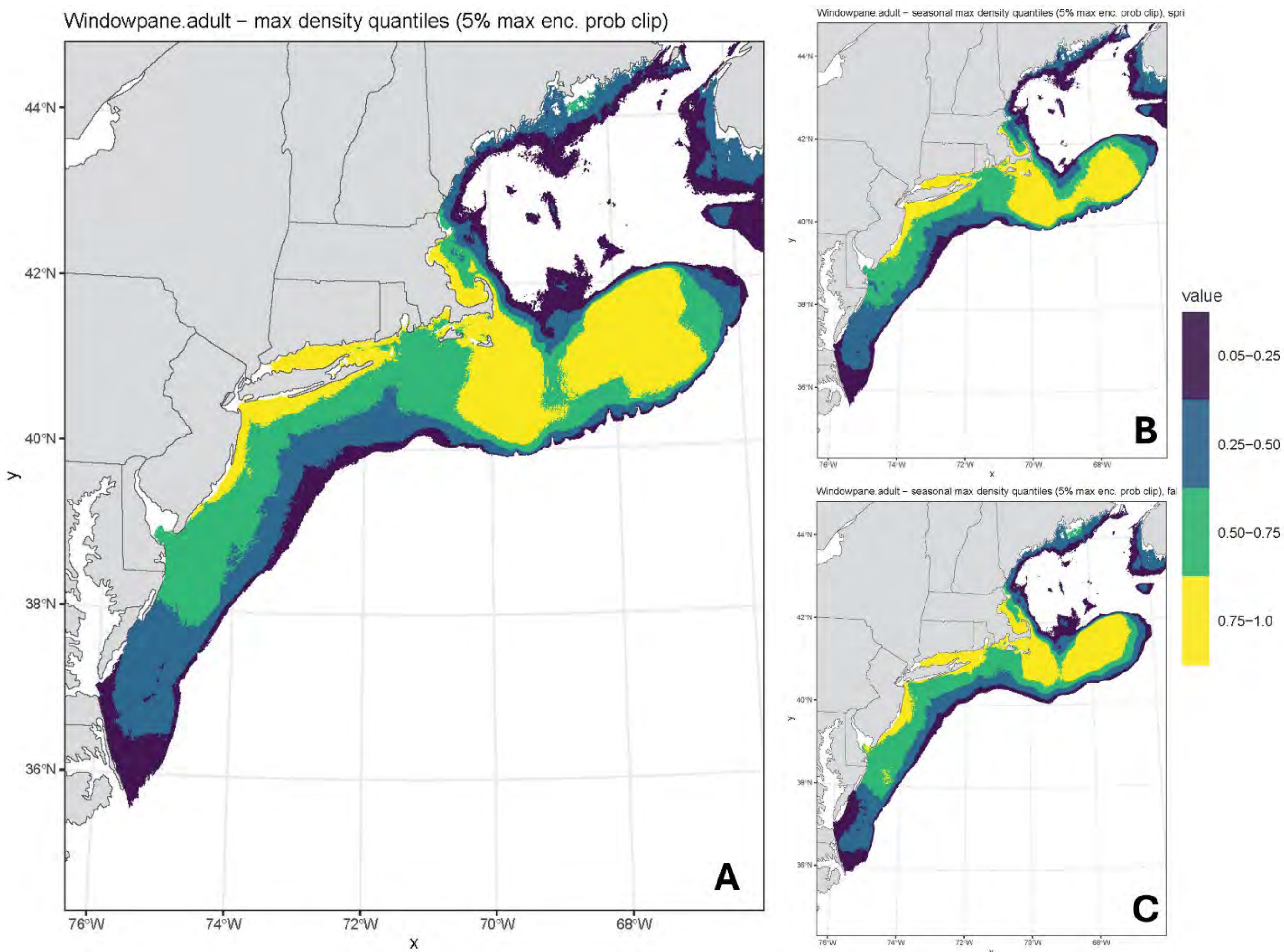

Figure 85. 20-year mean predicted density (species counts) for adult windowpane flounder (*Scophthalmus aquosus*). Maps depict the maximum of the 20-year averages across (A) the full temporal range of the model (six months); (B) spring survey months (March-May); and (C) fall survey months (September-November).

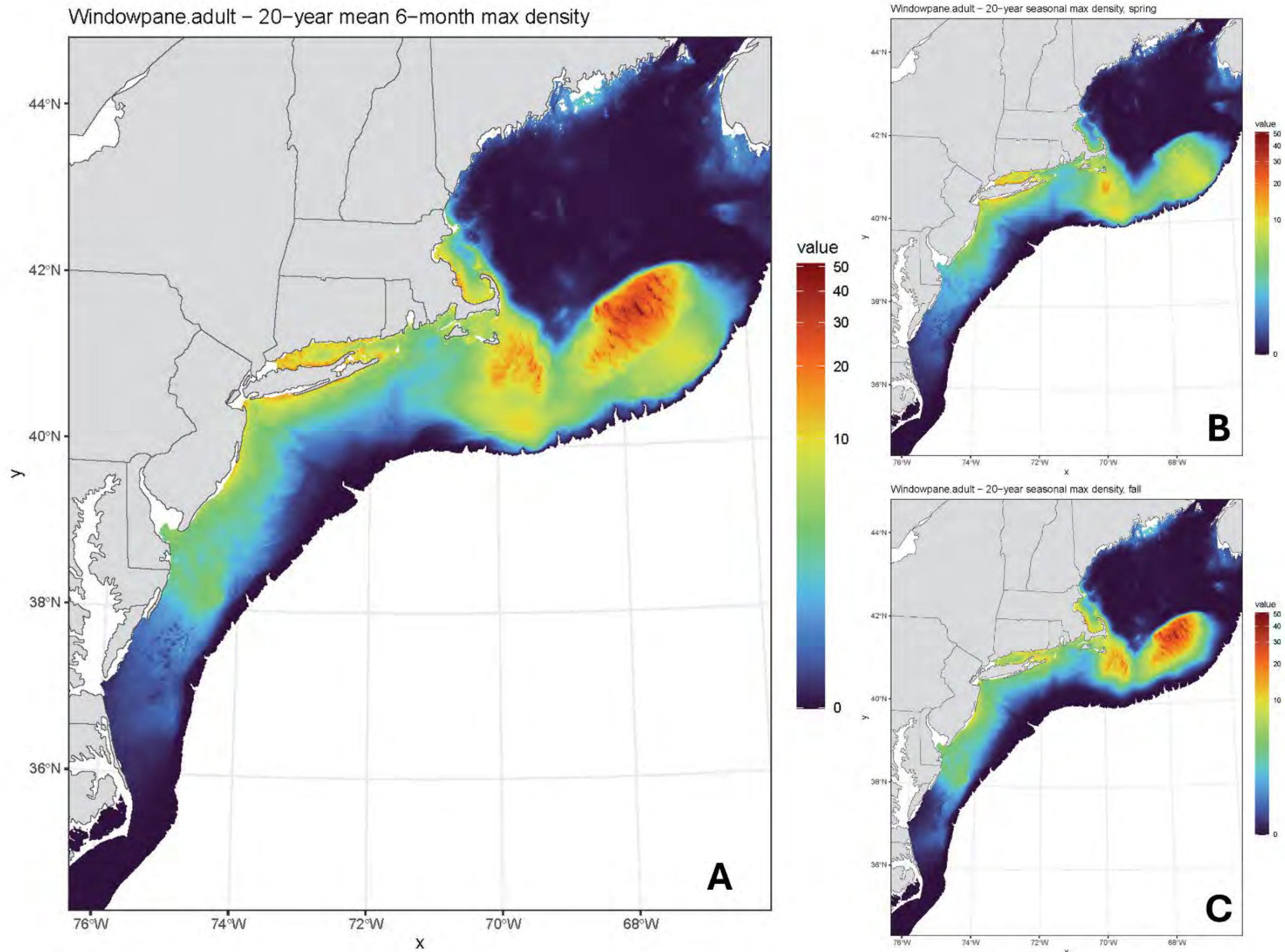

5.14 WINTER FLOUNDER

Figure 86. 20-year maximum predicted density (species counts) quantiles for juvenile winter flounder (*Pleuronectes americanus*). Maps depict the maximum of the 20-year averages across (A) the full temporal range of the model (six months); (B) spring survey months (March-May); and (C) fall survey months (September-November).

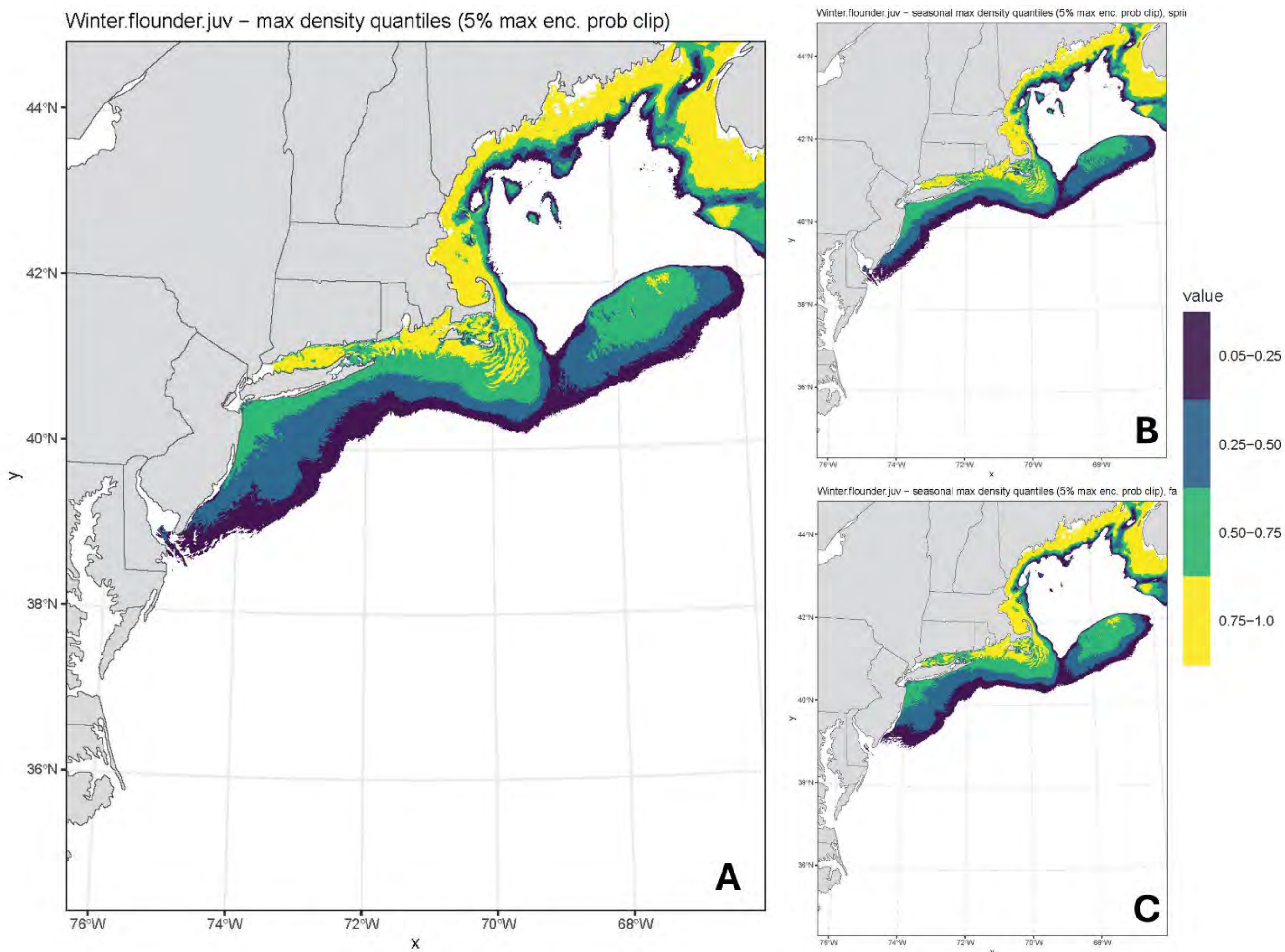

Figure 87. 20-year mean predicted density (species counts) for juvenile winter flounder (*Pleuronectes americanus*). Maps depict the maximum of the 20-year averages across (A) the full temporal range of the model (six months); (B) spring survey months (March-May); and (C) fall survey months (September-November).

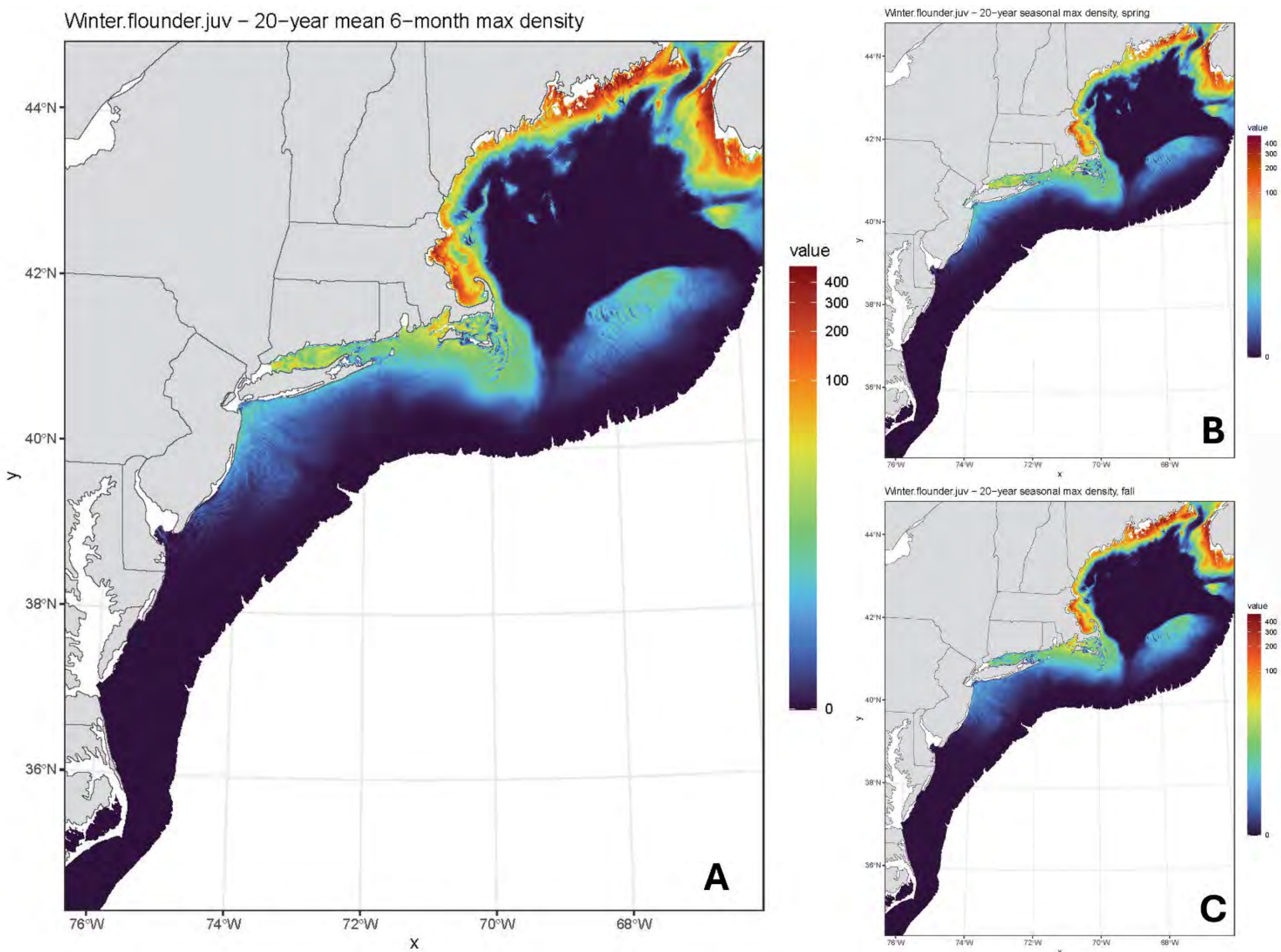

Figure 88. 20-year maximum predicted density (species counts) quantiles for adult winter flounder (*Pleuronectes americanus*). Maps depict the maximum of the 20-year averages across (A) the full temporal range of the model (six months); (B) spring survey months (March-May); and (C) fall survey months (September-November).

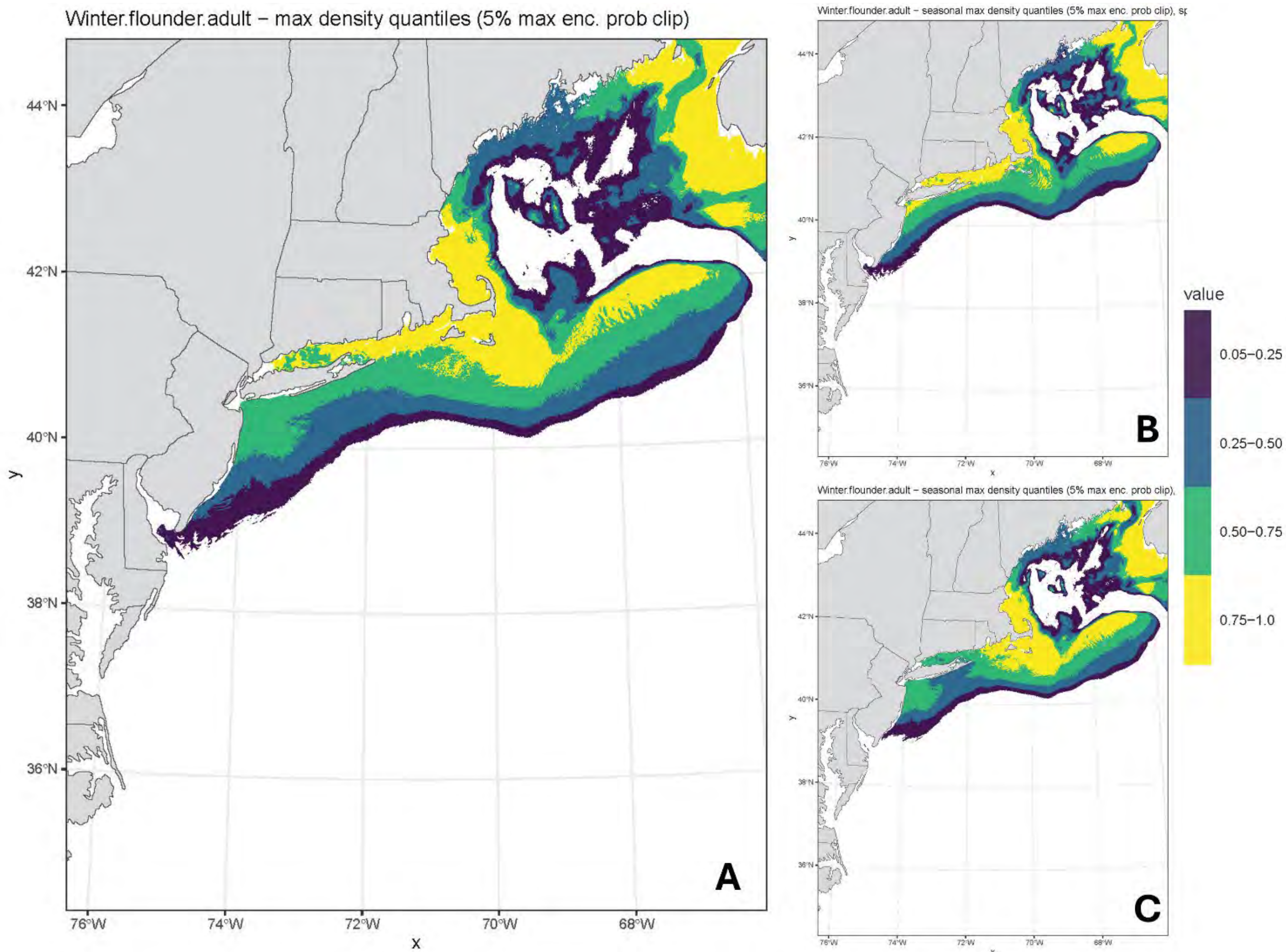

Figure 89. 20-year mean predicted density (species counts) for adult winter flounder (*Pleuronectes americanus*). Maps depict the maximum of the 20-year averages across (A) the full temporal range of the model (six months); (B) spring survey months (March-May); and (C) fall survey months (September-November).

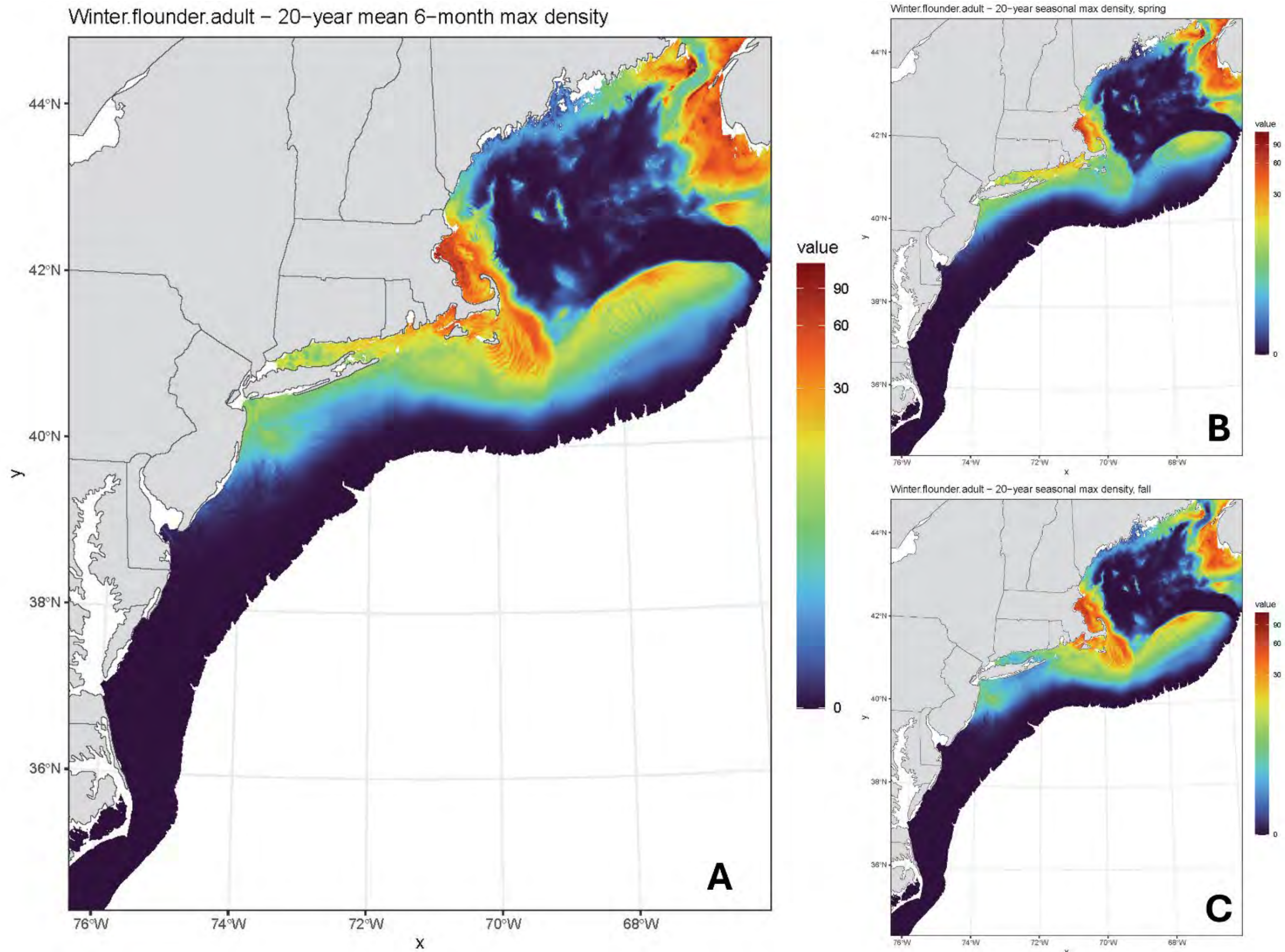

5.15 Witch flounder

Figure 90. 20-year maximum predicted density (species counts) quantiles for juvenile witch flounder (*Glyptocephalus cynoglossus*). Maps depict the maximum of the 20-year averages across (A) the full temporal range of the model (six months); (B) spring survey months (March-May); and (C) fall survey months (September-November).

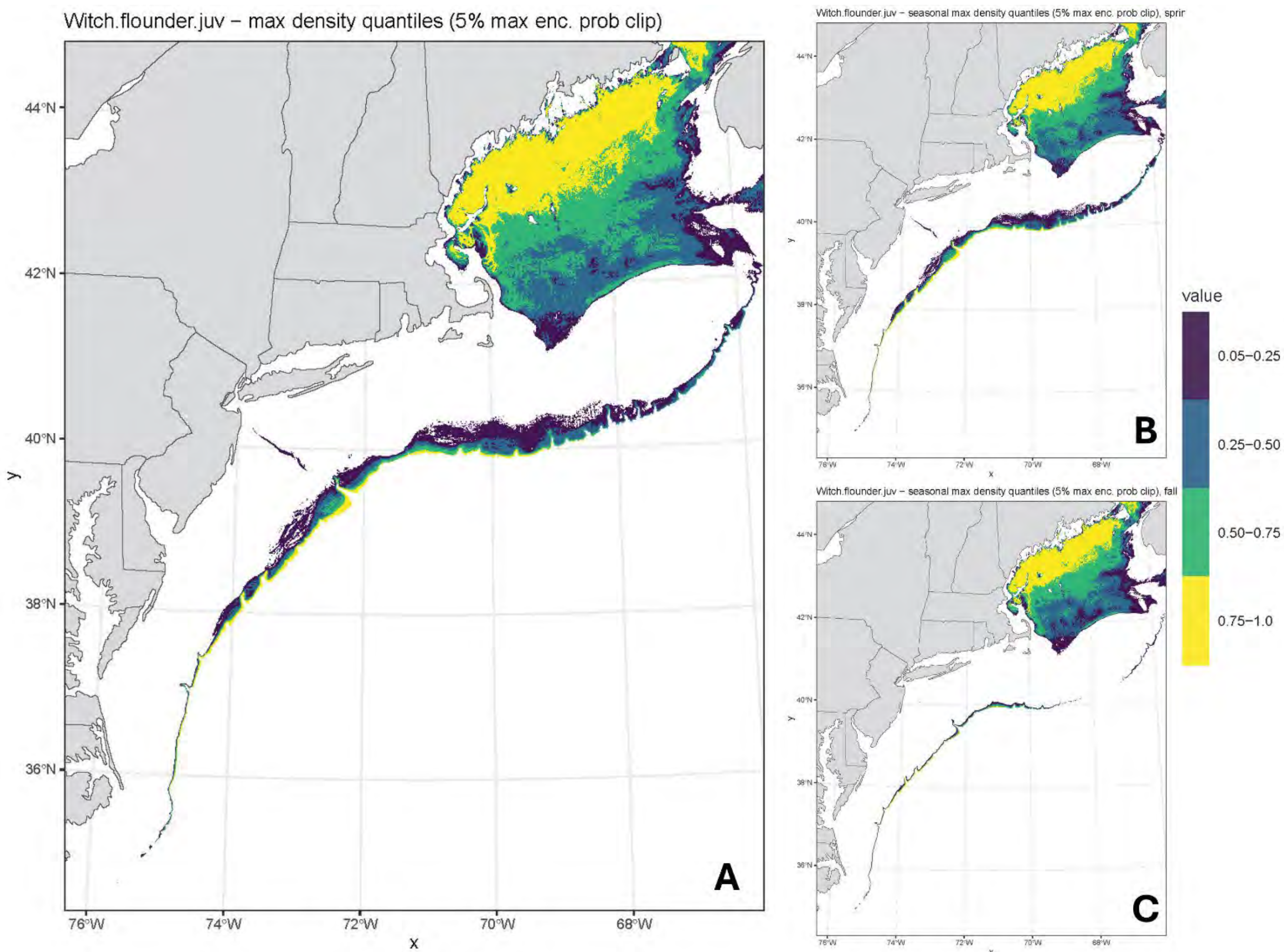

Figure 91. 20-year mean predicted density (species counts) for juvenile witch flounder (*Glyptocephalus cynoglossus*). Maps depict the maximum of the 20-year averages across (A) the full temporal range of the model (six months); (B) spring survey months (March-May); and (C) fall survey months (September-November).

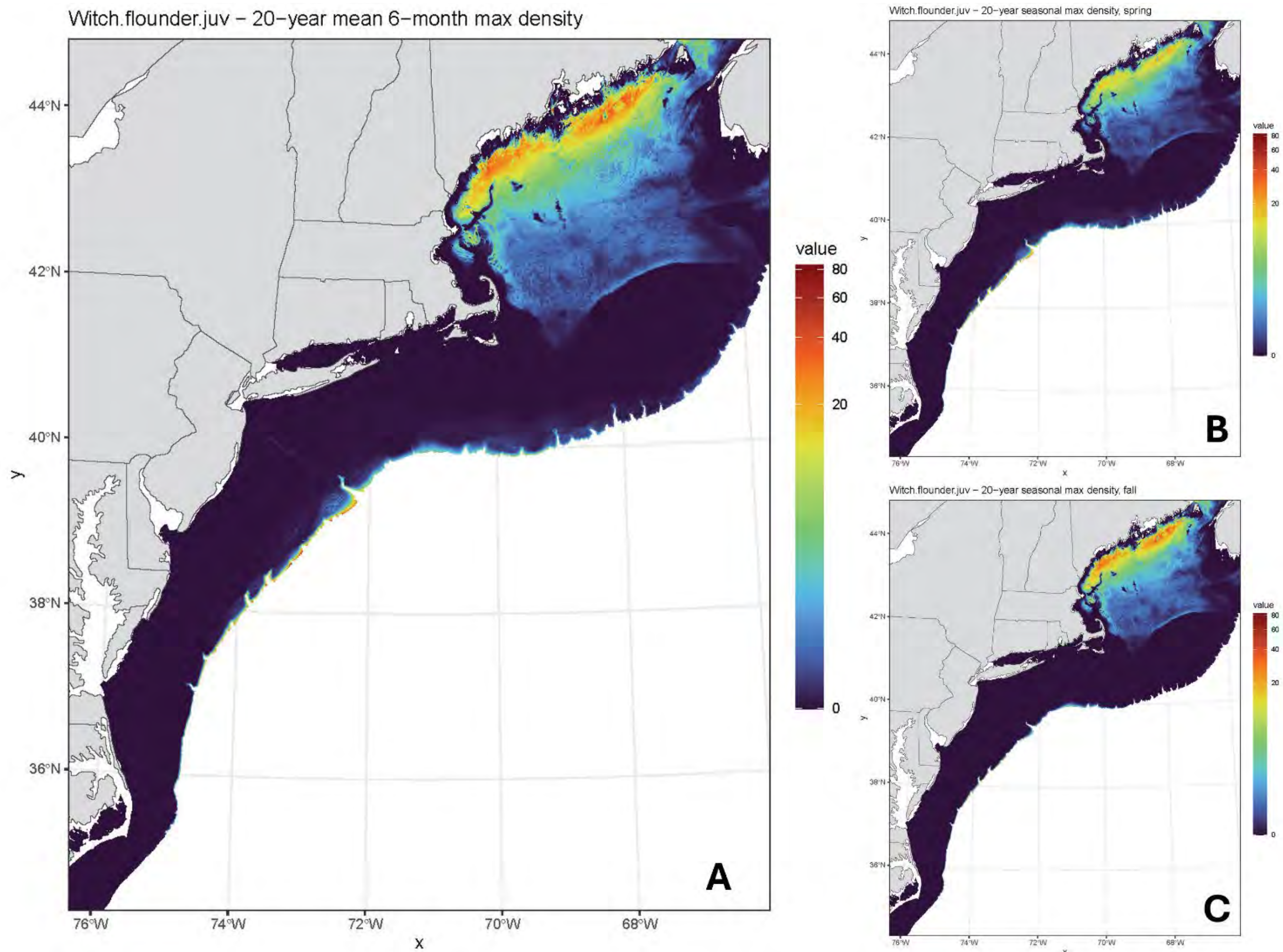

Figure 92. 20-year maximum predicted density (species counts) quantiles for adult witch flounder (*Glyptocephalus cynoglossus*). Maps depict the maximum of the 20-year averages across (A) the full temporal range of the model (six months); (B) spring survey months (March-May); and (C) fall survey months (September-November).

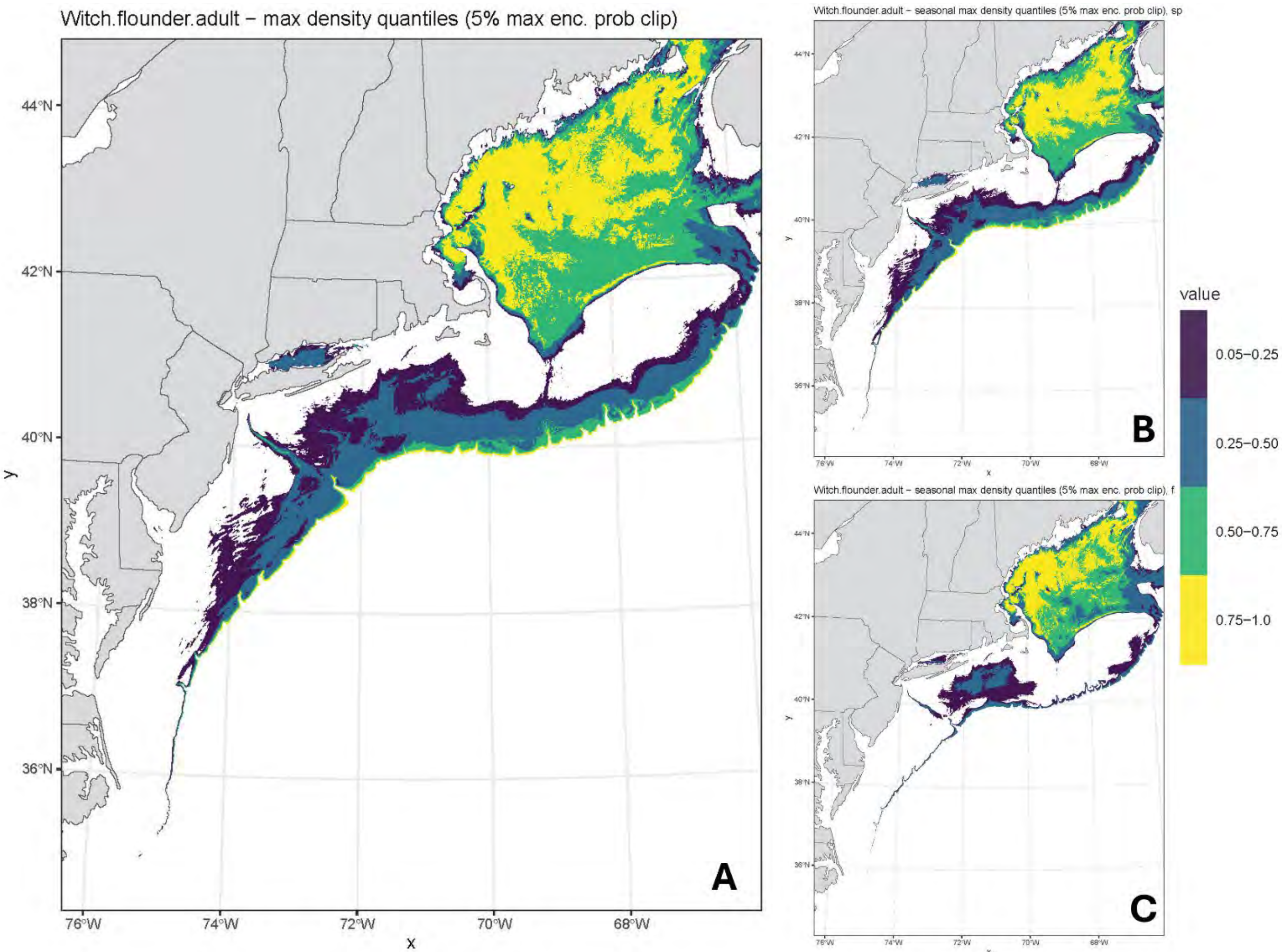

Figure 93. 20-year mean predicted density (species counts) for adult witch flounder (*Glyptocephalus cynoglossus*). Maps depict the maximum of the 20-year averages across (A) the full temporal range of the model (six months); (B) spring survey months (March-May); and (C) fall survey months (September-November).

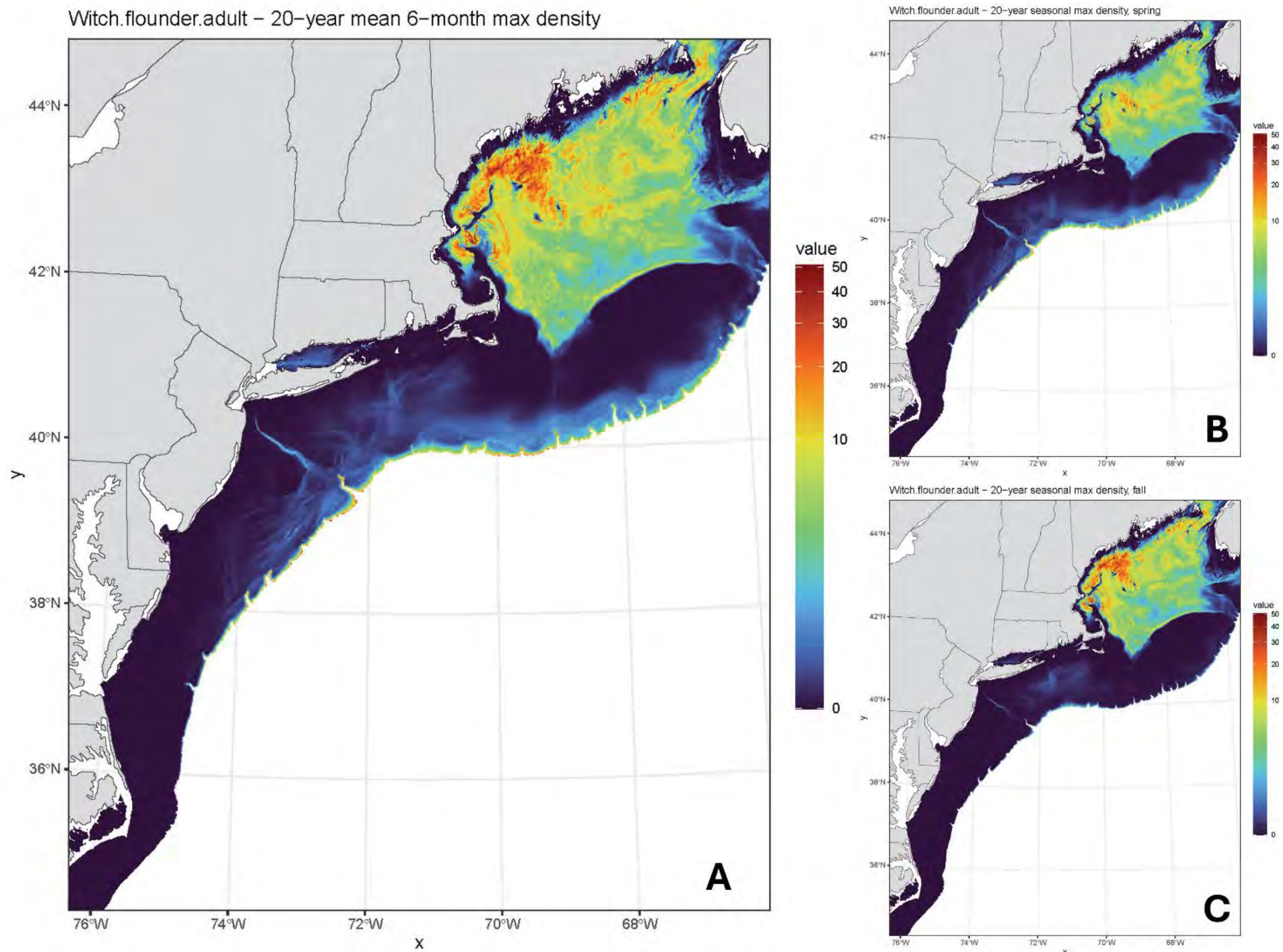

5.16 YELLOWTAIL FLOUNDER

Figure 94. 20-year maximum predicted density (species counts) quantiles for juvenile yellowtail flounder (*Limanda ferruginea*). Maps depict the maximum of the 20-year averages across (A) the full temporal range of the model (six months); (B) spring survey months (March-May); and (C) fall survey months (September-November).

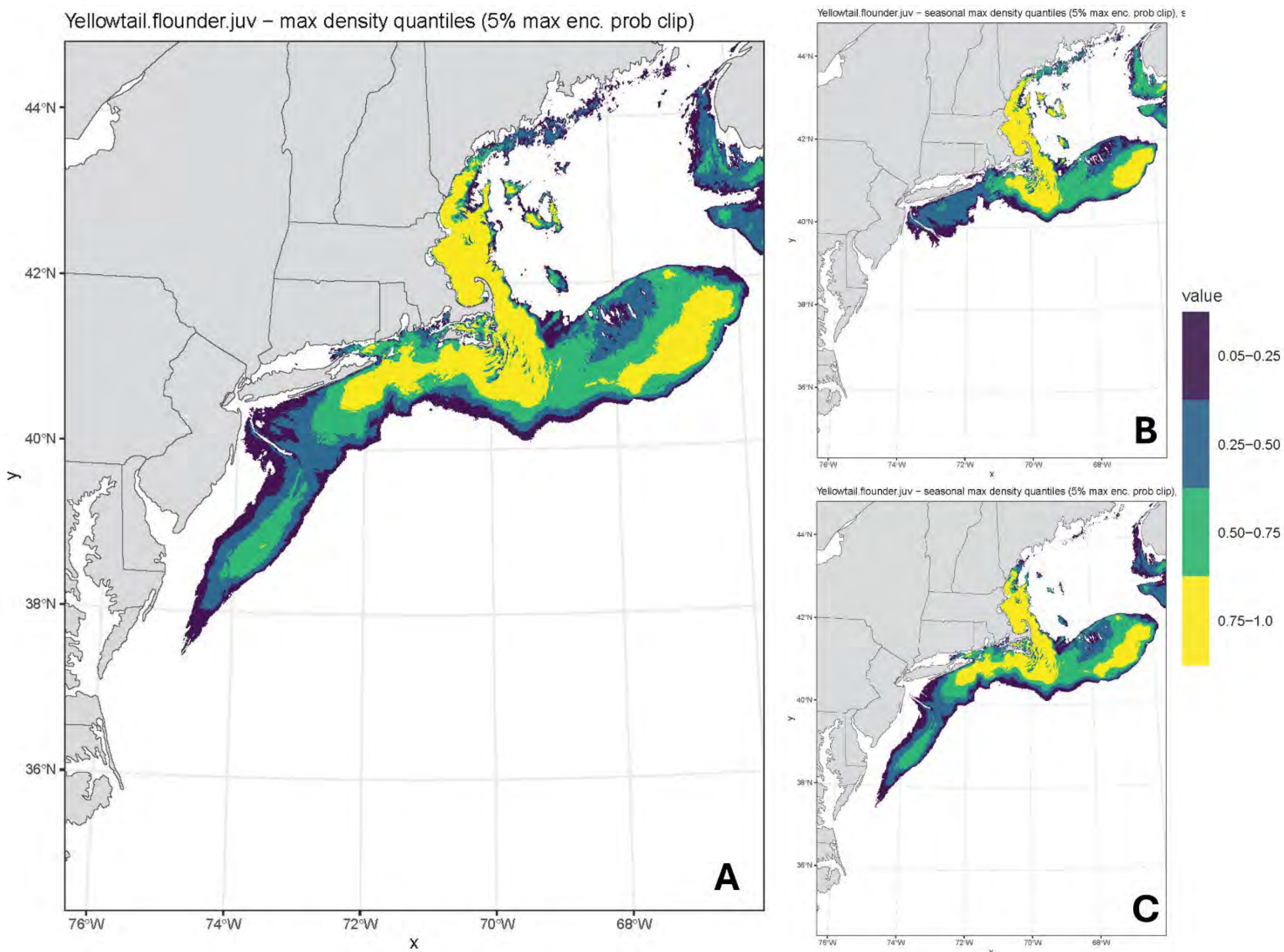

Figure 95. 20-year mean predicted density (species counts) for juvenile yellowtail flounder (*Limanda ferruginea*). Maps depict the maximum of the 20-year averages across (A) the full temporal range of the model (six months); (B) spring survey months (March-May); and (C) fall survey months (September-November).

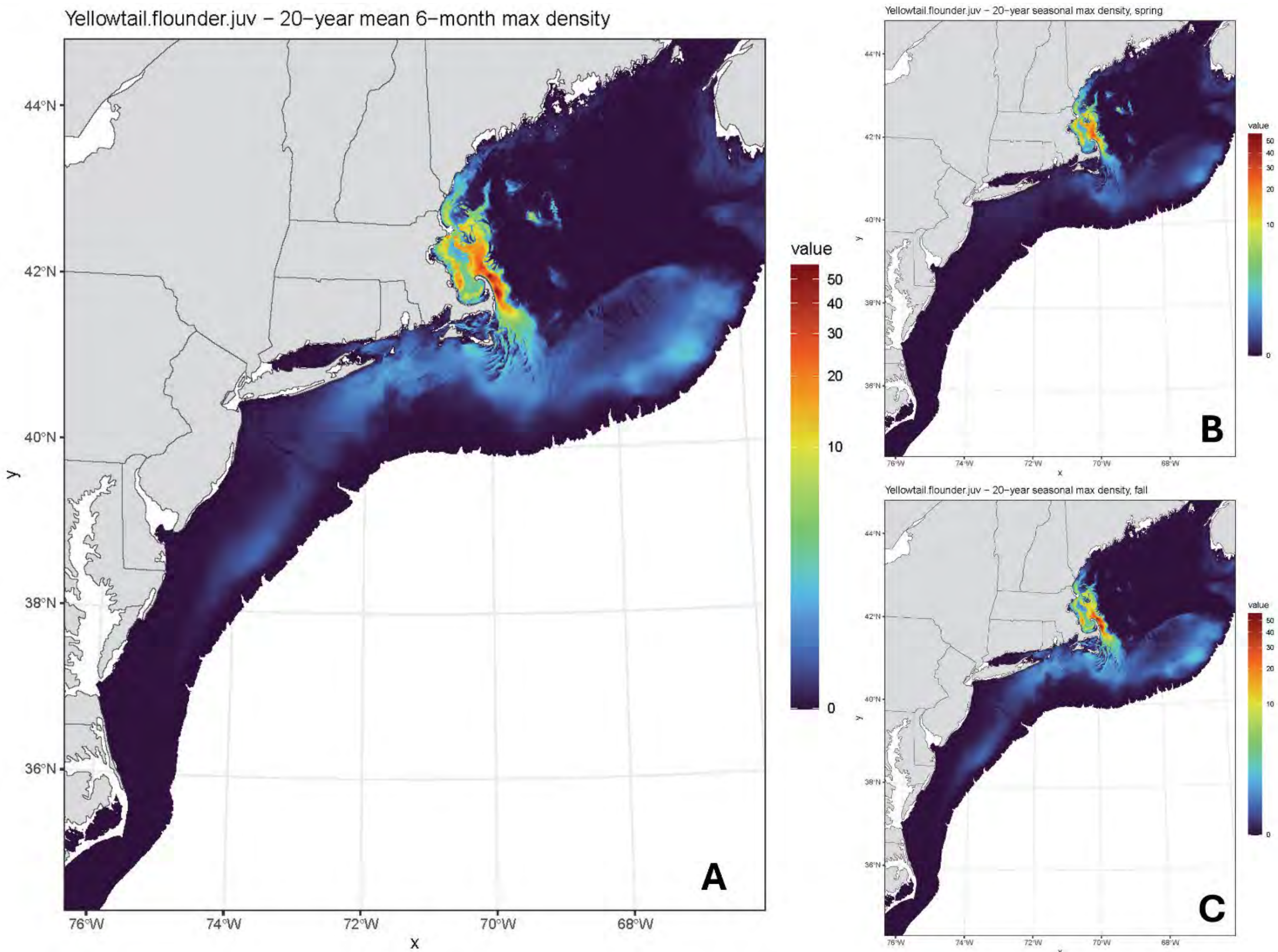

Figure 96. 20-year maximum predicted density (species counts) quantiles for adult yellowtail flounder (*Limanda ferruginea*). Maps depict the maximum of the 20-year averages across (A) the full temporal range of the model (six months); (B) spring survey months (March-May); and (C) fall survey months (September-November).

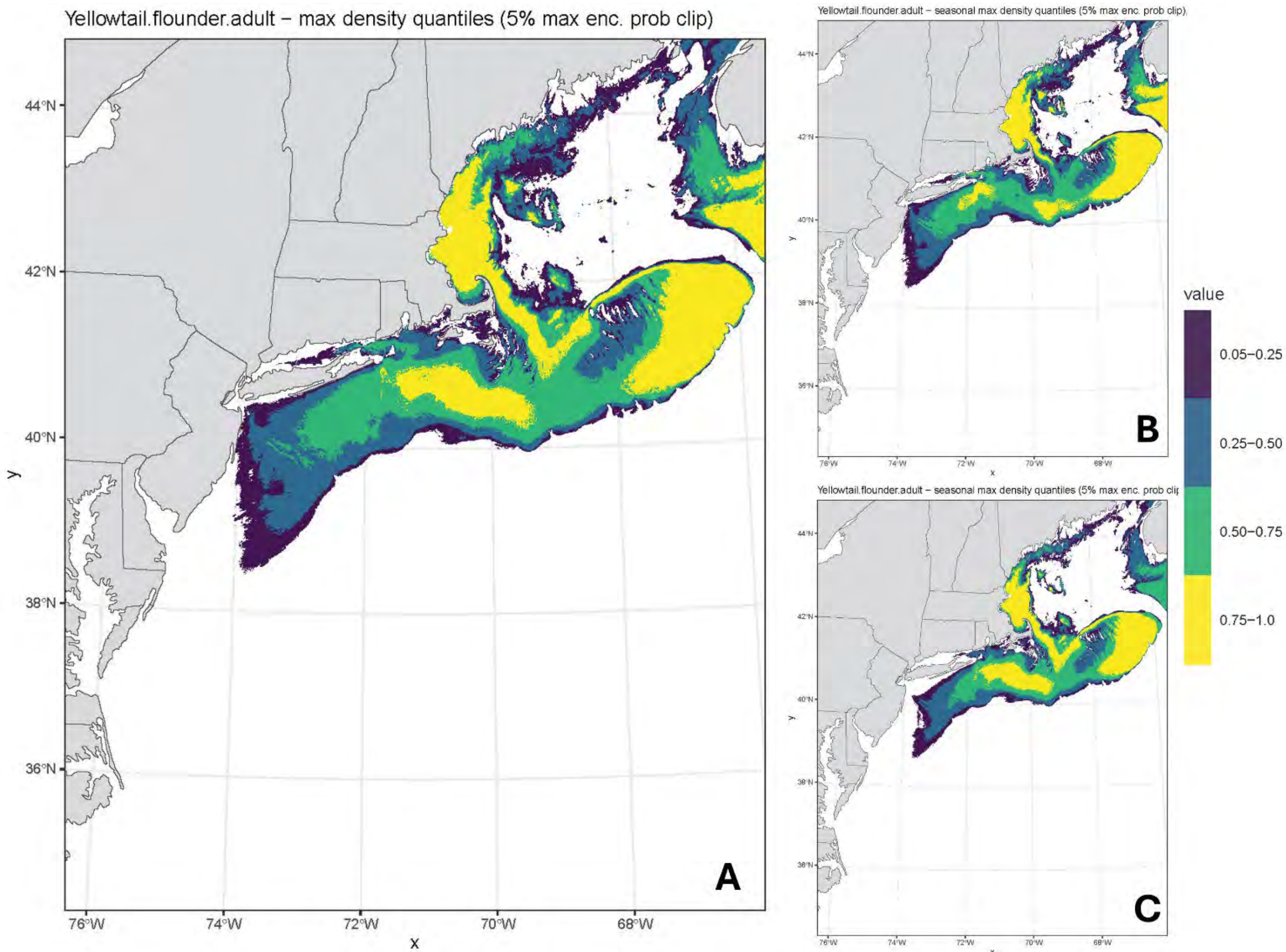

Figure 97. 20-year mean predicted density (species counts) for adult yellowtail flounder (*Limanda ferruginea*). Maps depict the maximum of the 20-year averages across (A) the full temporal range of the model (six months); (B) spring survey months (March-May); and (C) fall survey months (September-November).